

Praktikum zum Masterpflichtmodul *Anorganische Chemie* WS 2025/26

Teilbereich Metallorganische Chemie

Zum Vorgespräch:

Das **Vorgespräch** einer Praktikumswoche findet **montags** statt. Hierzu bereiten sich die Teilnehmenden auf die Versuchsblöcke aus dem Skript vor, die Ihnen für die jeweilige Praktikumswoche zugeordnet sind. Eine entsprechende Zuordnungsliste wird in ILIAS hochgeladen. Die einzelnen Versuche werden von den Teilnehmenden an der **Tafel** vorgestellt. Bestandteil des Vorgesprächs sind zum einen die **Reaktionsgleichungen, Mechanismen, aufgeführte Lerninhalte** etc. und zum anderen die **präparative Durchführung** der jeweiligen Versuche. Für eine sinnvolle Diskussion der chemischen Zusammenhänge der Präparate sind Kenntnisse im Bereich der **Koordinationschemie** (Ligandenfeldtheorie, spektrochemische Reihe etc.), der **Metallorganischen Chemie** (Metallocene, Metallcarbonyle, etc.) und Kenntnisse über **Methodik und Auswertung von NMR-Spektren** (Molekülsymmetrie, Anzahl und Multiplizität der NMR-Signale etc., siehe dazu z.B. das Skript *Crashkurs NMR-Spektroskopie* in ILIAS) unerlässlich und somit Bestandteil des Vorgesprächs. Sind grundlegende Kenntnisse nicht vorhanden, muss das Vorgespräch wiederholt werden. Wir bitten alle Teilnehmenden sich gut vorzubereiten, da der Beginn der praktischen Arbeit erst nach bestandenem Vorgespräch möglich ist.

Im Anschluss an das Vorgespräch erfolgt bereits eine kurze Einweisung in allgemeine Arbeitstechniken unter inerten Reaktionsbedingungen im Labor. Alle Arbeiten (sofern nicht anders erwähnt) sind unter Schutzgas und mit getrockneten bzw. entgasten Lösungsmitteln durchzuführen! Glasgeräte/Apparaturen sind vor Gebrauch bzw. Zugabe von Lösungsmitteln/flüssigen Reaktanden zu sekurieren. **Während der praktischen Arbeit ist ein Laborjournal zu führen**, in dem die tatsächlich erfolgte Versuchsdurchführung und die jeweiligen Beobachtungen notiert werden.

Ergänzend zur angegebenen Fachliteratur, werden noch folgende Bücher empfohlen:

- R. Alsfasser, C. Janiak, T. M. Klapötke, H.-J. Meyer, E. Riedel, *Moderne Anorganische Chemie*, de Gruyter.
- C. Elschenbroich, *Organometallchemie*, 6. Aufl., Teubner, Wiesbaden, **2008**.
- M. Hesse, H. Meier, B. Zeeh, *Spektroskopische Methoden in der organischen Chemie*, 8. Aufl. Thieme, **2012**.
- G. R. Fulmer *et al.* NMR Chemical Shifts of Trace Impurities: Common Laboratory Solvents, Organics, and Gases in Deuterated Solvents Relevant to the Organometallic Chemist, *Organometallics* **2010**, 29, 2176-2179.
- H. E. Gottlieb *et al.* NMR Chemical Shifts of Common Laboratory Solvents as Trace Impurities, *J. Org. Chem.* **1997**, 62, 7512-7514.

Zum Praktikumsverlauf:

Spätestens zum ersten Labortag muss das entsprechende Vorprotokoll vorliegen (pro Versuch ein Vorprotokoll, siehe Vordruck). Dabei ist die Ansatzberechnung wichtig (inkl. Massen, molare Massen, Stoffmengen, ggf. Dichten für Flüssigkeiten). Zusätzlich muss die entsprechende **Versuchsdurchführung aus der Fachliteratur in ausgedruckter Form** vorliegen. Die Versuchsbeschreibungen in diesem Skript dienen nur zur groben Orientierung. Die angegebene Fachliteratur sollte vor Versuchsbeginn verinnerlicht und befolgt werden, soweit nicht anders vom Assistenten angeordnet.

Die Durchführung der Versuche ist von Dienstag bis Freitag jeweils von 8:00 bis 18:00 Uhr möglich. **Die Vorlesungen bzw. Übungen haben stets Vorrang vor der Laborarbeit.** Bitte teilt euch eure Zeit so ein, dass am Ende der Woche alle Präparate fertig synthetisiert und charakterisiert, sowie die Ausrüstung und der Arbeitsplatz gereinigt sind. Hierbei ist zu beachten, dass **Arbeiten im Labor nur bei vollständiger Anwesenheit der gesamten Gruppe** durchzuführen sind. Eine Arbeitsteilung in Form eines „Schichtbetriebs“ ist nicht akzeptabel. Jeder Gruppe wird am Montag ein Arbeitsplatz zugewiesen, der alle benötigten Materialien/Geräte enthält. Spätestens am Freitag um 18:00 Uhr muss dieser Arbeitsplatz wieder abgegeben werden (inkl. gespülten Glasgeräten!).

Zu den Versuchsergebnissen:

Die Versuchsergebnisse werden durch eine kurze Powerpoint-Präsentation vorgestellt (Die Anfertigung eines ausführlichen schriftlichen Protokolls ist dagegen nicht erforderlich). Jede Gruppe erstellt dazu eine Präsentation von ca. 10 Minuten Dauer (maximal 10 Folien). Alle Gruppen einer Praktikumswoche vereinbaren für die Präsentationen mit den Assistenten einen gemeinsamen Termin in der auf die Praktikumswoche folgenden Woche. Bestandteile der Präsentation sollen sein: **Einleitung** (Vorstellung des Präparates, Lernziel des Versuchs), **Reaktionsgleichung(en)**, **Mechanismus**, **Versuchsdurchführung mit Ansatzgröße, Ausbeuteberechnung, Präsentation und Erläuterung der NMR-Spektren**. Ausbeuten und spektroskopische Daten werden mit der Primärliteratur verglichen, eventuelle Abweichung werden diskutiert.

Zusammengefasst:

Die Theorie zu den Versuchen (Stichwort: Lerninhalte) ist für das Kolloquium in der jeweiligen Woche vorher zu lernen. Ohne bestandenes Vorgespräch, korrektes Vorprotokoll und ausgedruckter Versuchsvorschrift (Primärliteratur und Skript!) ist ein Beginn der praktischen Arbeiten nicht möglich! Während der Versuchsdurchführung ist ein Laborjournal zu führen, in dem die Versuchsdurchführung und Beobachtungen notiert werden. Die Lerninhalte dienen außerdem als Rahmen für die Präsentation der Versuchsergebnisse.

Wir wünschen allen Teilnehmenden ein erfolgreiches Praktikum!.

Block 3

3.1 Darstellung von [1,3-Bis(2,6-diisopropylphenyl)imidazol-2-yliden]kupfer(I)iodid

Literatur:

- [1] Synthese: O. Santoro, A. Collado, A. M. Z. Slawin, S. P. Nolan, C. S. J. Cazin, *Chem. Commun.* **2013**, 49, 10483-10485.
- [2] Übersicht: E. A. Martynova, N. V. Tzouras, G. Pisano, C. S. J. Cazin, S. P. Nolan, *Chem. Commun.* **2021**, 57, 3836-3856.

Durchführung:

In einem 10-mL-MW-Gefäß wird das Imidazoliumsalz IPr*HCl zusammen mit CuI und K₂CO₃ (4 eq.: Abweichung zur Literatur!) vorgelegt und in 1 mL Aceton gelöst. Es wird 24 Stunden bei 60 °C gerührt. Die erhaltene Lösung wird über Silica filtriert und das Silicapad mit 3 x 1 mL Methylenechlorid gewaschen. Die Lösung wird im Hochvakuum auf die Hälfte ihres Volumens eingeengt und das Produkt mit n-Hexan gefällt. Das Produkt wird abzentrifugiert, mit 3 Portionen je 1 mL n-Hexan gewaschen und im Hochvakuum getrocknet. Ist das Produkt unter UV-Bestrahlung lumineszent?

Ansatzgröße:

0,235 mmol IPr*HCl

Charakterisierung:

- ¹H-NMR (CDCl₃)
- ¹³C{¹H}-NMR (CDCl₃)

Lerninhalte:

- Welche Darstellungsmöglichkeiten für Metall-NHC-Komplexe gibt es? Welchen „Vorteil“ bietet die in diesem Versuch durchgeführte Darstellungsmöglichkeit? Welche weitere Synthesemöglichkeit für Cu(I)-NHC-Komplexe gibt es ferner?
- Geben Sie den Reaktionsmechanismus/-verlauf für die durchgeführte Synthese an.
- Wieviel Signale liefert das Produkt im jeweiligen NMR-Spektrum und wie spalten diese auf?

3.2 Darstellung von [Bis(2,6-diisopropylphenyl)imidazol-2-yliden]kupfer(I)carbazolat

Literatur:

- [1] Synthese: N. V. Tzouras, E. A. Martynova, X. Ma, T. Scattolin, B. Hupp, H. Busen, M. Saab, Z. Zhang, L. Falivene, G. Pisano, K. van Hecke, L. Cavallo, C. S. J. Cazin, A. Steffen, S. P. Nolan, *Chem. Eur. J.* **2021**, 27, 11904-11911.
- [2] Eigenschaften: R. Hamze, J. L. Peltier, D. Sylvinson, M. Jung, J. Cardenas, R. Haiges, M. Soleilhaveoup, R. Jazzaar, P. I. Djurovich, G. Bertrand, M. E. Thompson, *Science* **2019**, 363, 601-606.

Durchführung:

In einem 10-mL-MW-Gefäß wird IPr*HCl zusammen mit CuCl und K₂CO₃ vorgelegt und in 1 mL Aceton gelöst. Es wird 24 Stunden bei 60 °C gerührt. Nach dem Abkühlen der Lösung werden Carbazol und K₂CO₃, gelöst in 0,5 mL Aceton, hinzugegeben. Die Suspension wird 20 Stunden bei Raumtemperatur gerührt. Das Lösungsmittel wird im Hochvakuum entfernt, der Rückstand in 2 mL Tetrahydrofuran suspendiert und über Al₂O₃ (basisch, Brockmann I) filtriert. Das Lösungsmittel wird im Hochvakuum aus dem Filtrat entfernt und der verbleibende farblose Feststoff mit Diethylether gewaschen. Ist das Produkt unter UV-Bestrahlung lumineszent?

Ansatzgröße:

0,235 mmol IPr*HCl

Charakterisierung:

- ¹H-NMR (CDCl₃)
- ¹³C{¹H}-NMR (CDCl₃)

Lerninhalte:

- Für Cu(I)-Komplexe kann die Farbigkeit häufig mit MLCT begründet werden. Was ist MLCT?
- Was bedeutet TADF? Erläutern Sie kurz, was TADF ist und wieso diese von besonderem Forschungsinteresse ist.
- Wieviel Signale liefert das Produkt im jeweiligen NMR-Spektrum und wie spalten diese auf?



Cite this: *Chem. Commun.*, 2021,
57, 3836

Received 15th December 2020,
Accepted 18th March 2021

DOI: 10.1039/d0cc08149c

rsc.li/chemcomm

The “weak base route” leading to transition metal–N-heterocyclic carbene complexes

Ekaterina A. Martynova, Nikolaos V. Tzouras, Gianmarco Pisanò, Catherine S. J. Cazin and Steven P. Nolan *

N-Heterocyclic carbenes (NHCs) are nowadays ubiquitous in organometallic chemistry and catalysis. Recently, a synthetic method which makes use of weak bases and desirable solvents has emerged as a simple, widely applicable and cost-effective pathway to well defined M–NHC complexes. Herein, recent studies devoted to the weak base approach are examined in detail, in order to showcase the simplicity, scope and variations of the method with regards to the azolium salts, bases and the metal sources, as well as the reaction conditions used. Mechanistic investigations are presented, illustrating the formation of intermediates which are air and moisture stable, prior to the metallation step. Finally, the importance, limitations and future prospects of the weak base route are discussed.

Introduction

The vast potential of N-heterocyclic carbenes (NHCs) as ancillary ligands in transition metal catalysis has been demonstrated and thoroughly explored during the last decade.^{1–3} In any catalytic method, the access to the catalyst is a crucial factor in determining its overall utility. Consequently, sustainable routes for the synthesis of transition metal-based catalysts are highly desirable to stock the synthetic chemist’s toolbox.

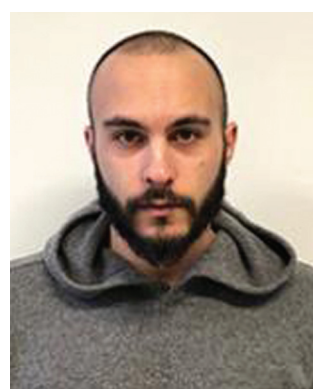
Department of Chemistry and Centre for Sustainable Chemistry, Ghent University, Building S3, Krijgslaan 281, 9000 Gent, Belgium. E-mail: steven.nolan@ugent.be



Ekaterina A. Martynova

Ekaterina A. Martynova received her specialist diploma (equivalent to MSc in Russia) in 2019 at Lomonosov Moscow State University under the supervision of Tatyana Podrugina. In 2020 she joined the group of Prof. Steven P. Nolan at Ghent University as a PhD candidate. Her research is primarily focused on the synthesis and reactivity of late transition metal N-heterocyclic carbene complexes and their application in homogeneous catalysis.

Historically, there have been three main approaches for the synthesis of transition metal–NHC complexes (Scheme 1).⁴ The first involves the formation of a free carbene as the initial step (Scheme 1a).^{5–9} Such species are usually obtained by the addition of a strong base to an azolium salt. The next step of this “free carbene route” is the introduction of a transition metal source to the reaction mixture (of the *in situ* generated NHC) or to the isolated NHC. It is worth mentioning that besides being a two-step procedure, the free carbene route is carried out under inert atmosphere, using strictly anhydrous conditions and strong bases, which are usually expensive and potentially hazardous. The second approach – the “transmetallation



Nikolaos V. Tzouras

Nikolaos V. Tzouras carried out his diploma thesis research at the University of Athens with Professor G. C. Vougioukalakis, on the synthesis of N-Heterocyclic carbene precursors. After obtaining a scholarship for graduate studies in organic synthesis, he carried out his MSc research on sustainable metal catalyzed C–H activation and multicomponent reactions, while he spent three months as a visiting researcher in Ghent university, working in the research group of Professor S. P. Nolan. Currently, he is pursuing a joint PhD degree with G.C. Vougioukalakis and S. P. Nolan as an FWO fellow, focusing on organometallic chemistry and catalysis.

Feature Article

ChemComm

route” – is also a two-step procedure (Scheme 1b).^{6,10–12} The first step is the reaction between an azolium salt and copper or silver oxides, in order to obtain the corresponding Cu- or Ag-NHC complexes. The next step consists of a NHC transfer to a desired second transition metal. Despite the advantageous features of this approach, such as the use of air-stable starting materials and the generation of water as by-product in the first step, it also has significant drawbacks. This route is limited to the use of only copper and silver oxides, usually requires high temperatures or toxic solvents, while it generates non-trivial amounts of waste. It is also troublesome when attempting to access metal complexes bearing bulky NHC ligands.

Importantly, these limitations render the scale-up of these routes challenging and not sustainable in terms of waste and



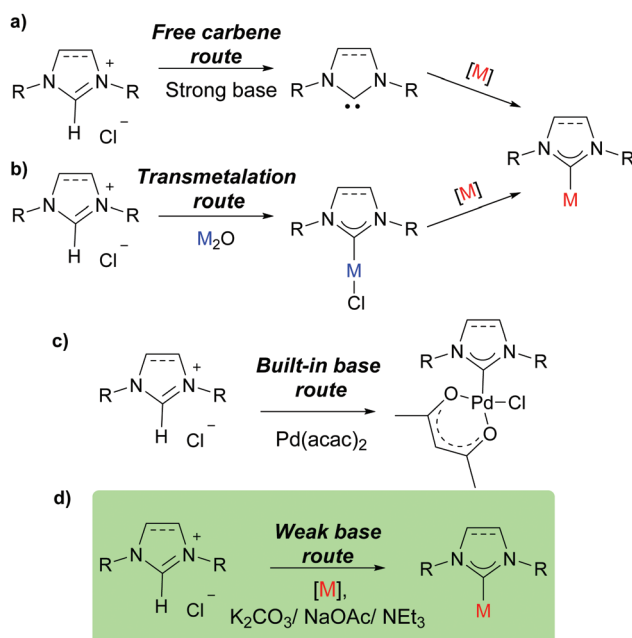
Gianmarco Pisano

developing new synthetic strategies for sustainable access to transition metal-N-heterocyclic carbene complexes through the implementation of mechanochemical methods.



Catherine S. J. Cazin

of Chemistry in St Andrews in 2009 where she held a Royal Society University Research Fellowship. She is now a Full Professor in the Department of Chemistry at Ghent University.



Scheme 1 Methods for the synthesis of metal–NHC complexes.

resource management. The third approach, the “built-in base route”,^{13,14} is not as general as the other two and requires the prior installation of a ligand onto the metal precursor that can act as a base (Scheme 1c). Some examples make use of commercially available precursors already possessing such ligands. A simple, one-pot synthetic procedure has been reported,¹⁴ where $\text{Pd}(\text{acac})_2$ and excess of an NHC salt were refluxed in 1,4-dioxane for 24 hours; after which time the desired compound, $[\text{Pd}(\text{acac})(\text{NHC})\text{Cl}]$, was obtained in almost quantitative yield.



Steven P. Nolan

Steven P. Nolan received his BSc in Chemistry from the University of West Florida and his PhD from the University of Miami where he worked under the supervision of Professor Carl D. Hoff. After a postdoctoral stay with Professor Tobin J. Marks at Northwestern University, he joined the Department of Chemistry of the University of New Orleans in 1990. In 2006 he joined the Institute of Chemical Research of Catalonia (ICIQ) as Group leader and ICRA Research Professor. In early 2009, he joined the School of Chemistry at the University of St Andrews and in 2017 joined the Department of Chemistry of Ghent University as Senior Full Professor. Professor Nolan's research interests revolve around the design and synthesis of catalytic complexes enabling organic transformations.

A limited number of works devoted to the synthesis of various M–NHC complexes ($M = \text{Rh, Ir, Au, Ni, Pd, Cu, Ag, etc.}$) via the reaction between metal sources and azolium salts in the presence of weak bases, such as NaOAc , K_2CO_3 and NEt_3 have also been described in the literature during the period from 2002 until 2012.^{15–22} It is worth mentioning that the reported procedures require high temperatures ($80\text{--}200\ ^\circ\text{C}$), microwave irradiation, long reaction times (9–24 hours) and toxic solvents (xlenes, 3-chloropyridine and acetonitrile). In addition, there are examples of using the weak base approach to obtain a cationic Pt–NHC complex by stirring a triazolium salt and Karstedt's catalyst in the presence of NaOAc in THF, at room temperature.²³ Unfortunately, these procedures cannot be applied to many NHC precursors.

The groups of Nolan and Gimeno,^{24,25} in 2013, independently reported an approach using a weak base (K_2CO_3 , among others), imidazol(in)ium salts and gold or silver sources, which allows the one-step synthesis of the corresponding metal–NHC complexes (Scheme 1d). These were some of the earliest systematic reports on the topic, describing the metallation of the most commonly used NHC salts under environmentally benign conditions and provided an in-depth investigation of the methodology, highlighting its importance for coinage metals specifically and also in general. This “weak base route” led to several significant improvements, namely to the use of aerobic conditions, the prospect of using greener solvents, such as acetone and ethyl acetate, and to the use of weak bases that are less toxic and more cost-efficient.

The objective of this contribution is to highlight the weak base approach as the state-of-the-art procedure for the synthesis of numerous metal–NHC complexes. An up-to-date overview of studies on the “weak base route” is presented herein. Particular attention is paid to key aspects of this chemistry including its large-scale applications and mechanistic understanding, highlighting the future prospects and limitations discovered thus far. Throughout this review, the term “weak base” refers to typically inorganic bases and triethylamine (with a pK_a value of their conjugate acid being less than 11 in water). Even though pK_a values depend on the solvent, comprehensive classification of the bases examined is not the objective and the reagents which will be encountered herein are typically regarded as mild or “weak” bases.

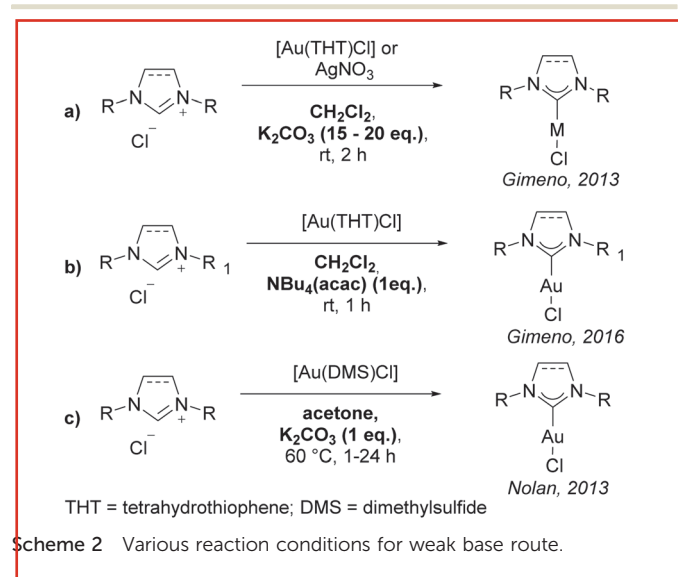
The weak base route in the synthesis of group 11 complexes

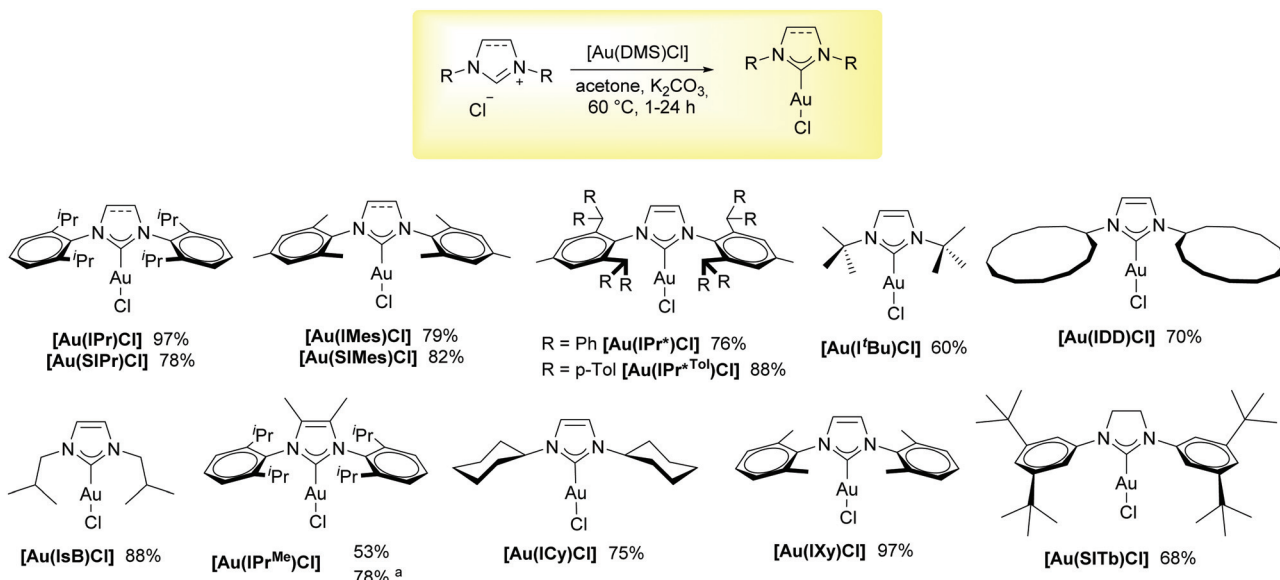
Gold–NHC complexes are valuable to the wide research community because of their various applications in catalysis^{26,27} medicinal chemistry and material science.^{28–30} For these reasons, complexes of the coinage metal have become a key point of interest during the last two decades. In 2011, Zhu and co-workers reported a new synthetic approach for gold–NHC complexes using a weak base route.³¹ It was shown that $[\text{Au}(\text{NHC})\text{Cl}]$ complexes can be obtained directly by heating $[\text{M}][\text{AuCl}_4]\cdot 2\text{H}_2\text{O}$ ($\text{M} = \text{Na, K}$) and various NHC ligands in

3-chloropyridine with potassium carbonate as a base. $[\text{Au}(\text{NHC})\text{Cl}_3]$ species were considered as intermediates for this reaction, which can be transformed into the desirable gold–NHC complexes by re-exposing the reaction conditions. The use of a toxic solvent and high temperature are among the main drawbacks of this route which are reminiscent of the approach used for Organ's palladium system (see the Pd–NHC chapter below). The Ananikov group attempted to obtain gold complexes containing ring-expanded NHC ligands using the same procedure, but did not succeed.³² Their work has demonstrated the unsuitability of this approach in the case of bulkier ligands (THP-Dipp, THD-Dipp).

The Nolan²⁴ and Gimeno groups,²⁵ independently reported an alternative approach implementing the use of weak bases for the synthesis of such complexes. This method allows the one-step synthesis of gold–NHC complexes using imidazol(in)ium salts and metal sources. The procedure reported by Gimeno requires an excess (15 eq.) of base and is carried out in dichloromethane. The same reaction conditions were also tested for the synthesis of Ag–NHC complexes (Scheme 2a). The reaction conditions described by Gimeno and co-workers were not applicable to NHC ligands bearing both very bulky and very small substituents, the latter compounds were observed to decompose to metallic gold under these conditions. In order to find a more versatile procedure, Gimeno reported the “acac method” in 2016.³³

Tetrabutylammonium acetylacetonate, $\text{NBu}_4(\text{acac})$, was used as the deprotonating reagent in this approach, however it is worth mentioning that $\text{NBu}_4(\text{acac})$ requires synthesis prior to use, thus adding a step in the M–NHC synthetic procedure. Reactions were carried out in DCM, a non-desirable solvent for sustainability reasons (Scheme 2b). The Nolan method makes use of only 1 equivalent of potassium carbonate and of the more sustainable acetone as solvent (Scheme 2c). The optimisation of this route was carried out on an example of $\text{IPr}\cdot\text{HCl}$ as the imidazolium salt and $[\text{Au}(\text{DMS})\text{Cl}]$. Different solvents (among them acetonitrile, acetone, THF and iPrOH), bases





Scheme 3 General synthetic procedure for $[\text{Au}(\text{NHC})\text{Cl}]$ complexes using optimized conditions. Scope of obtained gold–NHC complexes. Reaction conditions: 1 eq. of NHC·HCl salt, 1 eq. of $[\text{Au}(\text{DMS})\text{Cl}]$, 1 eq. of K_2CO_3 , ^a 2 eq. of K_2CO_3 .

(such as NaOAc , K_2CO_3 , NaHCO_3 , Na_2CO_3 , NET_3 and pyridine) and temperatures (from 25 to 60 °C) were tested. The best result was obtained in acetone with 1 eq. of potassium carbonate at 60 °C after 1 hour. To highlight the versatility of this approach, reactions with various saturated and unsaturated NHC ligands under the same user-friendly conditions were performed (Scheme 3). Both saturated and unsaturated Au–NHC complexes were obtained in good to excellent yields. In some cases, improved performance in comparison with previously reported methods was observed.⁶ $[\text{Au}(\text{IPr})\text{Cl}]$ was prepared in 97% yield in comparison to 76% yield while using the free carbene route. The yield was also improved for $[\text{Au}(\text{IMes})\text{Cl}]$ from 63% (using the transmetalation route) to 79%. It is worth mentioning that $[\text{Au}(\text{IPr}^*)\text{Cl}]$, bearing the very bulky IPr^* ligand, which could not be obtained by transmetalation,³⁴ was successfully prepared in 76% yield using the weak base route.²⁴ However, although the yields for gold complexes bearing ICy, IDD and I^tBu were good (60–88%), the reactions did not reach completion. Substituents on the backbone of IPr^{Me} decreased the yield to 53%, but this could be improved to 78% by the addition of 2 eq. of potassium carbonate. Usually for saturated NHC ligands, longer reaction times (24 hours) are required to reach full conversion.

The scalability of this approach was also tested.²⁴ Gram-scale experiments with various NHC salts ($\text{IPr}\text{-HCl}$, $\text{IMes}\text{-HCl}$, $\text{ICy}\text{-HCl}$, $\text{IPrMe}\text{-HCl}$, $\text{SIMes}\text{-HCl}$) demonstrated excellent results with 1 eq. of base. In order to shorten the reaction time, excess potassium carbonate (3 eq.) can be used. The desired gold complexes were obtained in high yields ((77–94%) (Table 1)).

The Cisneros group investigated the weak base route with the use of aqueous ammonia in order to obtain Cu–NHC complexes.³⁵ Despite the reaction proceeding under mild conditions, it has some drawbacks, for example, 6 eq. of NH_3 (aq.) are essential to reach full conversion. Also, the desired Cu–NHC complexes can be isolated from the aqueous solution only after

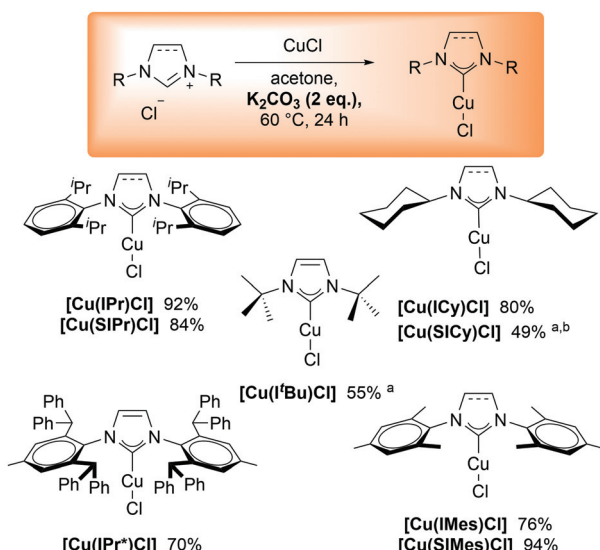
Table 1 Large-scale reactions

NHC·HCl (g)	Yield% (g)
IPr-HCl (21.7)	94 (29.8)
IMes-HCl (23.1)	87 (31.6)
ICy-HCl (3.0)	75 (3.9)
IPrMe-HCl (1.22)	77 (2.1)
SIMes-HCl (3.0)	79 (3.7)

numerous filtrations or extractions. Water appears cumbersome here as it is in numerous other workups. In addition, this route is not applicable to $\text{IAd}\text{-HCl}$ due to its higher pK_a value. So, the described synthetic procedure is restricted to NHC salts with lower pK_a values ($pK_a \approx 21$).

In order to find a more versatile approach to Cu–NHC complexes using milder bases, Cazin and co-workers investigated the weak base synthetic approach for copper–NHC complexes,³⁶ as simple access to such compounds would significantly streamline their use. Moreover, being in the same group, copper and gold were expected to both be amenable to such simple conditions.

However, the exploration of appropriate reaction conditions for the $[\text{Cu}(\text{IPr})\text{Cl}]$ complex revealed that 1 eq. of K_2CO_3 was not enough to reach full conversion (only 80% was achieved), while doubling the amount of the weak base allowed to isolate the desired compound in a 92% yield. In order to reduce the reaction time to 1 hour, 10 eq. of K_2CO_3 were employed. The weak base route with modified reaction conditions was tested on a large scope of Cu–NHC complexes, bearing both saturated and unsaturated NHC ligands. All the desired copper–NHC



Scheme 4 General synthetic procedure for $[\text{Cu}(\text{NHC})\text{Cl}]$ complexes using optimized conditions. Scope of obtained copper–NHC complexes. Reaction conditions: 1 eq. of NHC·HCl salt, 1 eq. of CuCl, 2 eq. of K_2CO_3 ,^a under Ar; ^b in CH_2Cl_2 .

complexes were obtained in moderate to high yields (Scheme 4).

Noteworthy is that the formation of side-products such as $[\text{Cu}(\text{NHC})_2]^+$ was never observed, in contrast with the free carbene route.³⁷ The described procedure allowed the isolation of the very bulky copper–IPr* complex without use of microwave irradiation as it was previously reported.³⁴ The use of the weak base approach improved the yield for the $[\text{Cu}(\text{ICy})\text{Cl}]$ complex from 70%³⁷ to 80%. The synthesis of $[\text{Cu}(\text{I}'\text{Bu})\text{Cl}]$ was carried out under inert atmosphere as it is known to be air- and moisture-sensitive.³⁷ It was revealed that $[\text{Cu}(\text{SICy})\text{Cl}]$ complex could not be obtained under batch conditions. The only reported procedure at that time included using of a continuous flow system.³⁸ As it was shown by the Cazin group, attempts to obtain the $[\text{Cu}(\text{SICy})\text{Cl}]$ complex from the appropriate NHC salt using the transmetalation route led to decomposition of the complex and concomitant formation of 1,3-dicyclohexylimidazolidin-2-one.¹² The copper complex bearing the SICy ligand was synthesized using the weak base approach in 49% yield. Under the optimized conditions, a mixture of the desirable $[\text{Cu}(\text{SICy})\text{Cl}]$ complex and 1,3-dicyclohexylimidazolidin-2-one was obtained. To avoid the formation of the by-product, DCM was used instead of acetone. The obtained results demonstrated the scalability and versatility of the weak base route both for gold- and copper–NHC complexes.

In order to gain insight into possible intermediates involved in this synthetic route, $[\text{Au}(\text{DMS})\text{Cl}]$ and IPr-HCl were stirred in acetone in the absence of base. The formation of a new compound was observed, an imidazolium aurate, which was isolated and fully characterized by ^1H , ^{13}C NMR and elemental analysis. Its formation in solution can be determined by the significant upfield shift of the imidazolium C2 proton in the ^1H -NMR spectrum. This shift is indicative of metallate

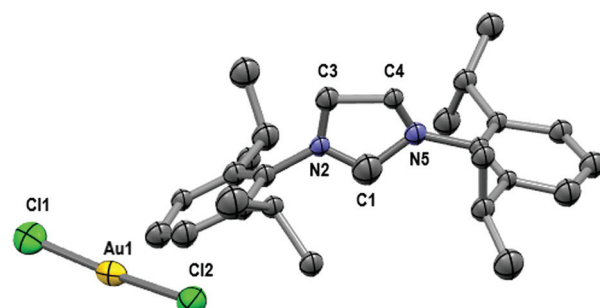


Fig. 1 Thermal ellipsoid representation of $[\text{IPrH}][\text{AuCl}_2]$ at 50% probability. A counterion $[\text{AuCl}_2]$ with a $\text{Cl}(1)\text{–Au}(1)\text{–Cl}(2)$ angle of $175.0(4)^\circ$.

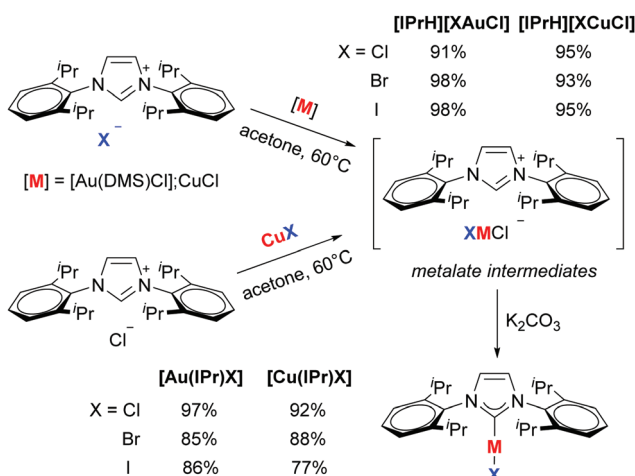
formation in most cases examined as part of the investigation of the weak base route. The structure of the intermediate was determined unequivocally using X-ray diffraction as $[\text{IPrH}][\text{AuCl}_2]$ (Fig. 1).²⁴

The same procedure was repeated for copper compounds: the reaction between CuCl and IPr-HCl salt without K_2CO_3 was carried out, and a product of similar structure $[\text{IPrH}][\text{CuCl}_2]$ was isolated.³⁶ The formation of both aurate and cuprate intermediates occurs at room temperature, while the desired metal–NHC complexes can be obtained by adding the corresponding amount of base to these.

The unusual structure of isolated intermediates prompted the authors to perform experiments with NHC salts containing various halides (Br, I, Cl). The authors investigated which halide would be included in the structures of intermediates and established the structures of the corresponding complexes in each case. Reactions of $[\text{Au}(\text{DMS})\text{Cl}]$ or CuCl with IPr-HBr, IPr-HI salts were carried out under the usual mild conditions. The desirable intermediates $[\text{IPrH}][\text{MClBr}]$ and $[\text{IPrH}][\text{MICl}]$ ($\text{M} = \text{Au}, \text{Cu}$) were isolated in high yields. The addition of 1 eq. of K_2CO_3 for gold compounds and 2 eq. of K_2CO_3 for copper compounds led to only one type of metal–NHC complex in each case. For copper complexes, the reactions between IPr-HCl and CuX ($X = \text{Br}, \text{I}$) were also explored, it was established that the same intermediates and Cu–IPr complexes were obtained (Scheme 5).

It is worth mentioning that a chloride-containing metal complex was never observed if IPr-HBr or IPr-HI was used. While the reaction between IPr-HBr and CuI was carried out, a new intermediate $[\text{IPrH}][\text{CuBrI}]$ was isolated in 94% yield. After the addition of potassium carbonate to this intermediate, only one copper complex $[\text{Cu}(\text{IPr})\text{I}]$ was obtained. We assumed that the trans effect of halides ($\text{I} \geq \text{Br} > \text{Cl}$) is the main reason for this observed phenomenon.³⁹

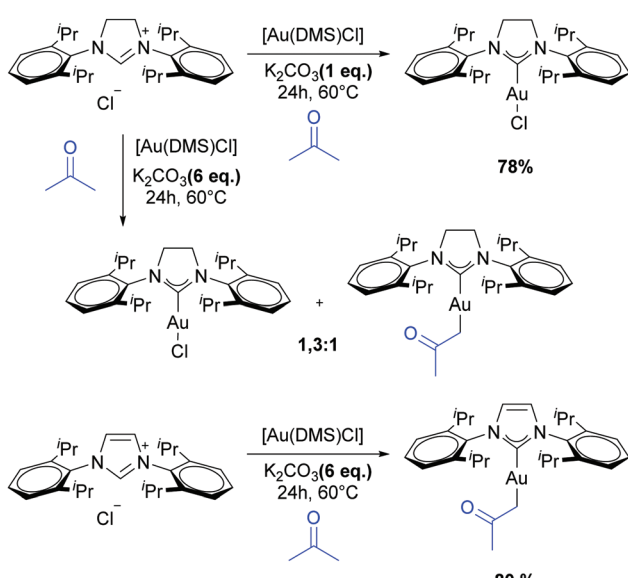
The Nolan group tested the described weak base approach on a large scope of different, both saturated and unsaturated NHC ligands. The influence of different NHC ligands on the reaction time was examined. For example, complexes $[\text{Au}(\text{IPr})\text{Cl}]$ and $[\text{Au}(\text{IMes})\text{Cl}]$ were obtained in 1 hour and 3 hours, respectively, whereas the corresponding saturated compounds $[\text{Au}(\text{SIPr})\text{Cl}]$ and $[\text{Au}(\text{SIMes})\text{Cl}]$ required 24 hours under the same reaction conditions. In order to decrease the



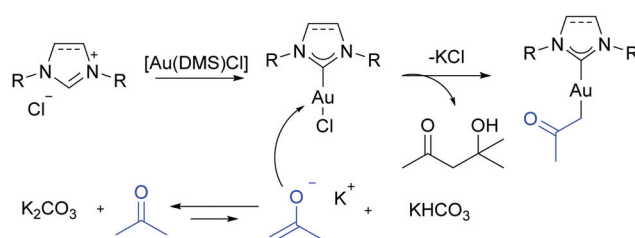
Scheme 5 Formation of $[\text{Au}(\text{IPr})\text{X}]$ and $[\text{Cu}(\text{IPr})\text{X}]$ complexes including intermediates $[\text{IPrH}][\text{XAuCl}]$ and $[\text{IPrH}][\text{XCuCl}]$.

reaction time for saturated NHC ligands, the same weak base approach using SIPr-HCl salt and $[\text{Au}(\text{DMS})\text{Cl}]$ with large excess (namely 6 equivalents) of potassium carbonate was tested.⁴⁰ Unexpectedly, a mixture of two different complexes, the desirable $[\text{Au}(\text{SIPr})\text{Cl}]$ and a new $[\text{Au}(\text{SIPr})(\text{CH}_2\text{COCH}_3)]$ was obtained in 1.3:1 ratio. The same reaction using unsaturated NHC salts led exclusively to the acetonyl compounds. Full conversion in the reaction between IPr-HCl salt and $[\text{Au}(\text{DMS})\text{Cl}]$ was obtained in 48 hours and the product $[\text{Au}(\text{IPr})(\text{CH}_2\text{COCH}_3)]$ was isolated in 80% yield (Scheme 6).

The authors suggested the following reaction mechanism (Scheme 7): the base, being in large excess, assists in the deprotonation/metallation of both the NHC salt and acetone, producing $[\text{Au}(\text{NHC})\text{Cl}]$ and generating an enolate. The latter reacts with the soft electrophilic gold center, leading to the acetonyl complex and releasing potassium chloride.



Scheme 6 The formation of acetonyl complexes.

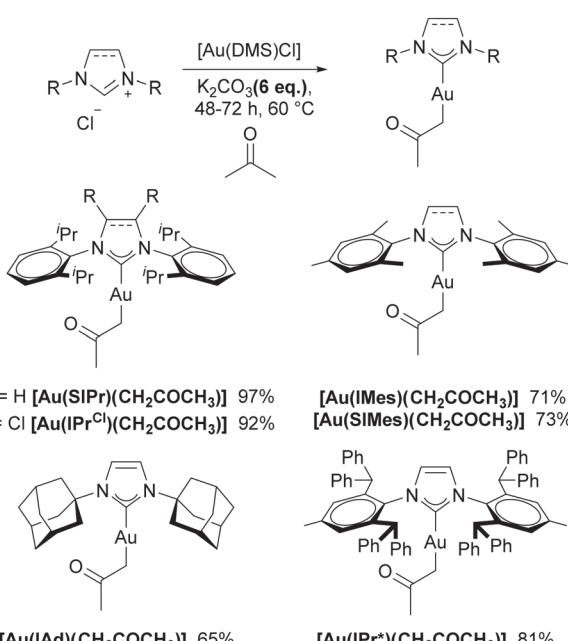


Scheme 7 The proposed mechanism of the acetonyl complex formation.

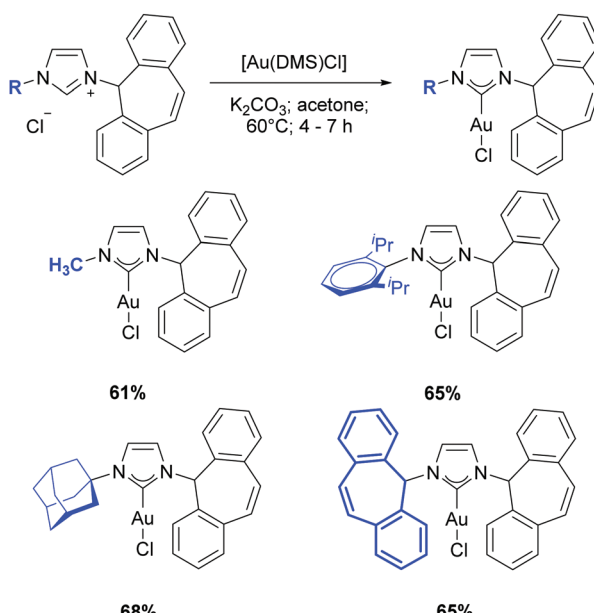
4-Hydroxy-4-methyl-2-pentanone, which is the product of aldol condensation of acetone in the presence of base, was found to be a side-product under these conditions, which supports the proposed mechanism.

This approach was proven to be efficient for various NHC ligands, namely IMes, SIMes, IPr, SIPr, IPr*, IAd. All complexes with the common structure $[\text{Au}(\text{NHC})(\text{CH}_2\text{COCH}_3)]$ were isolated in good to high yields (65–97%) (Scheme 8). Moreover, $[\text{Au}(\text{IPr})(\text{acetonyl})]$ complex showed high activity for the hydration of alkynes and intramolecular rearrangement/hydroarylation of propargylic acetates.³⁸ Importantly, the potential of these compounds as organometallic synthons for the installation of various molecular fragments on NHC-ligated gold was also demonstrated.

Our group also investigated the versatility of the weak base approach to unsymmetrical NHC ligands bearing bulky dibenzotropyliidene (Trop) as one of substituents on nitrogen.⁴¹ The free carbene route is not applicable for this type of ligands because of difficulties associated with the free carbene isolation. Rapid rearrangement occurs due to reaction between the carbene lone pair and the double bond of the dibenzotropyliidene ring.⁴² We reported a new synthetic approach for these



Scheme 8 Scope of $[\text{Au}(\text{NHC})(\text{acetonyl})]$ complexes.



Scheme 9 Synthesis of Trop-NHC Au(i)-complexes.

compounds, by the use of a weak base and technical grade acetone at 60 °C.⁴¹ It is worth mentioning that the weak base route is also applicable to the synthesis of gold complexes based on dibenzotropylidene-functionalized NHC ligands (Scheme 9).

Due to the growing interest in homogeneous gold catalysis, gold complexes in the higher oxidation state III were also investigated. The high redox potential of gold makes gold(III) compounds oftentimes tend to be reduced into gold(I) or gold(0) complexes.⁴³ Despite the facile synthesis of $[\text{Au}(\text{NHC})\text{X}_3]$ ($\text{X} = \text{Cl}, \text{Br}$) complexes, these were found to be photolytically unstable. Cationic gold(I)-bis(NHC) complexes then attracted attention due to the higher stability provided by the presence of a second NHC ligand. These compounds were then thought to be suitable precursors to obtain stable Au(III)-bisNHC complexes. The most frequently encountered synthetic approaches to Au(I)-bisNHC are the transmetalation and free carbene routes.^{44,45} Inspired by previous results and proven efficiency of the weak base route, we explored the applicability of this approach to Au-bis(NHC) complexes.⁴⁶ $[\text{Au}(\text{IPr})\text{Cl}]$ in the presence of $\text{IPr}\text{-HBF}_4$ and 2 eq. of K_2CO_3 was transformed to the desirable homoleptic gold complex $[\text{Au}(\text{IPr})_2]\text{[BF}_4]$. The investigation of the scope for this reaction showed applicability of this procedure for both saturated and unsaturated NHC ligands of different steric and electronic properties to obtain heteroleptic complexes. Moreover, different counterions were tested to prove the versatility of the method (Table 2).

The reaction between $[\text{Au}(\text{IPr})\text{Cl}]$ and $\text{SIMes}\text{-HBF}_4$ requires longer reaction times in comparison with other complexes. It was mentioned above that for $[\text{Au}(\text{NHC})\text{Cl}]$ complexes bearing saturated NHC the reaction proceeds more slowly compared to their unsaturated counterparts. Moreover, full conversion has not been reached even in six days. However, a modified strategy

Table 2 Application of weak base route to the synthesis of gold–bis(NHC) complexes, bearing NHC ligands with various electronic and steric properties

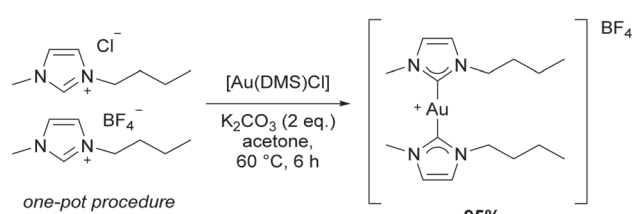
Au-bis(NHC) complex	Yields (%)
$[\text{Au}(\text{IPr})_2]\text{[BF}_4]$	95
$[\text{Au}(\text{IPr})(\text{IMes})]\text{[BF}_4]$	52
$[\text{Au}(\text{IPr})(\text{SIMes})]\text{[BF}_4]$	98 ^a
$[\text{Au}(\text{IPr})(\text{i'Bu})]\text{[BF}_4]$	82
$[\text{Au}(\text{IPr})(\text{ICy})]\text{[BF}_4]$	73
$[\text{Au}(\text{IPr})(\text{BMIM})]\text{[BF}_4]$	96
$[\text{Au}(\text{IPr})(\text{BMIM})]\text{[PF}_6]$	79
$[\text{Au}(\text{IPr})(\text{BMIM})]\text{[Cl]}$	62

^a $[\text{Au}(\text{SIMes})\text{Cl}]$ as a precursor, $\text{IPr}\text{-HCl}$, in the presence of K_2CO_3 .

was implemented for that compound. Using $[\text{Au}(\text{SIMes})\text{Cl}]$ and $\text{IPr}\text{-HBF}_4$ for the synthesis of $[\text{Au}(\text{IPr})(\text{SIMes})]\text{[BF}_4]$ complex proved successful. Full conversion was reached in 72 hours and the desired compound was isolated in excellent yield.⁴⁶

Two small NHC ligands on gold are favourable for oxidation reactions in gold(I)/gold(III) catalytic processes. The gold-bis(NHC) complex containing two small and flexible BMIM ligands was synthesized by our group. With the same procedure starting from $[\text{Au}(\text{BMIM})\text{Cl}]$ and $\text{BMIM}\text{-HBF}_4$, a mixture of various complexes was obtained, but $[\text{Au}(\text{BMIM})_2]\text{[BF}_4]$ could not be isolated. Nevertheless, the one-pot modification of the reaction starting from $[\text{Au}(\text{DMS})\text{Cl}]$ and mixture of BMIM salts led exclusively to the desired gold complex in high yield (Scheme 10).⁴⁶

In addition, the reaction of the synthesized gold complexes with hypervalent iodine in order to obtain the corresponding Au(III) compounds were explored, which is an important step in gold redox catalysis.⁴⁶ Further investigations of steric and electronic effects of NHC ligands were carried out. Small and more electron donating NHC ligands were found to be more desirable for the gold(I) center. The weak base approach was proven to be effective for the synthesis of Au(I)-bis(NHC) complexes both homo- and heteroleptic, bearing NHC ligands possessing various electronic and steric properties. The discussed weak base route was also proven to be efficient in the synthesis of dinuclear NHC–Au complexes.⁴⁷

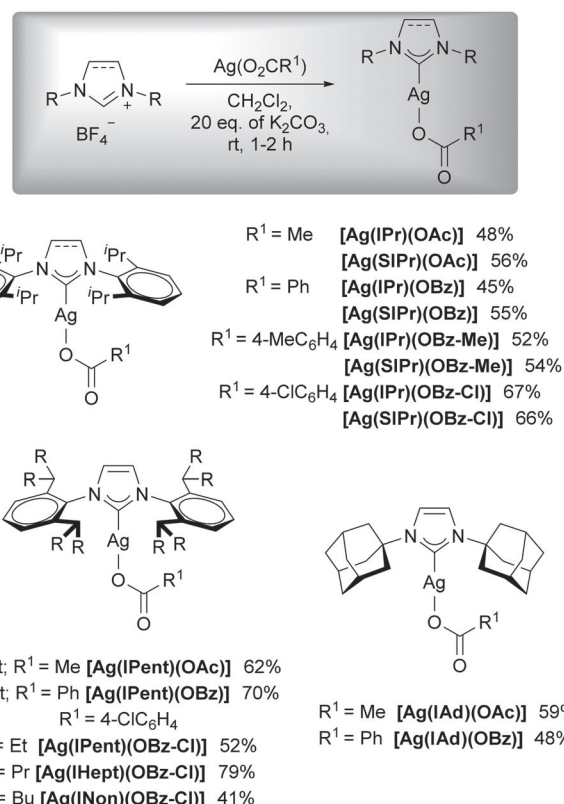
Scheme 10 One-pot procedure of the synthesis of $[\text{Au}(\text{BMIM})_2]\text{[BF}_4]$.

Another highly important metal in NHC chemistry is silver. It is worth mentioning that Ag–NHC complexes are highly valued in medicinal chemistry due to their anticancer and antimicrobial properties,^{28,48,49} but applications of Ag–NHC complexes in catalytic reactions remains relatively rare.^{1,50,51} The main reason for this can be the weakest M–C bond in Ag–NHC complexes among other metals in Group 11.⁵² The ability of $[\text{Ag}(\text{NHC})\text{X}]$ complexes to form bis-Ag (NHC) complexes of the formula $[\text{Ag}(\text{NHC})_2][\text{X}]$ in solution, is widely used in organometallic chemistry.⁵³ The described tendency has allowed Ag–NHC complexes to be employed as carbene-transfer reagents for the transmetallation route. Nowadays researchers are particularly interested in catalysts based on cheaper metals, such as silver. These catalysts can be used to facilitate the intermolecular addition of N–H and O–H bonds to alkynes to yield substituted oxazolines.^{54–56} Another significant application of silver complexes is in enantioselective transformations such as the aldol-type condensation, Mannich reactions, Michael reactions, 1,3-dipolar cycloadditions, among others.⁵⁷ In addition, Ag–NHC complexes are widely used as NHC transfer agents to copper, Cu–NHC complexes are essential catalysts for a large number of reactions.⁵⁸ This use is intriguing in view of the more efficient and direct route disclosed by Cazin.¹²

It was established that complexes such as $[\text{Ag}(\text{NHC})\text{Cl}]$ ($\text{NHC} = \text{IPr}$, SIMes), $[\text{Ag}(\text{IPr})_2]\text{PF}_6$ and $[\text{Ag}(\text{SIPr})(\text{OTf})]$ are inefficient as catalysts in cyclisation reactions involving propargylic-amide oxazoline derivatives.⁵⁹ In attempts to find active silver catalysts, the Nolan and Hii groups investigated the activity of $[\text{Ag}(\text{NHC})(\text{O}_2\text{CR})]$ complexes.⁵⁹ There are several independent sites in the structures of Ag–NHC carboxylate complexes that assist in optimizing catalytic activity. In order to accommodate steric and electronic properties of a potential catalyst, the degree of saturation in the NHC ligand that modifies σ donation properties can be changed. Bulky N -substituents also influence the properties of NHC ligands, as they prevent catalyst decomposition. The carboxylate ligand itself stabilizes these complexes and makes them more reactive, as the dissociation rate is higher for Ag-carboxylates than for Ag-halides.⁵⁹

Usually there are two possible approaches for the synthesis of Ag–NHC carboxylate compounds. The first one includes reaction between a Ag-carboxylate and the corresponding $[\text{Ag}(\text{NHC})\text{X}]$ ($\text{X} = \text{Cl}, \text{Br}, \text{I}$) complex.⁶⁰ According to the second approach, the NHC precursor salt and 2 eq. of $\text{Ag}(\text{O}_2\text{CR})$ are used in the reaction.⁶¹ Notably, these approaches have disadvantages, as AgX is generated during these reactions and also an excess of silver carboxylate is required. Both factors render the isolation of the desired compound difficult.

To overcome the described difficulties, the Hii group tested the weak base approach with previously described reaction conditions on silver–NHC compounds.⁵⁹ This synthetic procedure was adapted to a series of $[\text{Ag}(\text{NHC})(\text{O}_2\text{CR}^1)]$ complexes, bearing various saturated and unsaturated NHC ligands (IPr, IPent, IHept, INon, IAd, SIPr) and diverse substituents on the carboxylate fragment (Me or substituted Ph).



Scheme 11 Scope of silver–NHC carboxylate complexes $[\text{Ag}(\text{NHC})(\text{O}_2\text{CR}^1)]$.

The authors underlined that the key to success is the use of $\text{NHC}\cdot\text{HBF}_4$ instead of $\text{NHC}\cdot\text{HX}$ ($\text{X} = \text{Cl}, \text{Br}, \text{I}$) salts. The desired compounds were obtained in moderate to good yields (41–79%) (Scheme 11).

To obtain acetate complexes ($\text{R}^1 = \text{Me}$), an excess (namely 20 eq.) of potassium carbonate is essential.⁵⁹ The reason for using a large excess of the base is to prevent the formation of homoleptic Ag–NHC complexes $[\text{Ag}(\text{NHC})_2][\text{X}]$. This amount of K_2CO_3 is enough to assist in the deprotonation of the generated acetic acid and to form the counterion. The catalytic activity of these silver–NHC complexes was tested in the cyclisation of propargylic amides. Compared with the Ag–pyridyl complexes,⁵⁶ NHC Ag–carboxylate catalysts proved efficient for amides with electron-deficient substituents. Thus, the weak base route proved to be an efficient, scalable and versatile approach towards the synthesis of these coinage metal–NHC complexes as well.

The application of the weak base route to palladium– and platinum–NHC complexes

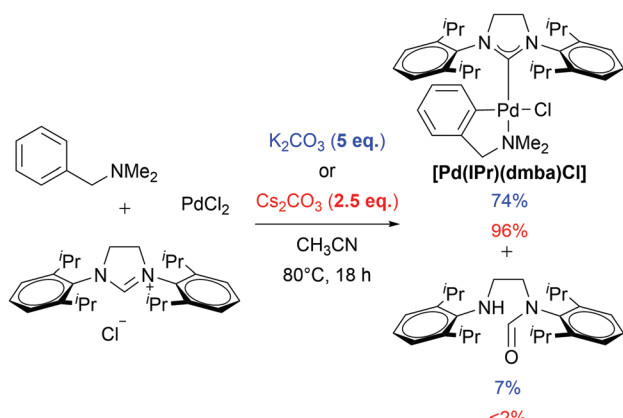
Pd–NHC complexes have been widely explored during the last decades and ubiquitously used in catalytic chemistry, especially in cross-coupling reactions.^{62–64} Complexes of the type $[\text{Pd}(\text{NHC})(\eta^3\text{-R-allyl})\text{Cl}]$ ($\text{R-allyl} = \text{allyl, methyl allyl, cinnamyl}$,

indenyl) revealed to be useful pre-catalysts in reactions generating C–C and carbon–heteroatom bonds.^{65–68} The most widespread approach to the synthesis of Pd–NHC complexes is using of a strong base in order to generate a free carbene, followed by the addition of Pd precursors, for example dimers such as $[\text{Pd}(\eta^3\text{-allyl})(\mu\text{-Cl})_2]$ or $[\text{Pd}(\eta^3\text{-cin})(\mu\text{-Cl})_2]$.^{5,9} Another approach, making use of a “built-in” base, does not require inert conditions, nevertheless high temperatures and 1,4-dioxane as a solvent are essential.⁶⁹ Taking into consideration the previously described disadvantages of the free carbene route, the development of more facile and cost-effective approach was highly desirable.

Ying and co-workers reported a one-pot procedure for the synthesis of palladacycle NHC complexes using a weak base.^{70–72} Although the described procedure allowed the synthesis of the desired palladacycle NHC compounds, bearing unsaturated NHC ligands in high yields, it required high temperatures and a toxic solvent (Scheme 12).

The same approach was also implemented for complexes with saturated NHC ligands.⁷¹ In the reaction of the commercially available SiPr-HCl salt, PdCl_2 , N,N -dimethylbenzylamine and 5 eq. of K_2CO_3 , the desired complex $[\text{Pd}(\text{SiPr})(\text{dmbo})\text{Cl}]$ was observed, with the concurrent formation of several other compounds. These side-products were unreacted NHC precursor salt and N,N' -bis(2,6-diisopropylphenyl)- N -formylethylenediamine, which is the ring opened product of the carbene precursor (Scheme 13).

The formation of by-product can be explained by lower acidity of saturated NHC salts in comparison to the unsaturated



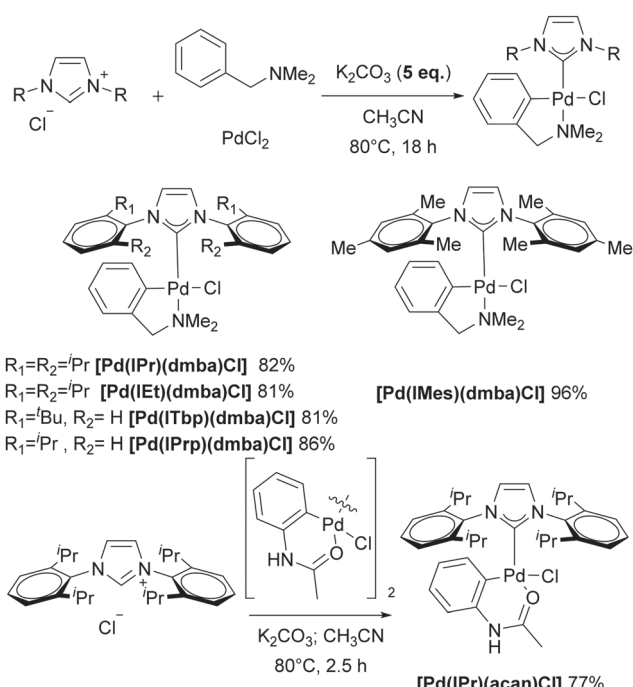
Scheme 13 The synthesis of palladacycle NHC complexes, bearing saturated NHC ligands.

counterparts and a tendency of saturated salts to hydrolyse. Using the more expensive Cs_2CO_3 instead of K_2CO_3 decreases the amount of by-product to appropriate level.

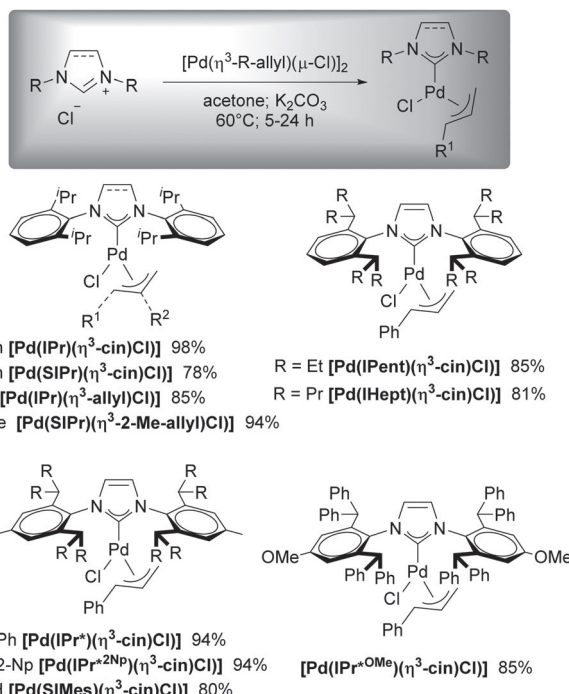
As it was previously discussed, our groups successfully established the weak base approach for Cu- and Au–NHC complexes. The experimental data revealed the existence of similar intermediates in both cases. In attempts to probe if the existence of such an intermediate, which is an “ate” complex, was more widespread than expected, Zinser *et al.* obtained a series of Pd–NHC complexes using the same reaction conditions as for the Cu- and Au–NHC compounds.^{73,74}

The palladium dimers $[\text{Pd}(\eta^3\text{-allyl})(\mu\text{-Cl})_2]$, $[\text{Pd}(\eta^3\text{-cin})(\mu\text{-Cl})_2]$ ^{73,74} and $[\text{Pd}(\eta^3\text{-2-Me-allyl})(\mu\text{-Cl})_2]$ ⁷⁴ were reacted with various saturated and unsaturated NHC salts in acetone in the presence of K_2CO_3 . While common NHC salts reacted well when simple heating of mixture in acetone at 60 °C for 5 hours, bulkier NHC ligands (namely IPr*, IPr*^{OMe}, IPr*^{2-Np}, IPent, IHep) required a modified procedure. The mixture of the corresponding NHC salt and palladium dimer in acetone was heated at 60 °C for 1 hour, to initially form the “ate” complex, then K_2CO_3 was added and the mixture was stirred for 24 hours. All the desired Pd–NHC complexes were obtained in good to excellent yields (78–98%) in this manner (Scheme 14).

The optimization of reaction conditions on the example of IPr complex revealed that 2.4:1 ratio for IPr-HCl and $[\text{Pd}(\eta^3\text{-cin})(\mu\text{-Cl})_2]$ was optimal to reach full conversion. Of note, while increasing the amount of the base leads to a decrease in reaction time, the amount of by-products however increases. Two equivalents of K_2CO_3 are enough to obtain $[\text{Pd}(\text{IPr})(\eta^3\text{-cin})\text{Cl}]$ in excellent yield (98%). The obtained results demonstrated the correlation between steric bulk of the NHC ligands and reaction conditions (time and the equivalents of a base) which are required for the formation of products and intermediates. The generation of Pd–NHC complexes, containing bulky ligands such as IPr*, IPr*^{OMe}, IPr*^{2-Np}, IPent and IHep, requires longer reaction time (namely 24 hours in comparison to less bulky ligands needing only 5 hours) and substantial excess of the weak base (4 eq.).⁷³



Scheme 12 Weak base route for the synthesis of palladacycle NHC complexes, bearing unsaturated NHC ligands.



Scheme 14 General synthetic procedure for $[\text{Pd}(\text{NHC})(\eta^3\text{-R'-allyl})\text{Cl}]$ complexes using optimized conditions. Scope of obtained palladium–NHC complexes.

The scalability of the weak base route for the synthesis of such complexes was demonstrated in the case of $[\text{Pd}(\text{IPr})(\eta^3\text{-cin})\text{Cl}]$, $[\text{Pd}(\text{IPr})(\eta^3\text{-allyl})\text{Cl}]$ and $[\text{Pd}(\text{IPr}^*)(\eta^3\text{-cin})\text{Cl}]$. The desired compounds were obtained in excellent yields of 97%, 92% and 98%, respectively, on gram-scale reactions without any modification of the smaller-scale reaction conditions.⁷³

To establish the structure of the palladate intermediate in the reaction between $\text{IPr}\text{-HCl}$ and $[\text{Pd}(\eta^3\text{-cin})(\mu\text{-Cl})]_2$, the reaction was carried out without the addition of K_2CO_3 .⁷³ A new compound was isolated and characterized by NMR spectroscopy and elemental analysis. The structure of the intermediate was determined using X-ray diffraction as $[\text{IPrH}][\text{Pd}(\eta^3\text{-cin})\text{Cl}_2]$ (Fig. 2).

The interaction between the most acidic proton of the imidazolium salt (H1) and both chloride atoms of the palladate counterion was observed. This stabilizing interaction hints at the formation of a strong ion-pair in the solid state, while it also prevents the palladate intermediate from decomposing. Reactions without the addition of base, in order to isolate palladates $[\text{IPrH}][\text{Pd}(\eta^3\text{-allyl})\text{Cl}_2]$, $[\text{IPr}^*\text{H}][\text{Pd}(\eta^3\text{-cin})\text{Cl}_2]$ and $[\text{SIPrH}][\text{Pd}(\eta^3\text{-cin})\text{Cl}_2]$, were also carried out. The desired compounds were obtained in almost quantitative yields. The formation of Pd–NHC complexes including the formation of intermediates is illustrated in Scheme 15.

It is worth noting that the obtained palladate intermediates are air- and moisture-stable, and these properties render them potentially valuable pre-catalysts. The use of inorganic bases in the Suzuki–Miyaura reaction in the presence of Pd–NHC complexes was previously reported.⁷⁵ Zinser *et al.* investigated

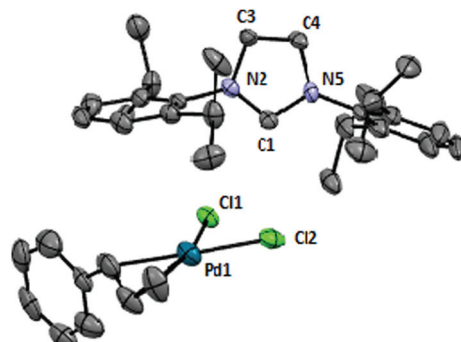
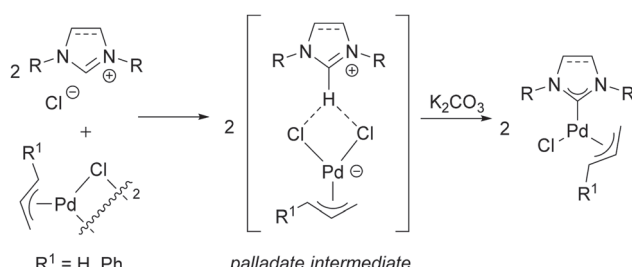
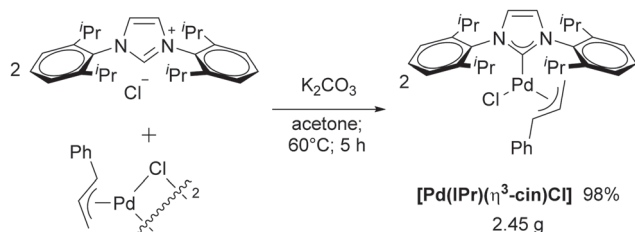


Fig. 2 Thermal ellipsoid representation of $[\text{IPrH}][\text{Pd}(\eta^3\text{-cin})\text{Cl}_2]$ at 50% probability.

the possibility of using potassium carbonate as a multi-functional component in this catalytic reaction. The palladate intermediates $[\text{IPrH}][\text{Pd}(\eta^3\text{-allyl})\text{Cl}_2]$, $[\text{IPr}^*\text{H}][\text{Pd}(\eta^3\text{-cin})\text{Cl}_2]$ and $[\text{IPrH}][\text{Pd}(\eta^3\text{-cin})\text{Cl}_2]$ were tested as pre-catalysts. The catalytic results were compared with that using well-defined Pd–NHC complexes such as $[\text{Pd}(\text{IPr})(\eta^3\text{-cin})\text{Cl}]$, $[\text{Pd}(\text{IPr})(\eta^3\text{-allyl})\text{Cl}]$ and $[\text{Pd}(\text{IPr}^*)(\eta^3\text{-cin})\text{Cl}]$. Two different reaction conditions were tested and palladates were inactive in both cases. The authors suggested that palladates should be converted into neutral Pd–NHC complexes prior to addition of the cross-coupling partners (phenylboronic acid and 4-chloroanisole). To activate the palladates, these were added into the reaction with 1.1 eq. of K_2CO_3 and then stirred in ethanol at 60 °C for 1 hour, after that time, phenylboronic acid and 4-chloroanisole were added and the mixture was stirred without heating for 20 hours. The modification of reaction conditions helped to obtain the desired cross-coupling product in high yield.⁷³ It is interesting that no reaction was observed while using NHC salts and palladium dimers, for example $[\text{Pd}(\eta^3\text{-cin})\text{Cl}]_2$. This highlights the importance of using pre-formed, well defined palladates, as this ensures the formation of the desired Pd–NHC complexes under the reaction conditions. When the activation time was changed from 1 hour to 30 minutes, lower yields for $[\text{IPrH}][\text{Pd}(\eta^3\text{-allyl})\text{Cl}_2]$ and $[\text{IPrH}][\text{Pd}(\eta^3\text{-cin})\text{Cl}_2]$ were observed. It was found that the steric bulk of the NHC ligand affects the activation step. $[\text{IPrH}][\text{Pd}(\eta^3\text{-cin})\text{Cl}_2]$ was also tested as a pre-catalyst in the Suzuki–Miyaura reaction with various coupling partners, among them were 2-chloropyridine, 2-bromopyrimidine and 2-chloro-6-trifluoromethylpyridine. All the desired



Scheme 15 General synthetic procedure for Pd–NHC complexes, including the formation of intermediate.

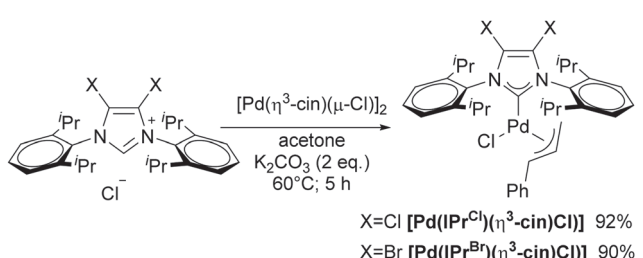
Scheme 16 Large-scale synthesis of $[Pd(IPr)(\eta^3\text{-cin})Cl]$.

compounds were obtained in high yields (85–99%). The applicability of the described palladates was also shown for the Mizoroki–Heck,^{73,74} the Buchwald–Hartwig arylamination and ketone arylation reactions.⁷⁶ The scalability of the weak base approach was also showcased. The reaction between IPr-HCl and the Pd source $[Pd(\eta^3\text{-cin})(\mu\text{-Cl})_2]$ with K_2CO_3 was carried out. The desired Pd–NHC complex was isolated in excellent yield (98%) (Scheme 16).⁷⁷

Hazari and co-workers investigated the activity of various Pd–NHC complexes in the Suzuki–Miyaura cross-coupling.⁷⁸ The obtained data showed the influence of allyl group substitution on the conversion of neutral Pd–NHC complex to Pd(i) allyl dimer.^{79,80}

The substitution of the backbone of the NHC ligands provides an opportunity to modify the electronic and steric properties of these ligands and the corresponding NHC–metal complexes and thus affect the catalytic activity.^{81–83} The catalytic activity of Pd–NHC complexes, containing IPr^{Cl} and IPr^{Br} ligands has been explored in the Suzuki–Miyaura cross-coupling reaction and compared to that of $[Pd(IPr)(\eta^3\text{-cin})Cl]$.⁸⁴ Both palladium compounds, bearing halogen substituents in the C^{4,5} – positions of imidazol-2-ylidene ring were obtained using the weak base route in high yields (Scheme 17).

In 2006, Organ and co-workers reported the air-stable palladium “PEPPSI” (PEPPSI = pyridine-enhanced precatalyst preparation, stabilisation and initiation) pre-catalysts.²⁰ The catalytic activity of the described complexes was tested in a large variety of cross-coupling reactions, including the Suzuki–Miyaura, Negishi, and Kumada–Tamao–Corriu reactions as well as in various carbon–heteroatom coupling reactions.^{5,85,86} The simple synthetic procedure leading to their isolation by action of a weak base is one of the most significant advantages of these complexes. Using potassium carbonate, various NHC salts, $PdCl_2$ and pyridine (or its derivatives), the desired PEPPSI

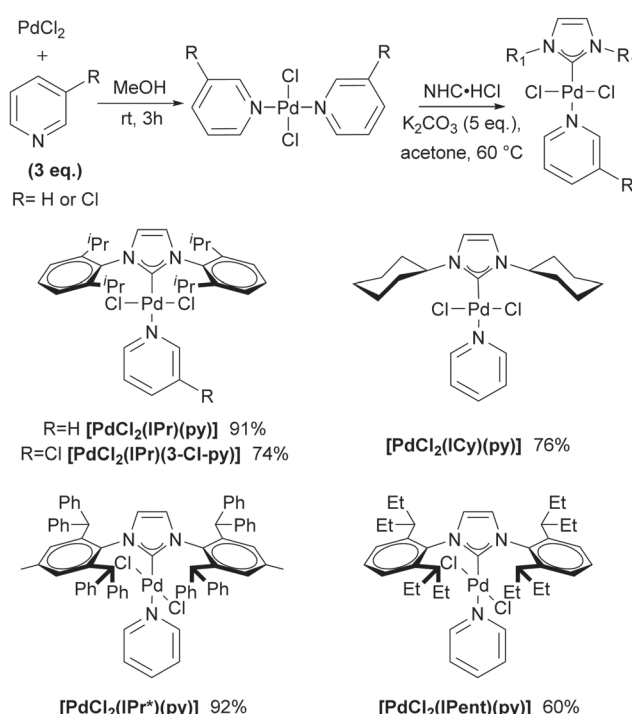
Scheme 17 General synthetic procedure for $[Pd(IPr^X)(\eta^3\text{-cin})Cl]$ complexes using optimized conditions.

complexes were obtained in high yields. Pyridine is used both as a solvent, and as a ligand in this procedure, therefore a large excess of pyridine is required. Of note, the use of high temperatures ($80^\circ C$) also proves essential.

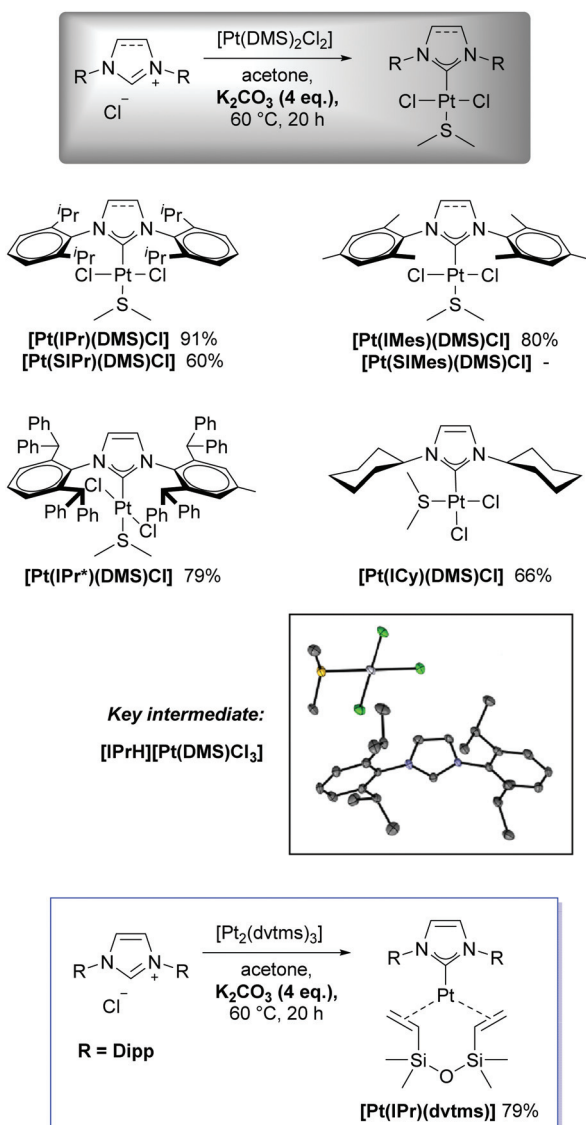
While attempting to understand the mechanism of formation at play in Organ’s synthetic procedure, Nolan and co-workers made use of the weak base route to obtain PEPPSI-type compounds. In a simpler and more environmentally benign approach, only 3 eq. of pyridine were used, high temperature was not essential, and acetone was used as the solvent.⁸⁷ The modified procedure was tested for various NHC ligands (IPr, IPr^* , ICy, IPent), and all the desired compounds were obtained in good to high yields (Scheme 18). Two intermediates were isolated and investigated, which shed light on the mechanism of the reaction and confirmed that 3 eq. of pyridine are enough to obtain the desired Pd–PEPPSI complexes.

As a continuation of the previous work regarding the development of general and robust synthetic methodologies towards transition metal–NHC complexes, Nolan and co-workers performed the first systematic study in the case of platinum.⁸⁸ This provided a new method for accessing a variety of well-defined Pt–NHC complexes that are active in the hydrosilylation of alkenes and alkynes, a field in which Pt–NHC complexes hold a prominent position.^{89,90}

Despite the existence of sporadic reports mentioning the use of a weak base in order to generate Pt–NHC complexes, this proves to be the first general and in-depth investigation (Scheme 19) of such a route in platinum systems.^{91–93} The development of the new methodology was enabled by the use of the platinum source $[Pt(DMS)_2Cl_2]$ in the presence



Scheme 18 General synthetic procedure for PEPPSI-type compounds.



Scheme 19 General synthetic procedure for Pt–NHC complexes using optimized conditions.

of an imidazolium salt and potassium carbonate in acetone, which was a system that had proven successful in past studies focusing on gold, copper and palladium. IPr-HCl was used in order to obtain proof of concept and optimize the reaction conditions. It was found that ethyl acetate is also a suitable, green solvent in which this reaction can be carried out. A profound effect of the base amount on the rate of the reaction was also found, while the carbonate base proved to be far more efficient than triethylamine in the case of platinum. The protocol was applied for a variety of imidazol(in)ium salts and led to satisfactory yields for the new complexes (Scheme 19). Structural investigation of the complexes revealed that only in $[\text{Pt}(\text{ICy})(\text{DMS})\text{Cl}_2]$, which bears the least sterically demanding NHC, the chloride anions are mutually *cis*. Limitations of the protocol were also encountered, as PEPPSI-type and DMSO-coordinated platinum complexes could not be obtained under these conditions when suitable platinum sources were

used. Furthermore, SIMes-HCl and IAd-HCl did not react under the operational conditions.

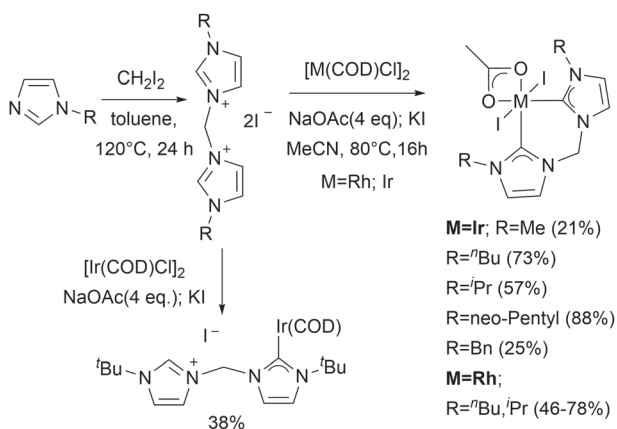
Importantly, when the reaction was carried out in the absence of base with IPr-HCl, an imidazolium platinate was observed and isolated as a key intermediate (Scheme 19).⁸⁸ Its molecular structure was unequivocally determined by single crystal X-ray diffraction analysis, and it is reminiscent of the aurate, cuprate and palladate salts reported previously. In the presence of a base, this intermediate is transformed into the desired Pt–NHC complex. Finally, the versatility of the weak base approach was demonstrated, when a Pt(0)–NHC complex was synthesized in 79% yield, using the standard conditions and Karstedt's catalyst as the platinum source (Scheme 19).

The application of the weak base route to the synthesis of rhodium and iridium–NHC complexes

The catalytic applications of Rh and Ir–NHC complexes were widely explored. These compounds proved to be efficient catalysts in numerous reactions, such as in the borylation of arenes, the hydrogenation of ketones, imines and olefins, the isomerization of allylic alcohols to ketones and the hydrosilylation of ketones.^{94–99} An important application of $[\text{M}(\text{NHC})(\text{CO})_2\text{Cl}]$ complexes ($\text{M} = \text{Rh}$ or Ir) is for the measurement of the Tolman Electronic Parameter (TEP) for novel ligands.^{83,100,101} The use of these compounds for that purpose is a good alternative to previously used $[\text{Ni}(\text{NHC})(\text{CO})_3]$ complexes.

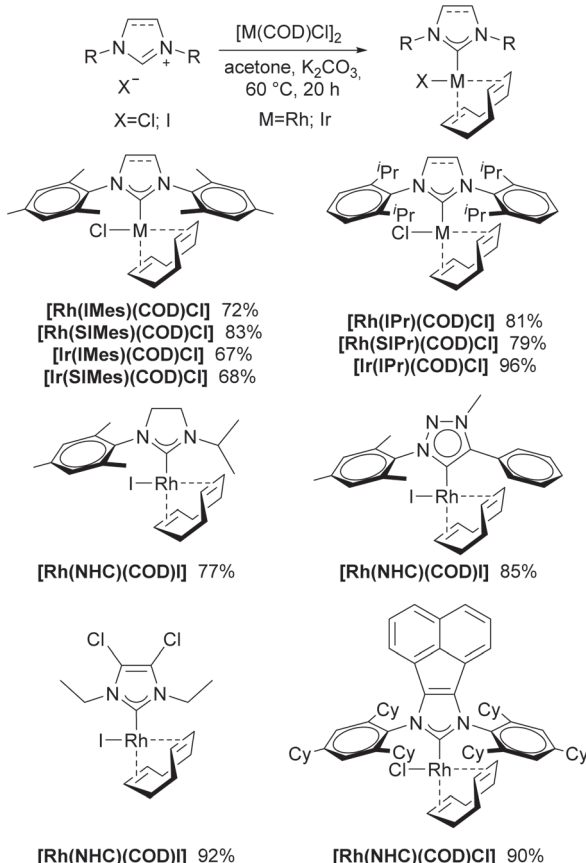
Early examples of using a mild base (NaOAc) to obtain Rh and Ir–NHC complexes were explored by Crabtree and Peris.^{18,19} In this manner, a series of bidentate NHC compounds were obtained, containing various NHC ligands. The influence of steric properties of NHC ligands was demonstrated. On the example of bulky ^tBu substituents, using the same reaction conditions, the possibility of isolating only one NHC complex $[\text{Ir}(\text{COD})(\text{NHC})\text{I}]$ ($\text{COD} = 1,5\text{-cyclooctadiene}$) was shown (Scheme 20). The addition of various bases (K_2CO_3 , NaOAc , KO^+Bu) or prolongation of the reaction time did not lead to formation of the chelated bis-NHC complex.¹⁸ The described procedures require refluxing for 16 hours in acetonitrile, the addition of 4 eq. of NaOAc and purification by column chromatography. The desired complexes were isolated in moderate to good yields, and the obtained compounds are air- and moisture-stable (Scheme 20).

Inspired by the work of Gimeno, the group of Plenio investigated the use of a simple and user-friendly procedure for the synthesis of $[\text{M}(\text{NHC})(\text{COD})\text{Cl}]$ and $[\text{M}(\text{NHC})(\text{CO})_2\text{Cl}]$ ($\text{M} = \text{Rh}$ or Ir) complexes.¹⁰² The procedure involves the use of potassium carbonate as a base and acetone or DCM as a solvent. Various NHC precursor salts, bearing both saturated and unsaturated backbones, were examined in the reaction with $[\text{Rh}(\text{COD})\text{Cl}]_2$ as the metal source in the presence of K_2CO_3 in acetone. All the desired complexes were isolated in high yields (Scheme 21). It is worth mentioning that more than

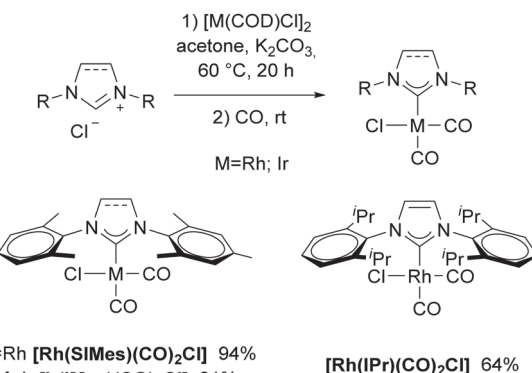


Scheme 20 General synthetic procedure for the synthesis of bidentate Rh and Ir-NHC complexes.

90% of conversion was observed for the described compounds, but lower isolated yields were obtained in some cases. Then experiments with $[\text{Ir}(\text{COD})\text{Cl}]_2$ as a metal source under the same reaction conditions were also carried out and lead to Ir-NHC complexes containing unsaturated ligands in high yields. Here, for saturated NHCs, the base amount was found to be the most important parameter. In those cases, 1.2 eq. of K_2CO_3



Scheme 21 General synthetic procedure for the synthesis of $[\text{M}(\text{NHC})(\text{COD})\text{Cl}]$ ($\text{M} = \text{Rh}$ or Ir) complexes.



Scheme 22 One-pot procedure for $[\text{M}(\text{NHC})(\text{CO})_2\text{Cl}]$ complexes.

were required in comparison to 3 eq. for Rh-NHC compounds. Various NHC-HX ($\text{X} = \text{Cl}$, I) salts were also tested. The formation of only one complex $[\text{M}(\text{NHC})(\text{COD})\text{X}]$, containing either Cl or I, depending on the counterion of the corresponding imidazolium salt was observed (Scheme 21).

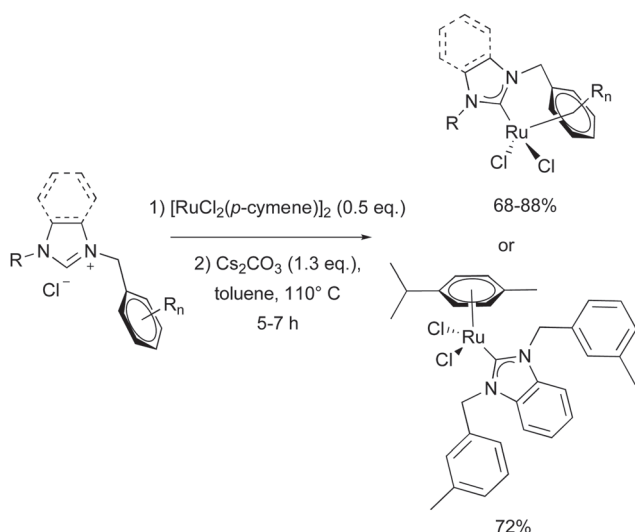
According to mechanistic investigations performed with SIMes-HCl and K_2CO_3 in the absence of a metal source, formamides were formed. These compounds are known to be the hydrolyzed products from free NHC ligands.¹⁰³ Despite this fact, the authors insisted that the formation of the free carbene during weak base route can be excluded as they decompose in acetone. Next, the reaction with $[\text{Rh}(\text{COD})\text{Cl}]_2$ and potassium carbonate was carried out and it was established that the spectra of the obtained product was the same as the hydroxo complex $[\text{Rh}(\text{COD})(\text{OH})]_2$. The authors assumed that a hydroxo complex is formed in the first step, which reacts with an NHC precursor leading to the formation of the desired M-NHC complexes.

Plenio and co-workers also studied the possibility of obtaining $[\text{M}(\text{NHC})(\text{CO})_2\text{Cl}]$ complexes directly from $[\text{M}(\text{COD})\text{Cl}]_2$ and CO.¹⁰²

The desired compounds were obtained in good to high yields (Scheme 22). The authors underlined that isolated yields in the case of complexes bearing CO were higher compared to those of compounds bearing COD ligands, because of the lower solubility of the former. Lower solubility in non-polar solvents resulted in minimized product loss during purification. A one-step, simple route to Rh systems enabling the TEP determination for the NHC ligand is highly desirable.

The application of the weak base route to the synthesis of ruthenium–NHC complexes

Ru-NHC complexes have been widely explored during the last decade, due to their high catalytic activity in a number of reactions, such as hydrogenation, alkene metathesis and amidation.^{104,105} Simplification of the synthetic access to well-defined Ru-NHC complexes is an important goal and has



Scheme 23 General synthetic procedure for the synthesis of $[\text{Ru}(\text{NHC})\text{Cl}_2]$ and $[\text{Ru}(\text{NHC})(p\text{-cymene})\text{Cl}_2]$ complexes.

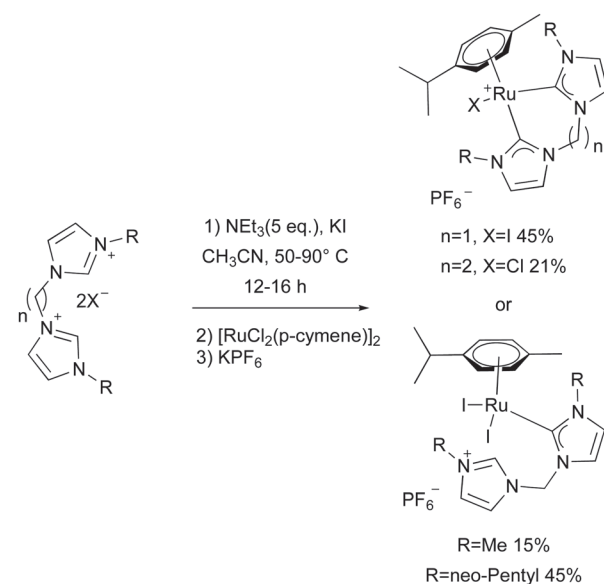
been sought after in sporadic reports, particularly through the application of the weak base route.¹⁰⁶

Özdemir and co-workers reported the synthesis of a series of $[\text{Ru}(\text{NHC})\text{Cl}_2]$ and $[\text{Ru}(\text{NHC})(p\text{-cymene})\text{Cl}_2]$ complexes using caesium carbonate as a base, in toluene.^{107,108} Ru–NHC complexes with bulky substituents were obtained in good to high yields (Scheme 23). Of note, the described procedure required a high temperature and a toxic solvent.

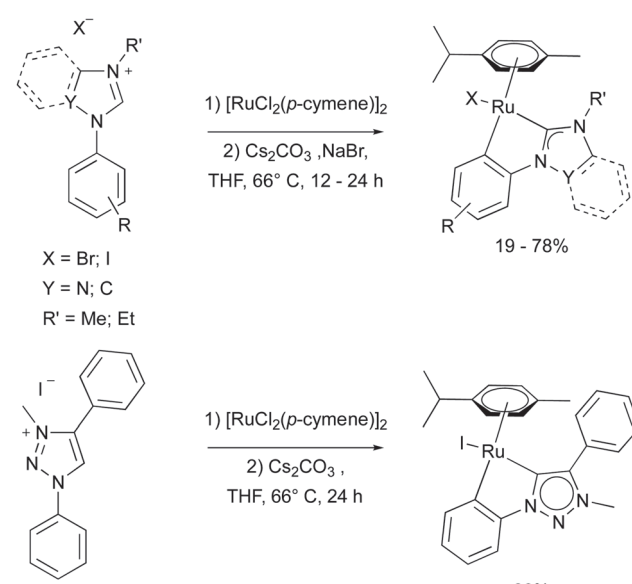
In 2004 Peris and co-workers reported the synthesis of Ru(II)-*p*-cymene complexes with mono- and bidentate ligands with the use of NEt_3 as a base.¹⁰⁹ The authors underlined that the use of NaOAc and Na_2CO_3 gave mixtures of products, which were difficult to identify. The formation of mono- or biscarbene complexes was found to be dependent on the steric bulk of the azolium precursor, as in the case of the larger neo-pentyl ligand only the monocarbene complex was formed. All the compounds were obtained in low yields and the reactions were carried out under an inert atmosphere (Scheme 24).

In some recent reports, synthetic routes to Ru(II)-*p*-cymene complexes containing various NHCs, through the use of a weak base, namely Cs_2CO_3 , were discussed (Scheme 25).^{110,111} The yields for the obtained Ru–NHC complexes range from low to good. It is worth noting that in these works, inert atmosphere and/or toxic solvents (THF) were required. Also, Cs_2CO_3 is more significantly more expensive than K_2CO_3 , an important factor for large scale synthesis.

In 2019, the research groups of Verpoort and Chen reported a simple synthetic pathway to the highly efficient in dehydrogenative amidation of alcohols Ru–NHC catalysts.^{112,113} In this work,¹¹² the authors used *in situ* generated Ru species in amide and amine synthesis. They also tested various bases for these catalytic reactions such as, K_2CO_3 , KOAc , $\text{KO}^\ddagger\text{Bu}$ and NaH , but only Cs_2CO_3 led to high yields of desired products and was effective for the selective amide formation. With these results in mind, the authors tried to isolate and characterize Ru

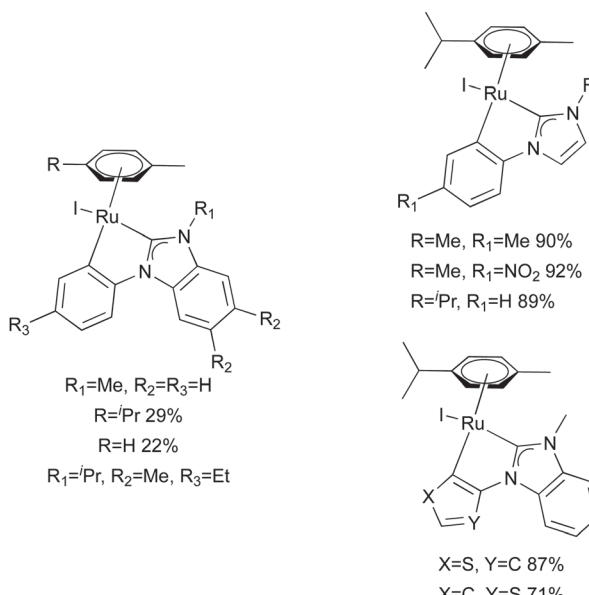


Scheme 24 General synthetic procedure for the synthesis of Ru-arene-monocarbene and biscarbene complexes.



Scheme 25 General synthetic procedure for the synthesis of Ru–NHC complexes.

species, which were formed during the catalysis. They described the synthesis of these Ru–NHC complexes from various NHC salts and $[\text{Ru}(p\text{-cymene})\text{Cl}_2]_2$ in the presence of Cs_2CO_3 in toluene and under inert atmosphere. Of note, in both cases column chromatography was used for the purification of the desired complexes and yields of the isolated compounds were low (22% and 29% respectively, Fig. 3). Moreover, these groups reported other Ru–NHC complexes, which were obtained with the use of the described weak base route.



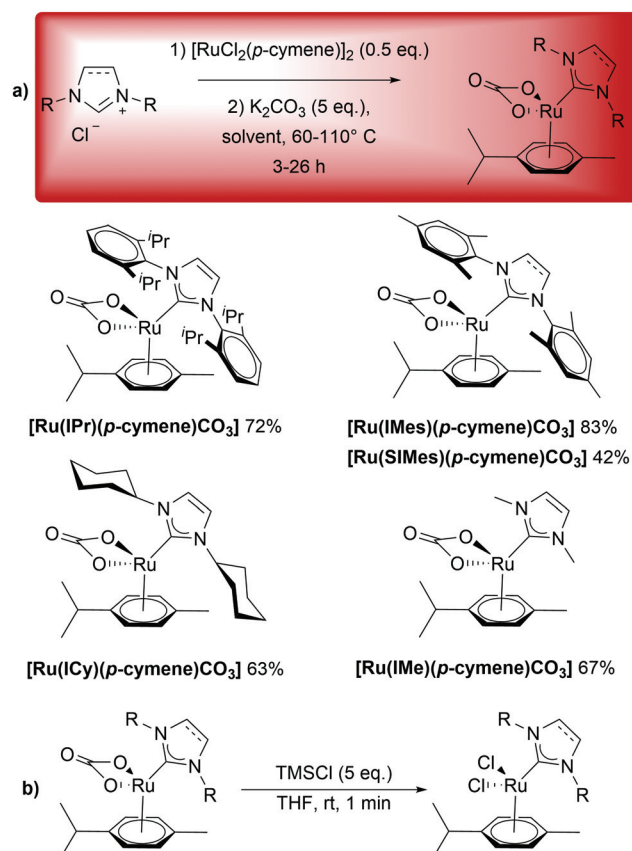
The desired Ru–NHC complexes were obtained in good to excellent yields (Fig. 3).¹¹³

Recently, Ma *et al.* investigated the previously described weak base route with NHC precursor salts and $[\text{RuCl}_2(p\text{-cymene})]_2$ in the presence of K_2CO_3 in acetone to obtain $[\text{Ru}(\text{NHC})(p\text{-cymene})\text{Cl}_2]$ complexes, but this reaction led to the formation of $[\text{Ru}(\text{NHC})(p\text{-cymene})\text{CO}_3]$ complexes instead through anion metathesis.¹¹⁴ The weak base route was tested with various NHCs, both saturated and unsaturated, and proved to be highly efficient for the synthesis of the carbo-nato-Ru complexes (Scheme 26a). The authors also reported an easy way to convert $[\text{Ru}(\text{NHC})(p\text{-cymene})\text{CO}_3]$ complexes into $[\text{Ru}(\text{NHC})(p\text{-cymene})\text{Cl}_2]$ complexes, using TMSCl. After 1 minute, 100% conversion was observed and the desired compounds were isolated in high yields (74–84%) (Scheme 26b).

It was demonstrated that these procedures can be carried out in one pot, thus simplifying the synthesis of $[\text{Ru}(\text{NHC})(p\text{-cymene})\text{Cl}_2]$ complexes.

Mechanistic investigations of the weak base route

The versatility of the weak base route has been shown for various metals, but the mechanism of the metallation is still unclear. Despite the fact that experimental results and thermodynamic values (pK_a) clearly show that free carbene formation is unlikely when weak bases (K_2CO_3 or NEt_3) are used, its formation should not be completely excluded.¹¹⁵ Perhaps a more practical and relevant approach than simply debating whether free carbene formation is feasible, would be to investigate the events that may occur in the presence of metal sources or other substrates in the reaction. Such studies would be more closely aligned with real reaction systems in both



Scheme 26 (a) General synthetic procedure for the synthesis of $[\text{Ru}(\text{NHC})(p\text{-cymene})\text{CO}_3]$ complexes via the weak base route. (b) General synthetic procedure for the synthesis of $[\text{Ru}(\text{NHC})(p\text{-cymene})\text{Cl}_2]$ complexes.

organocatalysis and M–NHC complex synthesis, providing a valuable perspective. The first report examining such systems concerned the role of azolium salts and weak bases in organocatalysis, and hypothesized/demonstrated that a concerted mechanism in which the base, the imidazolium salt and the substrate react simultaneously, is much more favourable than a stepwise free carbene generation and subsequent reaction with the substrate.¹¹⁶ A similar, concerted mechanism was proposed in the case of a study concerning deuterium exchange of azolium salts, in which there is no free carbene intermediate.¹¹⁷ A more recent study for the case of organocatalysis, further supported the concerted mechanism, in which the azolium salt interacts directly with the substrate without the involvement of a free carbene.¹¹⁸ Importantly, the study showed that the exact conditions of the system, including the solvent used, may determine whether or not the path involving a free carbene is favourable.

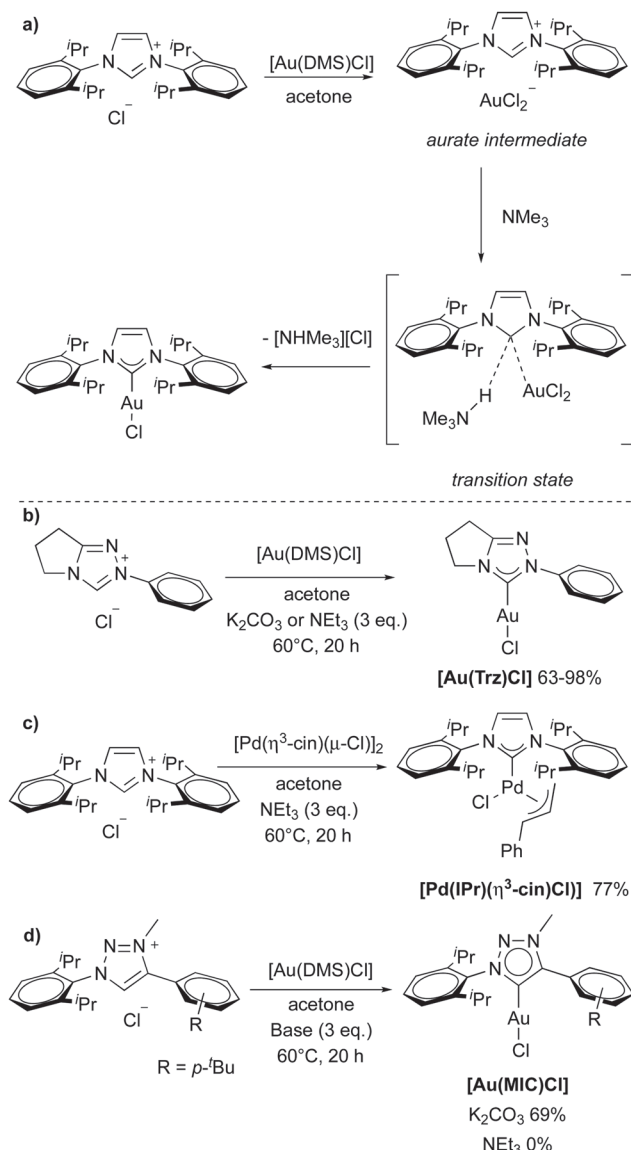
During the development of the weak base methodology for Au, Cu and Pd, observation and isolation of the metallate intermediates were common features. Later on, the same type of intermediate was isolated in the case of Pt. We reported mechanistic investigations on the role of the weak base in transition metal–NHC complex synthesis, using the metallate intermediate as a starting point.¹¹⁹ In the beginning, the

counterion in the aurate intermediate was suspected to be essential for the removal of the azolium proton while using a weak base, because of a decrease of the pK_a . However, further investigations revealed that pK_a values were the same for both IPr-HCl and the corresponding aurate intermediate.¹²⁰ Based on the results, the authors discounted an azolium deprotonation step from the transformation.

Another pathway of the reaction was tested with the aid of DFT. It included the simultaneous creation and scission of bonds in contrast to the previously discussed route, which consisted of deprotonation and subsequent metallation. For these investigations IPr-HCl and [Au(DMS)Cl] were chosen in the presence of NMe₃ as the base. The formation of the aurate intermediate was confirmed and shown to be energetically favourable. It is worth noting that the energy barrier when going from the metallate intermediate to the transition state depends on steric factors both for the base and NHC ligand. The transition state is followed by the dissociation of a chloride ion and formation of the ammonium salt [Me₃NH]⁺[Cl]⁻ which leads to the formation of the desired [Au(IPr)Cl] complex (Scheme 27a). Another pathway which includes deprotonation of IPr-HCl leads to a species which is higher in energy in comparison to the reactants and that is why a two-step route is not appropriate for the described process.

To address the influence of ligand structures on the energy barrier, the percent buried volume, % V_{Bur} , as steric descriptor and the snapping energy of the NHC-H bond were calculated for various ligands. The results showed that the energy barrier increases while using bulkier ligands (for IPr ligand $\Delta G_{Tr.s}^\# = 28.2 \text{ kcal mol}^{-1}$, for IMes ligand $\Delta G_{Tr.s}^\# = 24.9 \text{ kcal mol}^{-1}$). In addition, correlation between the strength of the NHC-H bond and energy barrier was found. TPT-Me (1,3,5-trimethyl-1,3,4-triazol-2-ylidene) (% $V_{Bur} = 24.0$) involved an energy barrier of 18.9 kcal mol⁻¹ and IMe (% $V_{Bur} = 25.8$)–25.6 kcal mol⁻¹. These differences in energy barrier values can be explained with weaker NHC-H bond, therefore the energy is lower for TPT-Me in comparison to IMe.

In order to establish whether the computational model had predictive value, reactions with a 1,2,4-triazolium salt and [Au(DMS)Cl] in the presence of both triethylamine (which closely resembles trimethylamine) and potassium carbonate were performed. The desired [Au(Trz)Cl] complex was efficiently obtained in all cases, while the yields were substantially higher when the corresponding aurate was subjected to the reaction conditions (Scheme 27b). These results confirmed the computationally predicted ease with which the triazolium salt should react under the conditions of the weak base approach. In order to probe the generality of the triethylamine-assisted protocol, the synthesis of a palladium-allyl-type NHC complex was attempted. Remarkably, the dimer-cleaving approach led to the desired complex in 77% yield without modification of the conditions (Scheme 27c). Furthermore, to test the limits of this protocol, the reaction between a mesoionic carbene (MIC) precursor and [Au(DMS)Cl] was carried out in the presence of both weak bases. The computational model predicted that this metallation should not be favoured, and indeed the reaction



Scheme 27 Synthetic pathway for [Au(IPr)Cl] using DFT calculations and experimental results with NEt₃.

was unsuccessful with triethylamine. However, potassium carbonate was able to facilitate this transformation, highlighting the importance of the identity of the weak base (Scheme 27d). The precise reasons behind the superiority of the carbonate base still remain unclear, although it is now evident that the pK_a of the base has little effect on the energy barrier of the reaction, as was demonstrated in a later work on the use of NaOAc for the synthesis of Au-NHC complexes.¹²¹ In fact, NaOAc led to a lower energy barrier than trimethylamine, despite having a significantly lower pK_a . The results suggest that although triethylamine is competent enough for some cases, in a synthetic scenario, the inorganic bases would be more reliable and robust. Lastly, the weak base approach was used to synthesize thiourea and selenourea derivatives of NHCs. This is possible with both triethylamine and potassium carbonate as demonstrated recently by Nahra and co-workers.¹²²

Application of the weak base route in mechanochemistry

In the context of the greener nature of the weak base approach, Cazin and co-workers have recently disclosed a solid state, solvent-free mechanochemical protocol that enables the access to complexes of the type $[\text{Cu}(\text{NHC})\text{Cl}]$ which drastically reduces reaction times and solvent use (Scheme 28).¹²³

By means of an automated device (namely, a planetary ball mill) and by leveraging on previously unreported reactivity of the NHC salt precursor, the Cazin group was able to assemble seven different complexes (including $[\text{Cu}(\text{MIC})\text{Cl}]$) in good to excellent yields and in short reaction times (only 1.5 hours). Under these conditions, solvent usage is limited to workup phase (simple filtration over a SiO_2 plug) and to acetone (a solvent listed among the “preferred” ones in many solvent selection guides – Pfizer, GSK, Sanofi, etc.). As in the solution-based chemistry, the reaction proceeds through the formation of a cuprate species, which is subsequently converted to the desired metal complexes upon addition of an excess of K_2CO_3 (3 eq.). No particular trend was observed regarding the steric properties of the employed NHC precursors, as opposed to the solution-based variant where long reaction times are observed for more encumbered NHC salts.³⁶

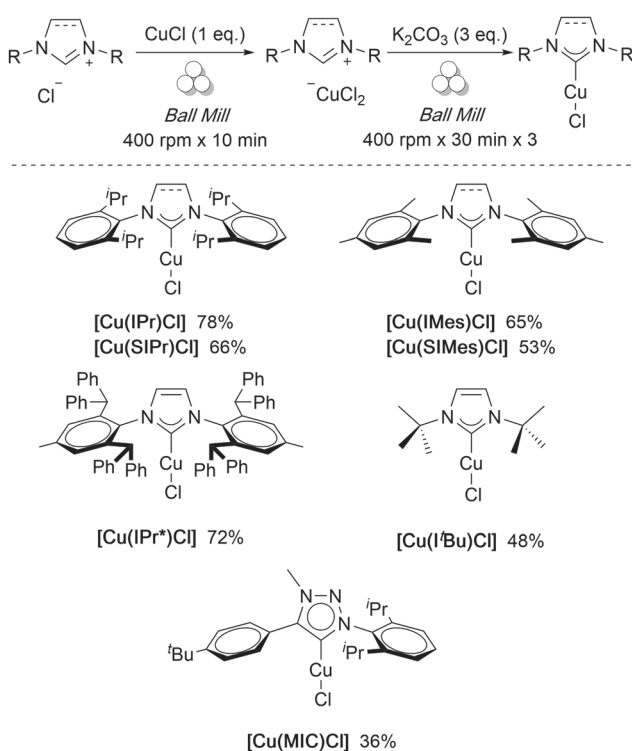
Principles of scalability of the protocol were also provided: mixing of 5 g of $\text{IPr}\text{-HCl}$, in the presence of CuCl (1 eq.) and K_2CO_3 (3 eq.), delivered 4.3 g of $[\text{Cu}(\text{IPr})\text{Cl}]$ (75% yield) in only 10 min: this further reduction of reaction time was attributed to an increase in temperature inside the reaction ball-mill vessel,

observed to concomitant increase with the number of milling bodies (which in turn increases the frequency of collisions during the milling process and therefore the energy transferred to the reactor).

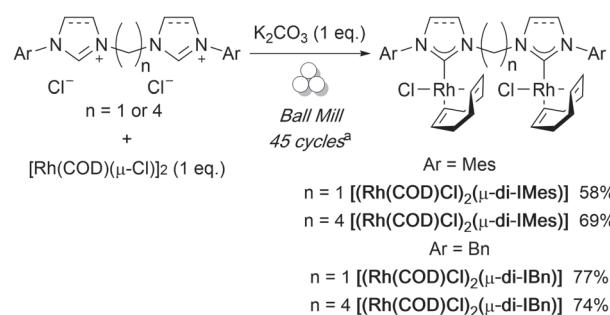
Concomitantly to this early communication, Udvárdy, Czégeéni & co-workers published a report reporting the mechanochemical synthesis of a small number of methylene bridged dinuclear rhodium(i)-NHC complexes of the type $[(\text{RhCl}(\text{COD}))_2(\mu\text{-di-NHC})]$ using K_2CO_3 as operational base (Scheme 29).¹²⁴ Again, as for the case of Cu(i)-complexes, the main features of such an approach were the short reaction times and the (partial) exclusion of solvents (only for the workup), thus eliminating the need of heating flammable acetone or toluene for prolonged periods of time.^{102,124}

In light of these early reports, Cazin and co-workers further expanded on the repertoire of metal–NHC complexes assembled using K_2CO_3 route under mechanochemical conditions, publishing an account in which general conditions for the assembly of different NHC-containing metal complexes are reported.¹²⁵ The synthetic approach adopted is simple and straightforward and consists of mixing the NHC salt together with the metal salt precursor of interest in the presence of an excess amount of the base.

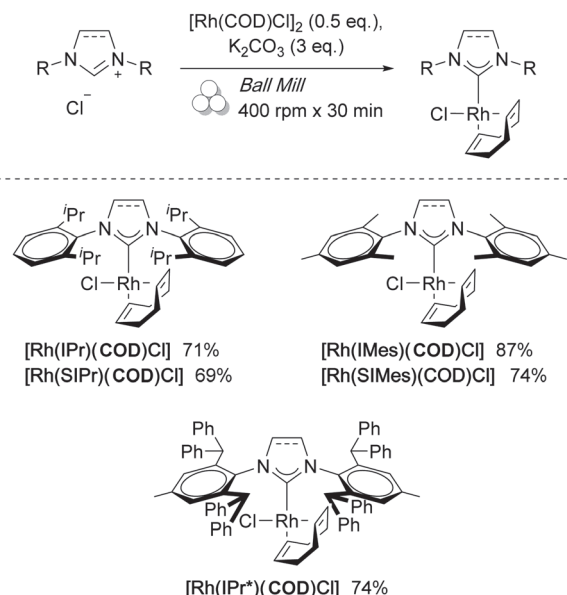
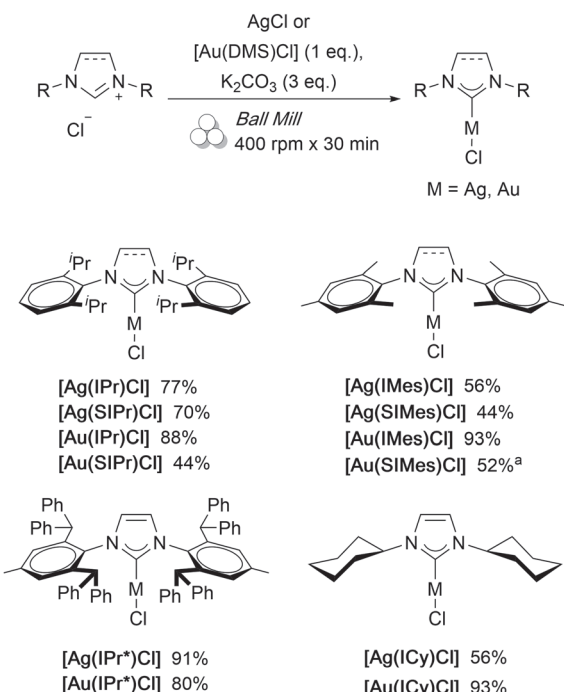
Using this approach, the Cazin group was able to complete the series of coinage metals describing the assembly of complexes of the type $[\text{M}(\text{NHC})\text{Cl}]$, with $\text{M} = \text{Ag}(\text{i}), \text{Au}(\text{i})$, by simple interchanging of the metal precursor (Scheme 30). Again, the most striking feature of such approach is that 30 min were sufficient to deliver these complexes in good to excellent yields, while limiting the use of (green) solvents (acetone and *n*-heptane) to the workup phase (thus, enhancing the E-factor for the overall process). Again, no particular trend is observed correlating the steric of the NHC salt precursors and the reaction time (trend that is observed in solution, as for the assembly of the $[\text{Au}(\text{X})\text{NHC}]$ complexes, with $\text{X} = \text{Cl}, \text{Br}, \text{I}$, reported by Nolan and co-workers).²⁴ Of note, the synthesis of the complex $[\text{Au}(\text{Cl})\text{SIMes}]$ could only be accomplished in 52% yield only when 6 eq. of the K_2CO_3 base were used: the addition of 3 eq. of K_2CO_3 invariably led to the formation of the corresponding aurate intermediate $[\text{IMes}\cdot\text{H}][\text{AuCl}_2]$.



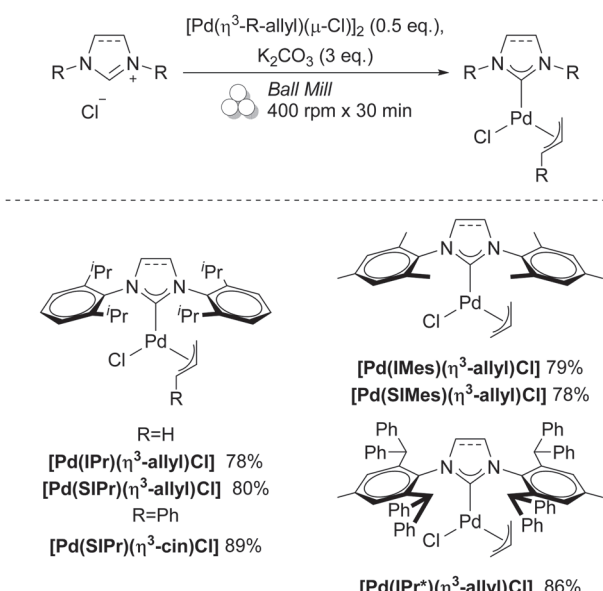
Scheme 28 Mechanochemical synthesis of $[\text{Cu}(\text{NHC})\text{Cl}]$ complexes.



Scheme 29 Mechanochemical synthesis of $[(\text{RhCl}(\text{COD}))_2(\mu\text{-di-NHC})]$ complexes. ^a1 cycle = milling for 2 min at 550 rpm, followed by 2 min resting.



The conditions reported were shown to be suitable also for the assembly of Pd(II)-complexes (Scheme 31). Simple exchange of the metal precursors to $[Pd(\eta^3\text{-allyl})(\mu\text{-Cl})_2]$ and $[Pd(\eta^3\text{-cin})(\mu\text{-Cl})_2]$, was sufficient in delivering the complexes of the general formula $[Pd(\eta^3\text{-R-allyl})(Cl)(NHC)]$, in good to excellent yields, again, after only 30 min. As for the synthesis of Cu(I) and Au(I) complexes, the formation of these complexes involves the



formation of a palladate intermediates, which have already been shown to be accessible by Nolan and Cazin, in the solid state by simple grinding of 0.5 eq. of the dimeric Pd(II) precursor to the NHC-HCl salt using mortar and pestle.⁷⁶ Again, under mechanochemical conditions, no particular trends were observed with respect to the bulkiness of the NHC-HCl salt or the allyl moiety (allyl or cinnamyl). Also in this case, proofs of scalability of the methodology were accomplished: 5.0 g of iPr-HCl were easily converted into 5.1 g (77% yield) of $[Pd(\eta^3\text{-allyl})(Cl)iPr]$. In the same report, Cazin and co-workers also successfully translated the protocol developed by Plenio and co-workers¹⁰² for the synthesis of $[Rh(NHC)(COD)Cl]$ complexes into a mechanochemical version (Scheme 32). This was, again, accomplished by simple interchanging of the metal salt precursor to $[Rh(COD)Cl]_2$.

From the viewpoint of green chemistry, this development (the previously unreported reactivity of the NHC precursors in the solid state and the use of mechanical forces to enable the assembly of NHC–metal complexes) is of great interest as this approach drastically reduces energy costs as well as waste production, by eliminating the need for heating highly flammable (although green) solvents and limiting their use in workups.

Conclusions and outlook

This feature article provides an overview of a simple and efficient route towards the synthesis of various NHC–metal complexes, using a weak base. All the advantages of this approach were fully described and illustrated with many specific examples. The versatility of this route was also shown to occur under mechanochemical conditions. The mechanistic aspects of the weak base route are also described. We strongly

believe this simple procedure can be successfully deployed as a method of choice to access a large variety of metal–NHC complexes and non-metal–NHC adducts. Given our continuous interest in the synthesis of well-defined M–NHC complexes and their use in organometallic synthesis and catalysis, we will pursue further advancements regarding the use of the weak base route in the near future. The contribution of our research groups, in addition to those of many others, has thus far highlighted the practicality and generality of this approach. As a result, we expect to encounter its use more frequently in the future, as it certainly renders the synthesis of various, highly useful M–NHC complexes a facile, routine operation. Moreover, the detailed reports in the literature which now cover most catalytically relevant transition metals, in combination with critical analysis provided in recent reviews,^{4,126} including the present one, are expected to provide a strong foundation for organometallic chemistry practitioners and researchers practicing M–NHC catalysis. A specific aspect of the weak base approach which has been emphasized by our groups is scalability. This aspect is highly important in our view, especially since it is a prerequisite for industrial applications, and has been demonstrated recently through the disclosure of detailed protocols for multigram scale (up to 200 grams) syntheses of Au–NHC complexes.¹²⁷ Of course, the various routes towards M–NHCs display complementarity in many cases and none should be disregarded, however the weak base route is the simplest and most user-friendly route so far, in addition to being superior in some cases, with the synthesis of [Au(IMes)Cl] being one example.¹²⁷

Keeping the recent advancements in mind, there are still challenges ahead on various frontiers of M–NHC synthesis. Currently, the weak base route is mainly applied for imidazol(in)ium salts as carbene precursors with few exceptions which can be found in the present review.^{102,112,113,119} Therefore, this route has to be extended towards other types of azolium salts, leading to the generation of metal–carbene complexes.¹²⁸ Additionally, other types of metal–NHC complexes can be targeted for each metal, with Pd being a case which may act as an example. In many cases, the scope limitations of the weak base route need to be investigated and overcome if possible, for example in the case of Pt–NHC complexes. Finally, the mechanistic aspects of this facile metalation have begun to emerge, however many questions remain unanswered, particularly regarding the superiority of carbonate bases over NEt_3 and the details concerning the mechanistic pathways and intermediates in the case of each transition metal.¹¹⁹

Conflicts of interest

There are no conflicts to declare.

Acknowledgements

We gratefully acknowledge support of this work through BOF research and starting grants to SPN and CSJC. Additionally,

CSJC and GP would like to thank the UGent IoF for support (TT grant). The Research Foundation – Flanders (FWO) is also gratefully acknowledged for a Fundamental Research PhD fellowship to NVT (11I6921N). The iBOF grant C³ to CSJC and SPN is acknowledged for partial support of the work.

Notes and references

- S. Díez-González, N. Marion and S. P. Nolan, *Chem. Rev.*, 2009, **109**, 3612–3676.
- S. P. Nolan, *Acc. Chem. Res.*, 2011, **44**, 91–100.
- Q. Zhao, G. Meng, S. P. Nolan and M. Szostak, *Chem. Rev.*, 2020, **120**, 1981–2048.
- T. Scattolin and S. P. Nolan, *Trends Chem.*, 2020, **2**, 721–736.
- A. Chartoire, C. Claver, M. Corpet, J. Krinsky, J. Mayen, D. Nelson, S. P. Nolan, I. Peñafiel, R. Woodward and R. E. Meadows, *Org. Process Res. Dev.*, 2016, **20**, 551–557.
- P. de Frémont, N. M. Scott, E. D. Stevens and S. P. Nolan, *Organometallics*, 2005, **24**, 2411–2418.
- N. Schneider, V. César, S. Bellemín-Lapponaz and L. H. Gade, *J. Organomet. Chem.*, 2005, **690**, 5556–5561.
- N. P. Mankad, T. G. Gray, D. S. Laitar and J. P. Sadighi, *Organometallics*, 2004, **23**, 1191–1193.
- M. S. Viciu, O. Navarro, R. F. Germaneau, R. A. Kelly, W. Sommer, N. Marion, E. D. Stevens, L. Cavallo and S. P. Nolan, *Organometallics*, 2004, **23**, 1629–1635.
- M. R. L. Furst and C. S. J. Cazin, *Chem. Commun.*, 2010, **46**, 6924–6925.
- I. J. B. Lin and C. S. Vasam, *Coord. Chem. Rev.*, 2007, **251**, 642–670.
- C. A. Citadelle, E. Le Nouy, F. Bisaro, A. M. Z. Slawin and C. S. J. Cazin, *Dalton Trans.*, 2010, **39**, 4489–4491.
- R. A. Kelly, N. M. Scott, S. Díez-González, E. D. Stevens and S. P. Nolan, *Organometallics*, 2005, **24**, 3442–3447.
- N. Marion, E. C. Ecarnot, O. Navarro, D. Amoroso, A. Bell and S. P. Nolan, *J. Org. Chem.*, 2006, **71**, 3816–3821.
- S. Zhu, R. Liang and H. Jiang, *Tetrahedron*, 2012, **68**, 7949–7955.
- B. Landers and O. Navarro, *Eur. J. Inorg. Chem.*, 2012, 2980–2982.
- F. Wang, S. Li, M. Qu, M.-X. Zhao, L.-J. Liu and M. Shi, *Beilstein J. Org. Chem.*, 2012, **8**, 726–731.
- M. Albrecht, J. R. Miecznikowski, A. Samuel, J. W. Faller and R. H. Crabtree, *Organometallics*, 2002, **21**, 3596–3604.
- M. Albrecht, R. H. Crabtree, J. Mata and E. Peris, *Chem. Commun.*, 2002, 32–33.
- C. J. O'Brien, E. A. B. Kantchev, C. Valente, N. Hadei, G. A. Chass, A. Lough, A. C. Hopkinson and M. G. Organ, *Chem. – Eur. J.*, 2006, **12**, 4743–4748.
- A. Bittermann, D. Baskakov and W. A. Herrmann, *Organometallics*, 2009, **28**, 5107–5111.
- C. Dash, M. M. Shaikh, R. J. Butcher and P. Ghosh, *Dalton Trans.*, 2010, **39**, 2515–2524.
- G. De Bo, G. Berthon-Gelloz, B. Tinant and I. E. Markó, *Organometallics*, 2006, **25**, 1881–1890.
- A. Collado, A. Gómez-Suárez, A. R. Martin, A. M. Z. Slawin and S. P. Nolan, *Chem. Commun.*, 2013, **49**, 5541.
- R. Visbal, A. Laguna and M. C. Gimeno, *Chem. Commun.*, 2013, **49**, 5642.
- N. Marion and S. P. Nolan, *Chem. Soc. Rev.*, 2008, **37**, 1776–1782.
- T. de Haro, E. Gómez-Bengoa, R. Cribeú, X. Huang and C. Nevado, *Chem. – Eur. J.*, 2012, **18**, 6811–6824.
- L. Mercs and M. Albrecht, *Chem. Soc. Rev.*, 2010, **39**, 1903–1912.
- A. M. Al-Majid, S. Yousuf, M. I. Choudhary, F. Nahra and S. P. Nolan, *ChemistrySelect*, 2016, **1**, 76–80.
- E. Sioriki, R. Lordan, F. Nahra, K. Van Hecke, I. Zabetakis and S. P. Nolan, *ChemMedChem*, 2018, **13**, 2484–2487.
- S. Zhu, R. Liang, L. Chen, C. Wang, Y. Ren and H. Jiang, *Tetrahedron Lett.*, 2012, **53**, 815–818.
- O. S. Morozov, A. V. Lunchev, A. A. Bush, A. A. Tukov, A. F. Asachenko, V. N. Khrustalev, S. S. Zalesskiy, V. P. Ananikov and M. S. Nechaev, *Chem. – Eur. J.*, 2014, **20**, 6162–6170.
- A. Johnson and M. C. Gimeno, *Chem. Commun.*, 2016, **52**, 9664–9667.

COMMUNICATION

[View Article Online](#)
[View Journal](#) | [View Issue](#)

Cite this: *Chem. Commun.*, 2013,
49, 10483

Received 19th July 2013,
Accepted 12th August 2013

DOI: 10.1039/c3cc45488f

www.rsc.org/chemcomm

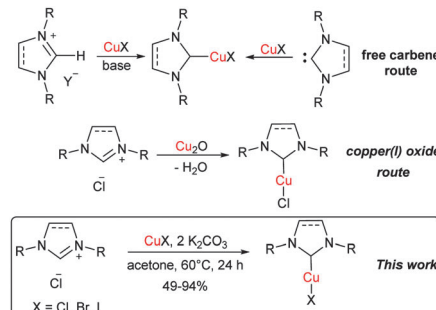
A one-pot procedure for the synthesis of $[\text{Cu}(\text{X})(\text{NHC})]$ ($\text{X} = \text{Cl}, \text{Br}, \text{I}$) is reported. The reaction is applicable to a wide range of saturated and unsaturated NHC ligands, is scalable and proceeds under mild conditions using technical grade solvents in air.

In transition metal-catalysed reactions the accessibility of the catalyst is one of the most important factors in dictating the usefulness of any catalytic method. The development of catalytic systems based on inexpensive metals such as iron¹ and copper² have gained increased attention during the last few years. In this context, N-heterocyclic carbene (NHC) copper species of the type $[\text{Cu}(\text{X})(\text{NHC})]$ ($\text{X} = \text{Cl}, \text{Br}, \text{I}$) have shown to be efficient catalysts for several transformations,³ such as the reduction of carbonyl compounds,⁴ hydrosilylation⁵ and [3+2] cycloaddition of alkynes and azides.⁶ They can also be used as carbene transfer reagents to other transition metals such as gold or palladium.⁷ In addition, these systems have exhibited interesting biological activity as antitumour agents.⁸

The most common synthetic strategy to prepare $[\text{Cu}(\text{X})(\text{NHC})]$ ($\text{X} = \text{Cl}, \text{Br}, \text{I}$) complexes is the reaction of a free carbene with a copper source.⁹ The free carbene can be isolated in the first instance or generated *in situ* (Scheme 1). The main drawbacks of this procedure are the need for an inert atmosphere and strictly anhydrous conditions as well as the use of strong and expensive bases.^{5a,10} In 2010 an improved procedure was developed by our group: the synthesis of several $[\text{Cu}(\text{Cl})(\text{NHC})]$ complexes using Cu_2O as a copper source in different solvents was reported (Scheme 1).¹¹ This methodology allows the use of air-stable and economical starting materials and generates water as the only side-product. McQuade and co-workers have employed this system to validate their hypothesis that such syntheses could be performed in a continuous flow apparatus.¹² In 2012, Jiang and co-workers reported the synthesis of some $[\text{Cu}(\text{Cl})(\text{NHC})]$ by treatment of imidazolium salts with weak bases in the presence of a copper source.¹³ However, this protocol requires

A general synthetic route to $[\text{Cu}(\text{X})(\text{NHC})]$ (NHC = N-heterocyclic carbene, X = Cl, Br, I) complexes†

Orlando Santoro, Alba Collado, Alexandra M. Z. Slawin, Steven P. Nolan and Catherine S. J. Cazin*



Scheme 1 Synthetic routes to $[\text{Cu}(\text{X})(\text{NHC})]$ complexes.

high temperature and environmentally unfriendly solvents such as 3-chloropyridine. Very recently, Cisnetti and co-workers showed that aqueous ammonia can promote the formation of Cu–NHC complexes from the corresponding imidazol(idin)ium salts.¹⁴

Despite these recent improvements, access to a general synthetic route leading to $[\text{Cu}(\text{X})(\text{NHC})]$ complexes under milder and environmentally friendly conditions remains highly desirable.

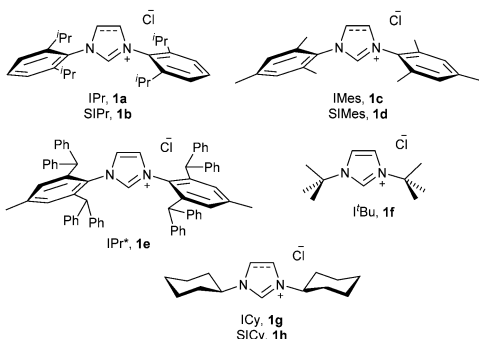
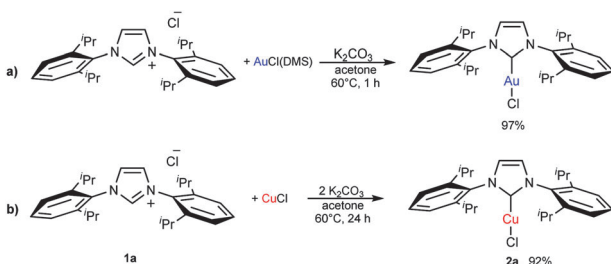
Recently, one of us has reported a one-step methodology to prepare $[\text{Au}(\text{X})(\text{NHC})]$ ($\text{X} = \text{Cl}, \text{Br}, \text{I}$) complexes, using imidazol(idin)ium salts, a gold source and a weak base. This protocol proceeds under mild conditions and has proven to be robust and general, as it is applicable to the synthesis of a wide range of NHC–Au complexes.^{15,16} Due to the great versatility of this protocol and the closely related chemistry of gold and copper, we were interested in extending this straightforward methodology to the preparation of $[\text{Cu}(\text{X})(\text{NHC})]$ complexes (Fig. 1). Therefore we carried out the synthesis of $[\text{Cu}(\text{Cl})(\text{IPr})]$ (**2a**) following the optimised conditions for gold, *e.g.*, treating, in air, $\text{IPr}\text{-HCl}$ (**1a**) with CuCl in the presence of 1 equivalent of K_2CO_3 , using technical grade acetone at 60 °C. After 24 h an encouraging 80% conversion to the desired complex **2a** was observed. By doubling the amount of base, **2a** was isolated in 92% yield (Scheme 2). Noteworthily, the reaction time can be reduced to 1 h by using 10 equivalents of base.

After a brief optimisation of the reaction conditions (see ESI†), we found the best conditions for the synthesis of $[\text{Cu}(\text{Cl})(\text{IPr})]$ are the ones used for the synthesis of $[\text{Au}(\text{Cl})(\text{IPr})]$. In order to

EaStCHEM School of Chemistry, University of St Andrews, St Andrews, KY16 9ST, UK. E-mail: cc111@st-andrews.ac.uk; Fax: +44 (0)1334 463808

† Electronic supplementary information (ESI) available: Optimisation details and full characterisation data. CCDC 940850–940853. For ESI and crystallographic data in CIF or other electronic format see DOI: 10.1039/c3cc45488f



**Fig. 1** NHC-HCl salts used in this study.**Scheme 2** Optimised conditions for (a) $[\text{Au}(\text{Cl})(\text{IPr})]$ and (b) 2a .

evaluate the versatility of this protocol we carried out the reaction using different NHC ligands and copper salts under the optimised conditions. The results are summarised in Table 1.[†] It should be noted that, although the reaction time can be significantly decreased by adding a large excess of base, all reactions were carried out with 2 equivalents in order to minimise waste.

This methodology is efficient for the synthesis of a wide variety of $[\text{Cu}(\text{Cl})(\text{NHC})]$ complexes. All complexes were obtained with moderate to excellent yields and were characterised by ^1H and ^{13}C - ^1H NMR spectroscopy with data in agreement with the literature.^{11,12,17} The reaction was tested for the most common saturated and unsaturated NHC ligands bearing *N*-aryl moieties (Table 1, entries 1–4). This procedure allowed the preparation of NHC–copper(I) complexes in air using mild conditions, while previous methods required either an inert atmosphere (free carbene routes)^{17a} or harsher conditions (toluene or water reflux).¹¹ Moreover, these reactions proceed cleanly and the formation of undesired side-products such as $[\text{Cu}(\text{NHC})_2]^+$ was never observed,

Table 1 Scope of $[\text{Cu}(\text{Cl})(\text{NHC})]$ synthesis^a

Entry	NHC·HCl	Complex	Yield (%)	$\text{NHC} \cdot \text{HCl} + \text{CuCl} + 2\text{K}_2\text{CO}_3 \xrightarrow[60^\circ\text{C}, 24\text{ h}]{\text{acetone}} [\text{Cu}(\text{Cl})(\text{NHC})]$	
				acetone	$60^\circ\text{C}, 24\text{ h}$
1	IPr, 1a	$[\text{Cu}(\text{Cl})(\text{IPr})]$, 2a	92		
2	SIPr, 1b	$[\text{Cu}(\text{Cl})(\text{SIPr})]$, 2b	84		
3	IMes, 1c	$[\text{Cu}(\text{Cl})(\text{IMes})]$, 2c	76		
4	SIMes, 1d	$[\text{Cu}(\text{Cl})(\text{SIMes})]$, 2d	94		
5	IPr*, 1e	$[\text{Cu}(\text{Cl})(\text{IPr}^*)]$, 2e	70		
6 ^b	tBu, 1f	$[\text{Cu}(\text{Cl})(\text{tBu})]$, 2f	55		
7	ICy, 1g	$[\text{Cu}(\text{Cl})(\text{ICy})]$, 2g	80		
8 ^{b,c}	SICy, 1h	$[\text{Cu}(\text{Cl})(\text{SICy})]$, 2h	49		

^a Reaction conditions: NHC·HCl (100 mg), CuCl (1 equiv.), K_2CO_3 (2 equiv.), acetone, 60°C , 24 h. ^b Under Ar. ^c In CH_2Cl_2 .

which is a common problem in the synthesis *via* the free carbene route.^{17a} The reaction involving the very bulky IPr^* (**1e**) also succeeded (Table 1, entry 5), avoiding the microwave irradiation employed in its previously reported synthesis.^{17b} Copper complexes containing *N*-alkyl NHC ligands were also prepared (Table 1, entries 6–8). $[\text{Cu}(\text{Cl})(\text{ICy})]$ (**2g**) was obtained in a higher yield (80%) than by previously reported routes (70–71%).^{17a} $[\text{Cu}(\text{Cl})(\text{tBu})]$ (**2f**) was prepared under an Ar atmosphere as the complex is known to be air- and moisture-sensitive.^{17a} Although the reaction did not reach completion, the pure complex was isolated in 55% yield, avoiding the isolation of the free carbene or toluene reflux. In this case the formation of the $[\text{Cu}(\text{NHC})_2]^+$ species was also not observed either.^{11,17a} A remarkable example is the synthesis of $[\text{Cu}(\text{Cl})(\text{SICy})]$ (**2h**) (Table 1, entry 8). To the best of our knowledge, this complex has never been isolated in batch conditions and the only reported synthesis requires the use of a continuous flow system apparatus.¹² Synthetic attempts following the Cu_2O route led to the formation of a single species identified as the ketone 1,3-dicyclohexylimidazolidin-2-one.¹¹ The optimal conditions to synthesise $[\text{Cu}(\text{Cl})(\text{IPr})]$ led to an equimolar amount of **2h** and of the ketone when applied to SICy. For this reason, a new synthetic approach is needed for this complex. Gratifyingly, when using dichloromethane instead of acetone, the formation of the ketone was not observed and pure $[\text{Cu}(\text{Cl})(\text{SICy})]$ was isolated as a white powder. While this complex decomposes to a green gel when stored for extended periods under an Ar atmosphere, this methodology enabled its preparation.

As the nature of the halide has shown to influence the catalytic behaviour of $[\text{Cu}(\text{X})(\text{NHC})]$,^{17a} the protocol described above was applied to access NHC–Cu derivatives containing different halides. Therefore, the reactions between IPr·HCl (**1a**) and CuBr and CuI in the presence of K_2CO_3 were carried out (Table 2). These reactions gave access to the corresponding bromide (**2i**) and iodide (**2j**) $[\text{Cu}(\text{X})(\text{IPr})]$ complexes, respectively.

In order to obtain more information about the mechanism of this transformation, the reaction of IPr·HCl and CuCl in the absence of base was performed. A new species was obtained in almost quantitative yield and characterised by ^1H and ^{13}C - ^1H NMR spectroscopy and by elemental analysis in addition to diffraction studies on a single crystal. The data revealed the product to be $[\text{IPrH}][\text{CuCl}_2]$ (**3a**),¹⁸ which consists of an imidazolium cation paired with a $[\text{CuCl}_2]^-$ counterion. **3a** is the copper counterpart of $[\text{IPrH}][\text{AuCl}_2]$, obtained in the reaction between IPr·HCl and $[\text{Au}(\text{Cl})(\text{DMS})]$.¹⁵ As in the gold reaction, the formation of **3a** occurs at room temperature within the mixing time and can be further reacted with 2 equivalents of base in acetone, affording the final $[\text{Cu}(\text{Cl})(\text{IPr})]$ complex (Scheme 3).

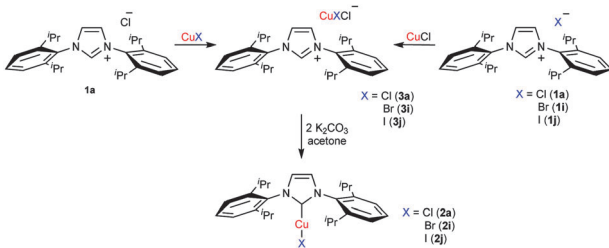
Next, the reactions between IPr·HCl and CuX (X = Br, I) were studied and two new $[\text{IPrH}][\text{CuClX}]$ species (**3i** and **3j**) were obtained.

Table 2 Synthesis of $[\text{Cu}(\text{X})(\text{IPr})]$ (X = Br, I) complexes^a

Entry	NHC·HCl	CuX	Complex	Yield (%)	$\text{IPr} \cdot \text{HCl} + \text{CuX} + 2\text{K}_2\text{CO}_3 \xrightarrow[60^\circ\text{C}, 24\text{ h}]{\text{acetone}} [\text{Cu}(\text{X})(\text{IPr})]$	
					acetone	$60^\circ\text{C}, 24\text{ h}$
1	IPr·HCl, 1a	CuBr	$[\text{Cu}(\text{Br})(\text{IPr})]$, 2i	88		
2	IPr·HCl, 1a	CuI	$[\text{Cu}(\text{I})(\text{IPr})]$, 2j	77		

^a Reaction conditions: NHC·HCl (100 mg), CuX (1 equiv.), K_2CO_3 (2 equiv.), acetone, 60°C , 24 h.



**Scheme 3** Formation and further reaction of the [IPrH][CuClX] species.**Table 3** Larger-scale reactions^a

Entry	IPr-HCl (g)	CuX (g)	Complex	Time (h)	Yield (%)	acetone 60 °C, 8–15 h		
						[Cu(Cl)(IPr)], 2a	[Cu(Br)(IPr)], 2b	[Cu(I)(IPr)], 2c
1	1.00	CuCl (0.22)	[Cu(Cl)(IPr)], 2a	15	90			
2	1.00	CuBr (0.33)	[Cu(Br)(IPr)], 2b	8	91			
3	0.88	CuI (0.36)	[Cu(I)(IPr)], 2c	8	85			

^a Reaction conditions: acetone, 60 °C, 1 equiv. of IPr-HCl, 1 equiv. of CuX, 3 equiv. of K₂CO₃.

The same complexes can also be obtained by the reaction between the corresponding IPr-HX salts and CuCl. Subsequent treatment of **3i** and **3j** with K₂CO₃ afforded the corresponding [Cu(X)(IPr)] **2i** and **2j** (Scheme 3). It should be noted that the formation of the analogous chloride complex **2a** was never observed. A new intermediate species, [IPrH][CuBrI] (**3k**), was prepared by treatment of CuI with IPr-HBr. Further treatment of **3k** with K₂CO₃ afforded [Cu(I)(IPr)] as a single product. This trend, also observed for gold,¹⁵ can be explained by considering the halide *trans* effect series: I > Br > Cl.¹⁹ On the basis of this evidence we postulated that the halide exerting a higher *trans* effect stabilises the bond *trans* to it and then this halide remains coordinated to the copper in the final complex. In addition, the lattice energies for the formation of the KX salts (KCl > KBr > KI) are in agreement with the observed reactivity.

Due to the interesting nature of these species, [SIPrH][CuCl₂] (**3b**), [IMeshH][CuCl₂] (**3c**), [SIMeshH][CuCl₂] (**3d**) and [ICyH][CuCl₂] (**3g**) analogues were synthesised and their structures have been confirmed by X-ray diffraction studies on single crystals.²⁰ Also in this case, the treatment of these species with K₂CO₃ under the reaction conditions led to the formation of the corresponding complexes. These results reinforce the hypothesis that the [(NHC)H][CuCl₂] species are the actual intermediates in this transformation.

Finally, we were interested in testing the efficiency of this protocol in the synthesis of [Cu(X)(IPr)] complexes on a larger scale (Table 3). It should be noted that the reaction time increased to several days when 2 equiv. of base were used and, in order to provide a practical synthetic protocol, an additional equivalent of K₂CO₃ was used.

In summary a one-pot general procedure for the synthesis of [Cu(X)(NHC)] (X = Cl, Br, I) under mild and aerobic conditions was developed. This synthetic method was shown to proceed via a [(NHC)H][CuX₂] intermediate species. A wide variety of NHC ligands, as well as halide sources, were efficiently used. Moreover, this protocol allowed for the synthesis of [Cu(Cl)(SICy)]

which has not been previously achieved under batch conditions. Further synthetic and theoretical studies dealing with the mechanism of the reaction are currently ongoing.

The authors gratefully acknowledge the Royal Society (University Research Fellowship to C.S.J.C.), EaStCHEM School of Chemistry, the ERC (Advanced Investigator Award-FUNCAT and PoC project GOLDCAT) and the EPSRC for funding. S.P.N. is a Royal Society Wolfson Research Merit Award holder. We also thank Mr Adrián Gómez-Suárez for early synthetic contributions and discussions.

Notes and references

‡ General synthetic procedure: a vial was charged with NHC-HCl (100 mg), CuCl (1 equiv.), K₂CO₃ (2 equiv.). The resulting mixture was suspended in acetone (1.0 mL) and stirred at 60 °C for 24 h. After this time the mixture was filtered through silica. The pad of silica was washed with dichloromethane (3 × 1 mL). The solvent was concentrated and pentane (3 mL) was added affording the desired product that was washed with further portions of pentane (3 × 1 mL) and dried under vacuum.

- (a) K. Gopalaiah, *Chem. Rev.*, 2013, **113**, 3248; (b) T. Mesganaw and N. K. Garg, *Org. Process Res. Dev.*, 2012, **17**, 29; (c) S. Prateepthongkum, I. Jovel, R. Jackstell, N. Vogl, C. Weckbecker and M. Beller, *Chem. Commun.*, 2009, 1990; (d) B. D. Sherry and A. Fürstner, *Acc. Chem. Res.*, 2008, **41**, 1500.
- (a) M. Carril, R. SanMartin and E. Dominguez, *Chem. Soc. Rev.*, 2008, **37**, 639; (b) V. Jurkauskas, J. P. Sadighi and S. L. Buchwald, *Org. Lett.*, 2003, **5**, 2417; (c) G. Lefèvre, G. Franc, A. Tlili, C. Adamo, M. Taillefer, I. Ciolfini and A. Jutand, *Organometallics*, 2012, **31**, 7694.
- J. D. Egbert, C. S. J. Cazin and S. P. Nolan, *Catal. Sci. Technol.*, 2013, **3**, 912.
- (a) S. Díez-González and S. P. Nolan, *Acc. Chem. Res.*, 2008, **41**, 349; (b) H. Kaur, F. K. Zinn, E. D. Stevens and S. P. Nolan, *Organometallics*, 2004, **23**, 1157.
- (a) S. Díez-González, H. Kaur, F. K. Zinn, E. D. Stevens and S. P. Nolan, *J. Org. Chem.*, 2005, **70**, 4784; (b) S. Díez-González, E. D. Stevens, N. M. Scott, J. L. Petersen and S. P. Nolan, *Chem.-Eur. J.*, 2008, **14**, 158.
- (a) S. Díez-González, A. Correa, L. Cavallo and S. P. Nolan, *Chem.-Eur. J.*, 2006, **12**, 7558; (b) S. Díez-González and S. P. Nolan, *Angew. Chem., Int. Ed.*, 2008, **47**, 8881; (c) S. Díez-González, E. D. Stevens and S. P. Nolan, *Chem. Commun.*, 2008, 4747.
- M. R. L. Furst and C. S. J. Cazin, *Chem. Commun.*, 2010, **46**, 6924.
- (a) M.-L. Teyssot, A.-S. Jarrousse, A. Chevry, A. De Haze, C. Beaudoin, M. Manin, S. P. Nolan, S. Díez-González, L. Morel and A. Gautier, *Chem.-Eur. J.*, 2009, **15**, 314; (b) M.-L. Teyssot, A.-S. Jarrousse, M. Manin, A. Chevry, S. Roche, F. Norre, C. Beaudoin, L. Morel, D. Boyer, R. Mahiou and A. Gautier, *Dalton Trans.*, 2009, 6894; (c) W. Liu and R. Gust, *Chem. Soc. Rev.*, 2013, **42**, 755.
- S. Díez-González and S. P. Nolan, *Synlett*, 2007, 2158.
- (a) N. P. Mankad, T. G. Gray, D. S. Laitar and J. P. Sadighi, *Organometallics*, 2004, **23**, 1191; (b) C. Michon, A. Ellern and R. J. Angelici, *Inorg. Chim. Acta*, 2006, **359**, 4549; (c) N. Schneider, V. César, S. Bellemín-Lapennaz and L. H. Gade, *J. Organomet. Chem.*, 2005, **690**, 5556.
- C. A. Citadelle, E. L. Nouy, F. Bisaro, A. M. Z. Slawin and C. S. J. Cazin, *Dalton Trans.*, 2010, **39**, 4489.
- S. M. Opalka, J. K. Park, A. R. Longstreet and D. T. McQuade, *Org. Lett.*, 2013, **15**, 996.
- S. Zhu, R. Liang and H. Jiang, *Tetrahedron*, 2012, **68**, 7949.
- C. Gibard, H. Ibrahim, A. Gautier and F. Cisnetti, *Organometallics*, 2013, **32**, 4279.
- A. Collado, A. Gómez-Suárez, A. R. Martin, A. M. Z. Slawin and S. P. Nolan, *Chem. Commun.*, 2013, **49**, 5541.
- Concurrently, a similar procedure has been reported R. Visbal, A. Laguna and M. C. Gimeno, *Chem. Commun.*, 2013, **49**, 5642.
- (a) S. Díez-González, E. C. Escudero-Adán, J. Benet-Buchholz, E. D. Stevens, A. M. Z. Slawin and S. P. Nolan, *Dalton Trans.*, 2010, **39**, 7595; (b) A. Gómez-Suárez, R. S. Ramón, O. Songis, A. M. Z. Slawin, C. S. J. Cazin and S. P. Nolan, *Organometallics*, 2011, **30**, 5463.
- E. D. Blue, T. B. Gunnoe, J. L. Petersen and P. D. Boyle, *J. Organomet. Chem.*, 2006, **691**, 5988.
- F. R. Hartley, *Chem. Soc. Rev.*, 1973, **2**, 163.
- CCDC-940850 (**3b**), CCDC-940851 (**3c**), CCDC-940852 (**3d**) and CCDC-940853 (**3g**) contain the supplementary crystallographic data for this contribution.



VIP Simple Synthetic Routes to Carbene-M-Amido (M=Cu, Ag, Au) Complexes for Luminescence and Photocatalysis Applications

Nikolaos V. Tzouras,^[a] Ekaterina A. Martynova,^[a] Xinyuan Ma,^[a] Thomas Scattolin,^[a] Benjamin Hupp,^[b] Hendrik Busen,^[b] Marina Saab,^[a] Ziyun Zhang,^[c] Laura Falivene,^[c] Gianmarco Pisanò,^[a] Kristof Van Hecke,^[a] Luigi Cavallo,^[c] Catherine S. J. Cazin,^[a] Andreas Steffen,^{*[b]} and Steven P. Nolan^{*[a]}

Abstract: The development of novel and operationally simple synthetic routes to carbene-metal-amido (CMA) complexes of copper, silver and gold relevant for photonic applications are reported. A mild base and sustainable solvents allow all reactions to be conducted in air and at room temperature, leading to high yields of the targeted compounds even on multigram scales. The effect of various mild bases on the N–H metallation was studied in silico and experimentally, while a mechanochemical, solvent-free synthetic approach was also

developed. Our photophysical studies on [M(NHC)(Cbz)] (Cbz=carbazolyl) indicate that the occurrence of fluorescent or phosphorescent states is determined primarily by the metal, providing control over the excited state properties. Consequently, we demonstrate the potential of the new CMAs beyond luminescence applications by employing a selected CMA as a photocatalyst. The exemplified synthetic ease is expected to accelerate the applications of CMAs in photocatalysis and materials chemistry.

Introduction

In the course of the last five years, carbene-metal-amido (CMA) complexes of the coinage metals have emerged as highly promising candidates for application in organic light-emitting diodes (OLEDs) and other next-generation photonic applications.^[1–14] Some examples have already been demonstrated in highly luminescent OLEDs.^[4,6,7,9,11–13] The excited state properties of these donor-bridge-acceptor organometallic emitters have been investigated thoroughly and the structural features which modulate those properties have been largely established.^[15–18] The key structural components needed are: i) a

simple amide donor such as the carbazole framework, ii) a linear, two-coordinate d¹⁰ coinage metal (Cu, Ag, Au), and iii) an acceptor ligand of the carbene type.^[17] For the latter, the most frequently encountered ones are those of the cyclic (alkyl)(amino) carbene and monoamido- or diamido-carbene (MAC and DAC, respectively) families,^[3–14] while examples bearing the more common (benz)imidazolylidene framework and a mesoionic carbene have been reported only very recently.^[19,20] The peculiar combination of electronic properties of the single components enables the population of ligand-to-ligand (LL)CT states with a small energy gap between the singlet and triplet excited states, which is highly beneficial for emission via Thermally Activated Delayed Fluorescence (TADF) with extraordinarily high radiative rate constants k_r.^[3–14,17–19,21] However, variations of the general formula, specifically to make it more suitable for other photophysical, -chemical or -catalytic applications, has been of comparatively lower priority. A rare exception is a recent study by Li et al., where the Cu-carbazolyl moiety was combined with common imidazolylidenes as weak π-acceptors.^[19a] The authors postulate that the balance of LLCT and ligand centered (LC) ππ* states localized at the carbazolyl was tipped towards the latter, resulting in dual fluorescence and remarkably long-lived phosphorescence on the millisecond timescale in the solid state, at room temperature. Although this study was confined to CMAs of Cu and is, from our point of view, not fully consistent in the interpretation of the photophysical properties (see below), there is clear indication of great potential of this class of photoactive compounds beyond TADF. Importantly, while the origins of their photochemical behaviour are rigorously being studied,^[15–18] an aspect of the chemistry of

[a] N. V. Tzouras, E. A. Martynova, X. Ma, Dr. T. Scattolin, M. Saab, G. Pisanò, Prof. Dr. K. Van Hecke, Prof. Dr. C. S. J. Cazin, Prof. Dr. S. P. Nolan
Department of Chemistry and Centre for Sustainable Chemistry
Ghent University
Krijgslaan 281,S-3, 9000 Ghent (Belgium)
E-mail: steven.nolan@ugent.be

[b] Dr. B. Hupp, H. Busen, Prof. Dr. A. Steffen
Faculty of Chemistry and Chemical Biology
TU Dortmund University
Otto-Hahn-Str. 6, 44227 Dortmund (Germany)
E-mail: andreas.steffen@tu-dortmund.de

[c] Z. Zhang, Dr. L. Falivene, Prof. Dr. L. Cavallo
KAUST Catalysis Center, Physical Sciences and Engineering Division
King Abdullah University of Science and Technology
Thuwal 23955-6900 (Saudi Arabia)

Supporting information for this article is available on the WWW under
<https://doi.org/10.1002/chem.202101476>

© 2021 The Authors. Published by Wiley-VCH GmbH. This is an open access article under the terms of the Creative Commons Attribution License, which permits use, distribution and reproduction in any medium, provided the original work is properly cited.

CMAs (and of metal-amido complexes in general) which has remained largely stagnant deals with their synthesis.

The fundamental point of focus in the case of metal-amido complexes, regardless of the ancillary ligand employed, is the formation of the M–N bond. Synthetic routes leading to the vast majority of CMAs reported thus far make use of the well-defined [MCl(L)] complexes in combination with carbazole and a strong base such as KO^tBu, NaO^tBu, or KHMDS in THF as the solvent, in order to achieve N–H metallation.^[3–14,19] Other approaches include the early use of NaOH and NBu₄Cl as a phase transfer catalyst in a biphasic DCM/H₂O solvent system,^[22] the use of lithium amides and reaction of the latter with a [AuCl(L)] complex or a cationic gold precursor,^[23] as well as the use of the well-defined [Au(OH)(IPr)] synthon and more recently a new, commercially available Au-Aryl synthon for N–H auration in THF and benzene, respectively.^[24] In the case of Cu, amido complexes bearing phosphines have been synthesized using lithium amides or by using KHMDS as the base,^[25] while NHC-bearing complexes have been synthesized by addition of amines to a [CuMe(NHC)] complex (Me = methyl) and later by using CsOH.^[26] In the case of Ag, the amine lithiation approach was recently described for the synthesis of phosphine-stabilized Ag-amido complexes.^[27] All of these synthetic routes have been described in the literature as straightforward and practical on a small scale, yet in reality these have important flaws with regard to sustainability, atom- and step-economy and operational simplicity. For example, the use of strong bases requires strictly inert conditions, excluding air and moisture, regardless of the stability of the initial or final organometallic materials. Furthermore, many protocols are carried out in toxic solvents and require either two synthetic steps or the presence of a phase transfer catalyst and long reaction times, without being necessarily applicable to all ligand types and all coinage metals.

Therefore, we were intrigued by the possibility of providing a simplified and general synthetic protocol to access photoactive CMAs of Cu, Ag and Au bearing various carbene-type ligands, studying the excited state properties of new complexes and showcasing their application in photocatalysis. As a starting point, the use of a mild, cost-efficient and robust base should be sought to render the synthesis amenable to operationally simpler and milder conditions, as we have demonstrated in a number of recent reports.^[24b,28,29]

Results and Discussion

We began our studies by utilising the optimal reaction conditions developed for the transmetallation of organoboranes to gold,^[24b] [MCl(NHC)] complexes **1a–3a** and carbazole as the most frequently encountered amido framework (Entries 1, 7 and 11, Table 1). In these initial experiments, full conversion was not achieved in the case of gold, while in the case of silver the reaction also led to unidentified species which could only be removed from the final material by filtration through basic alumina. Increasing the temperature in the case of gold led to full conversion, while using acetone as the solvent proved to be the optimal choice as it leads to full conversion at ambient

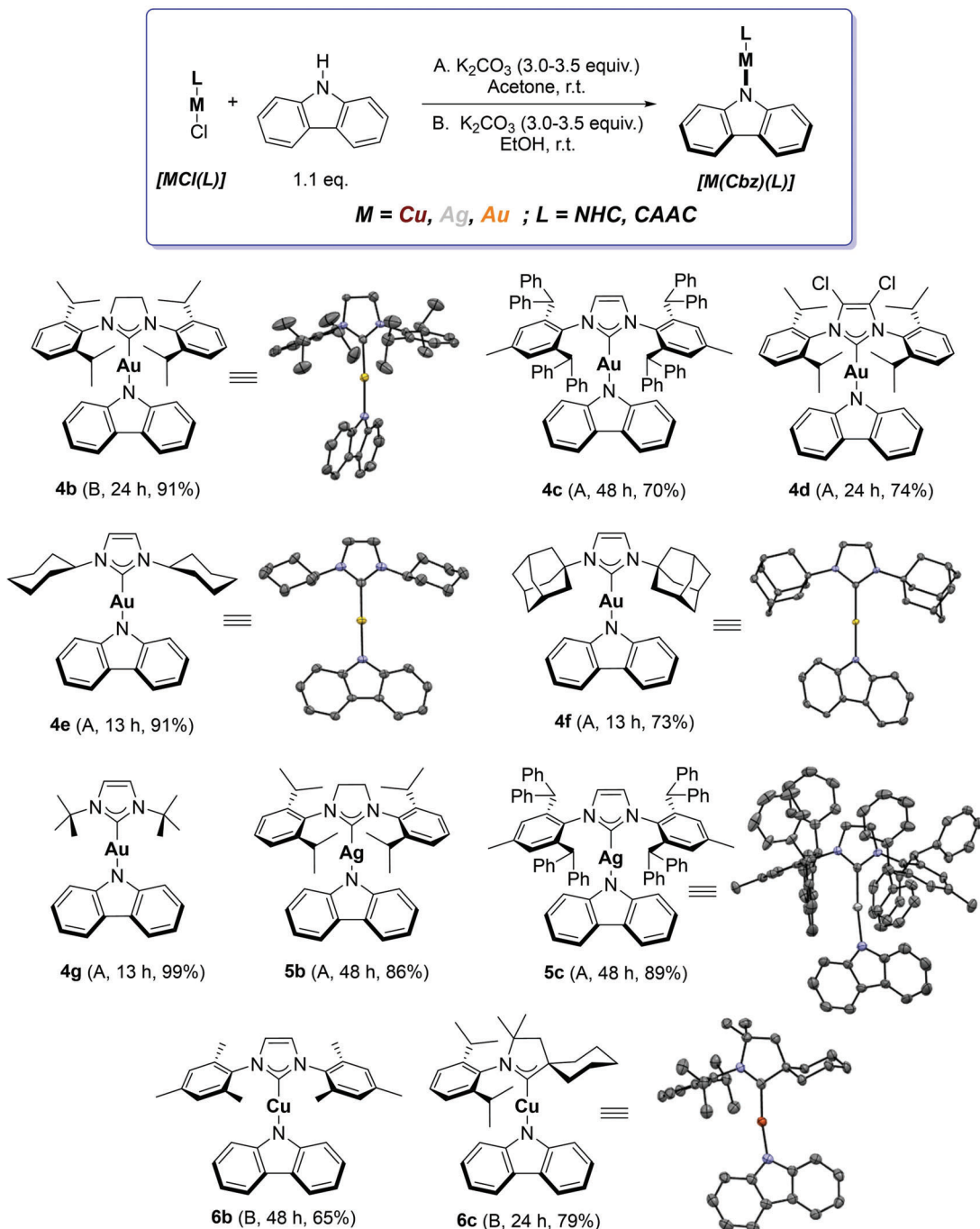
Table 1. Optimization of the synthetic protocols.

Entry/Metal ^[a]	Solvent	Base	T [°C]	Conversion/Yield [%]
1/Au	EtOH	K ₂ CO ₃	40	85
2/Au	EtOH	K ₂ CO ₃	60	100
3/Au	Acetone	K ₂ CO ₃	RT ^[b]	100/88
4/Au	Acetone	NEt ₃	40	26
5/Au	Acetone	NEt ₃	60	30 ^[c]
6/Au	EtOAc/H ₂ O 1:1	K ₂ CO ₃	60	80
7/Ag	EtOH	K ₂ CO ₃	40	100/70 ^[d]
8/Ag	THF/EtOH 4:1	K ₂ CO ₃	40	100/72 ^[d]
9/Ag	Acetone	K ₂ CO ₃	RT ^[b]	100/79
10/Ag	THF	KO ^t Bu	RT	100/72 ^[e]
11/Cu	EtOH	K ₂ CO ₃	RT ^[b]	100/87
12/Cu	Acetone	K ₂ CO ₃	40	93
13/Cu	Acetone	K ₂ CO ₃	40	93 ^[c]
14/Cu	Acetone	K ₂ CO ₃	60	100 ^[f]
15/Cu	iPrOH	K ₂ CO ₃	80	100
16/Cu	Acetone	NEt ₃	40–60	0 ^[c]

[a] Conditions unless otherwise noted: [MCl(IPr)] (50 mg), carbazole (1.1 equiv.), base (3.0 equiv.), 0.5 mL of solvent, 24 h. [b] Room temperature (RT) under operating conditions can range from 25 to 40 °C. [c] 48 h. [d] Impurities in the product spectra. [e] Inside a glovebox. [f] 3.5 equiv. of base.

temperature. Using NEt₃ as the base, or using a biphasic system, led to incomplete conversion (Entries 4–6, Table 1). DFT calculations were used to investigate the effect of different weak bases on the metallation step and a concerted N–H deprotonation/metallation with K₂CO₃ has the lowest kinetic barrier and was more thermodynamically favoured, thus supporting the fact that this base was experimentally optimal (see Supporting Information for details). In the case of silver, acetone also proved to be the superior solvent, leading to full conversion (Entry 9, Table 1). To provide a comparative test, the synthesis of **5a** was performed in a glovebox using a strong base and led to a slightly lower isolated yield (Entry 10, Table 1). Finally, in the case of copper, the use of ethanol (Entry 11, Table 1) proved best while other sets of conditions proved inferior (Entries 12–16, Table 1). Note here that solvents used are reagent grade solvents and used as received.

With the optimal conditions for all three coinage metals in hand, we began to explore the ligand scope of the synthetic method (Scheme 1). While investigating the scope, we found that the synthesis of each specific complex may benefit by slight variations of the optimal conditions shown in Table 1, such as alternating between ethanol and acetone as solvents. In the case of gold, a saturated backbone on the NHC did not affect the reaction and product **4b** was obtained in high yield. When a bulkier ligand is present, unsurprisingly the reaction is slower and requires more than 24 h to reach full conversion (see Supporting Information for detailed description). Substitu-



Scheme 1. Scope of the CMA synthetic route. The X-ray molecular structure of complexes **4b**, **4e**, **4f**, **5c** and **6c** are presented, showing thermal displacement ellipsoids at the 50% probability level and hydrogen atoms omitted for clarity (see Supporting Information for more detailed structural information).^[30]

tion on the NHC backbone did not affect the reaction, with complex **4d** obtained under the standard conditions. Complexes bearing *N*-alkyl substituted NHCs were also amenable to these conditions and the CMAs **4e–4g** were synthesized in high yields in only 13 h. In the case of silver, compounds **5b** and **5c** were successfully synthesized in high yields, and require longer reaction time, because of the increased bulk of the ligands. Interestingly, the X-ray molecular structure of **5c** shows that the plane of the carbazolyl fragment is forced to adopt a

parallel orientation with respect to the plane of the imidazolylidene moiety, which is a unique feature among complexes with *N*-aryl substituted NHC ligands reported here. This feature of **5c** in the solid state is attributed to the steric profile of the specific NHC ligand. In the case of copper, complex **6b** bearing a less bulky NHC was also synthesized but requires 48 h of reaction time. Finally, in order to showcase the versatility of the route, complexes beyond imidazol(in)ylidenes ligands were targeted. Compound **6c**, bearing a cyclic (alkyl)(amino) carbene ligand

was successfully synthesized using the very mild standard conditions.

In order to establish whether this methodology is applicable to alternative amines, we targeted the synthesis of other gold-NHC amido complexes (Scheme 2). Amines with significantly higher pK_a values than carbazole were also metallated efficiently (**4h–4j**). In the case of 2-aminopyridine, we found that use of other weak bases led to no conversion (see Supporting Information for details). The calculated energy profiles of the reaction, suggest that the kinetic barrier for a concerted deprotonation/metallation are similar for all other weak bases and theoretically should allow all transformations, however the case of K_2CO_3 is significantly more favoured thermodynamically (see Supporting Information for details) and it appears to hold a privileged position in enabling this methodology. Interestingly, the alternative use of ethanol

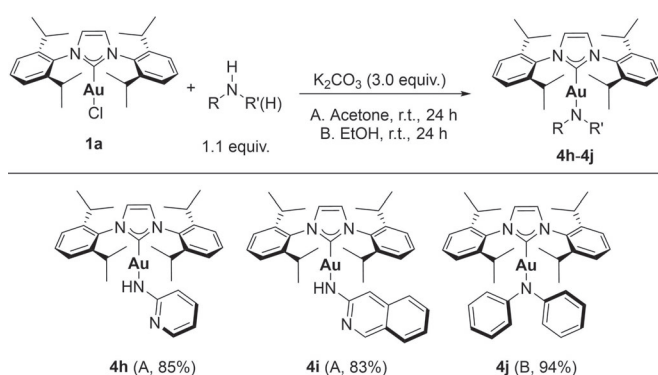
instead of acetone proved to be essential in order to achieve full conversion in the case of complex **4j**. This complex was synthesized on a gram scale, thus highlighting the scalability and versatility of the synthetic route.

Scalability is an important aspect of any synthetic method. As shown in Scheme 3, the methods described here can be carried out on multigram scale, leading to products in high purity and yields, using equimolar amounts of starting materials. Furthermore, in the case of gold and copper, one-pot syntheses of the desired CMA compounds were successfully carried out directly from the imidazolium salt and metal sources. In order to showcase potential further improvements and inspired by previous advances in mechanochemical synthesis of Cu–NHC complexes,^[29] we also performed a mechanochemical, solvent-free, high-yielding synthesis of **6a** in a planetary ball-mill, with a reaction time of 30 minutes (Scheme 3) to demonstrate an initial proof-of-concept using solvent-free methods. This is currently being further investigated in our laboratories.

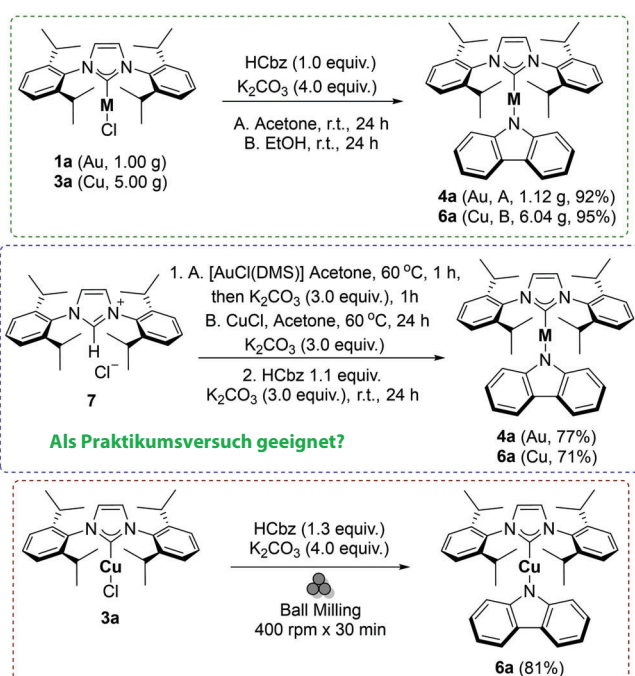
With a variety of imidazolylidene-based CMA complexes in hand, we wanted to take a closer look at their photophysical properties and applicability in photocatalysis, for which long-lived excited states are beneficial. It has previously been shown that $[\text{Au}(\text{MeIm})(\text{Cbz})]$ exhibits dual vibronically resolved phosphorescence ($\lambda_{\text{max}} = 404$ and 584 nm) in the solid state, where it forms π -stacked aggregates and intermolecular H–Au bonds.^[22a] Recently, $[\text{Cu}(\text{NHC})(\text{Cbz})]$ complexes were reported to emit from the S_1 state in solution, turning into dual fluorescence at 400–550 nm and remarkably ultralong phosphorescence at 580–750 nm on the millisecond timescale at RT in the solid state, which was attributed to the population of both $^1\pi\pi^*$ and $^3\pi\pi^*$ states localized on the carbazolyl ligand.^[19a]

The authors indicated that intermolecular forces in the single-crystals may be responsible for the long-lived emission, but do not provide further details. It is important to note that the observed phosphorescence is bathochromically shifted to that reported for HCbz, KCbz and their derivatives (ca. 400–540 nm),^[7,31,32] which excludes the interpretation of simple ^3Cbz emission. Thompson et al. previously reported that some structurally related $[\text{Cu}(\text{CAAC})(\text{Cbz})]$ complexes exhibit in the microcrystalline solid state ^3Cbz emission (ca. 430–550 nm) and in addition, due to the formation of aggregates, the same vibrationally resolved phosphorescence as reported for $[\text{Cu}(\text{NHC})(\text{Cbz})]$.^[7] Although the nature of this particular aggregate state has not been further clarified, it is feasible that its emission is due to exciton diffusion in the microcrystals, which may explain the very long lifetimes as also found for HCbz.^[32] However, the question remains whether persistent long-lived triplet states of $[\text{M}(\text{NHC})(\text{Cbz})]$ can be realized in solution and, more fundamentally, whether higher homologues of Cu could exert any influence on the excited state properties as found for coinage metal CAAC carbazolyl complexes.^[9]

For the photophysical studies, the gold and silver complexes bearing IPr (**4a**, **5a**) and SIPr (**4b**, **5b**) were chosen as they provide the best comparison with the $[\text{Cu}(\text{NHC})(\text{Cbz})]$ room temperature phosphorescence (RTPs)^[19a] and TADF emitters bearing benzimidazolylidenes.^[19b] An overview of all spectra



Scheme 2. Scope of amines in the case of gold.



Scheme 3. Large scale synthesis, one-pot synthesis and mechanochemical synthesis of CMA complexes.

and photophysical data is presented in the Supporting Information, Table S4 and Figures S5–S13.

The absorption spectra of CMA complexes **4a,b** and **5a,b** are very similar with multiple overlapping bands and shoulders between 235–380 nm (Figure 1). The high-energy bands with maxima at 239, 278 and 311 nm are assigned to LC transitions of the carbene and carbazole ligands as the metal ions neither influence the extinction coefficients nor the energies significantly.

The absorption band between 320–350 nm is considerably broadened and the corresponding extinction coefficients of the gold complexes **4a,b** of ca. $\epsilon = 11,000 \text{ M}^{-1} \text{cm}^{-1}$ surpass those of their silver congeners **5a,b** ($\epsilon \approx 4,000 \text{ M}^{-1} \text{cm}^{-1}$) by a factor of 2–3. Furthermore, this absorption band shows a minor bathochromic shift from the IPr (**4a, 5a**) to the SiPr complexes (**4b, 5b**) that most likely derives from the differences in acceptor strength between the NHC ligands. These features would be in line with the conclusion that it is a Cbz→NHC charge transfer (LLCT) with significant contribution from metal-centered orbitals. The lowest energy absorption at ca. 370 nm is only weakly allowed and independent of the nature of the carbenes, but shifts with the metal ion. Thus, it is most likely a symmetry forbidden MLCT to the Cbz. Our DFT and TD-DFT calculations generally support these assignments (see Supporting Information). However, we note that since rotation of the Cbz ligand around the M–C bond can occur with a very low energy barrier, the absorption spectrum in solution is the sum of all rotamers, each of which has different Franck-Condon-factors for the respective transitions, which can also shift in energy.^[4b,33,34]

When investigating the emission properties, stability issues were encountered (see Supporting Information), in particular for the silver complexes **5a,b**. In THF solution, **5a** displays multiple emission bands with distinct vibrational progression and an overall quantum yield of $\phi = 0.08$. The fluorescence at $\lambda_{\text{em}} = 343 \text{ nm}$ ($\tau = 13.5 \text{ ns}$) appears to stem from free carbazole as a photodecomposition product because the excitation spectrum of that band differs significantly from the absorption

(Figure S10). Between 380–440 nm, fluorescence from the ${}^1\text{C}\text{bz}$ LC state occurs as a result of insufficient spin-orbit coupling mediated by the Ag ion, leading to very slow intersystem-crossing to the triplet moieties. In addition, very weak phosphorescence from the ${}^3\text{C}\text{bz}$ state is hidden underneath the fluorescence band at $\lambda_{\text{em}} = 437 \text{ nm}$ with a significantly longer lifetime of at least 1–10 μs . A similar solution behavior is observed for **5b**, with a more pronounced ${}^3\text{C}\text{bz}$ LC emission with $\tau = 332 \mu\text{s}$, although we note that concentration and time influence the photolytic stability to a much greater extent (Figure S12). However, **4a/b** are much more stable under photolytic conditions and, in contrast to their Cu^[19] and Ag congeners **5a,b**, emit solely via phosphorescence in THF solution from a high-energy ${}^3\text{C}\text{bz}$ state at $\lambda_{\text{em}} = 430 \text{ nm}$ ($\phi = 0.32$) with exceptionally long lifetimes of $\tau = 332$ and 266 μs , respectively. The stronger spin orbital coupling (SOC) of Au apparently facilitates ISC $S_1 \rightarrow T_n$ with much higher efficiency, i.e. $k_{\text{ISC}} > 10^{10} \text{ s}^{-1}$, quenching any prompt fluorescence. Interestingly, the emissive T_1 state is not well coupled to the ground state, resulting in very small oscillator strength and low $k_{\text{phos}} \approx 10^3 \text{ s}^{-1}$, which is beneficial for photocatalytic applications (see below). We also note that the nature of the carbene ligand does not seem to influence the luminescence properties, although our TD-DFT calculations predict the ${}^3\text{LLCT}$ state to be lowest in energy for the SiPr complexes **4b/5b**, while the weaker π -acceptor IPr leads to a T_1 state of ${}^3\text{LC}$ character localized at the Cbz ligand for **4a/5a** (Supporting Information). Linearly coordinated coinage metal carbazolyl complexes are very flexible with regard to the dihedral angle between the ligand planes, which has an enormous influence on the luminescence properties.^[4b,7,14,35] Furthermore, the ordering of the excited states highly depends on the environment, i.e. polarity and specific solvent interactions. Therefore, we conclude that benzimidazole-based carbenes present a borderline in terms of π -acceptor strength to facilitate S_1/T_1 states of LLCT nature for TADF,^[7,19b] while weaker acceptors provide access to longer-lived triplet states.

In the solid state, we find that aggregation influences the luminescence properties of both the silver and gold complexes. Due to insufficient SOC, **5a,b** show significantly broadened dual fluorescence from the LC ${}^1\text{C}\text{bz}$ state at $\lambda_{\text{fl}} \approx 390 \text{ nm}$ with nanosecond lifetimes, indicative for $k_{\text{ISC}} < 10^9 \text{ s}^{-1}$, and phosphorescence between $\lambda_{\text{phos}} \approx 480$ –700 nm ($\tau = 45$ and 335 μs for **5a** and **5b**, respectively). The triplet state emission is vibrationally not well resolved and the excitation spectra display low-energy transitions between 400–480 nm distinctly different from the molecular absorption spectrum in solution (Figures S11 and S13). Gold complexes **4a,b** retain the ${}^3\text{C}\text{bz}$ emission ($\lambda_{\text{phos}} = 424 \text{ nm}$) already observed in solution. However, their respective lifetimes are significantly decreased to 74 (**4a**) and 38 (**4b**) μs , and a second, vibrationally resolved phosphorescence is detected with $\tau = 885$ and 374 μs , respectively (Figures 2 and S6). The excitation spectra of the two simultaneously phosphorescent states are very similar and in line with the absorption spectra in solution, although the longer-lived emission exhibits additional excitation bands between 400–440 nm. This leads us to conclude that besides direct excitation of the aggregate

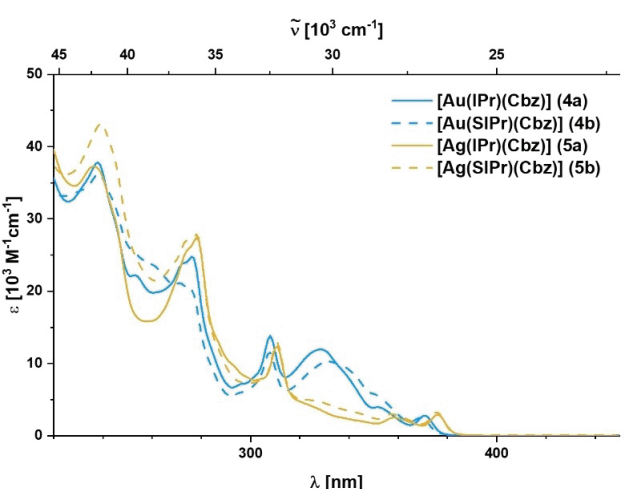


Figure 1. Absorption spectra of **4a,b** and **5a,b** in THF solution at room temperature.

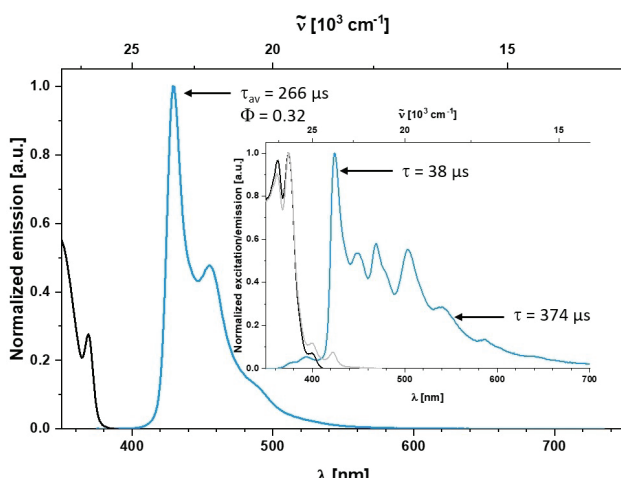


Figure 2. Normalized emission (blue) and excitation (black for $\lambda_{\text{em}} = 430 \text{ nm}$, grey for $\lambda_{\text{em}} = 540 \text{ nm}$) spectra of **4b** in THF solution and in the solid state (inset) at room temperature.

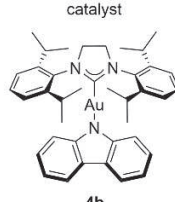
state, its emission is also triggered by triplet energy transfer from the ${}^3\text{Cbz}$ excited state of the monomers, also explaining the change in lifetime mentioned above. The implication of these findings is that the aggregate is already formed in the ground state, and its emission not merely the result of excimer formation in the solid state.

Although aggregation induced emission occurs in our Ag and Au analogs in the solid state, and despite the intermolecular interactions of **4b** in the single crystals being very similar to those reported for $[\text{Cu}(\text{IMes})\text{IPr}](\text{Cbz})$, we do not observe such remarkably long-lived RTP as reported for those Cu complexes.^[19a] But bearing in mind that it has also been reported for $[\text{Au}(\text{MeIm})(\text{Cbz})]$ and some $[\text{Cu}(\text{CAAC})(\text{Cbz})]$ complexes,^[7,22a] and that the aggregate emission of **4a,b** and **5a,b** is energetically different, it is possible that the specific crystalline environment or defect sites are responsible for the formation of very long-lived charge-separated excitons as recently reported for HCbz.^[32]

Complex $[\text{Au}(\text{SiPr})(\text{Cbz})]$ (**4b**) demonstrated the highest photostability, high-energy phosphorescence in the blue-green range with a remarkable long lifetime in solution, and showed an indication to undergo energy transfer, and was thus chosen as triplet state sensitizer for a proof-of-concept photocatalysis reaction. We selected (E,E')-dicinnamyl ether as the substrate for a [2+2] cycloaddition via triplet energy transfer^[36] upon irradiation at 365 nm with a 18 W LED, where **4b** still offers a reasonable extinction coefficient and absorption by common borosilicate glass does not appear to be a major issue. Both catalyst loading and irradiation time were varied to screen the performance limit of **4b** (Table 2, Entries 1–5) in this initial photocatalytic study.

Full conversion to the desired cycloaddition product was only achieved with **4b** acting as a photocatalyst. While some conversion (12%) was observed in the absence of **4b** after irradiation for 21 h (entry 6), most likely the result of direct excitation of the triplet state of (E,E')-dicinnamyl ether, the

Table 2. Optimization and control studies for the photocatalytic [2+2] cycloaddition.

Entry	Catalyst Load ^[a] [mol %]	Time [h]	Conversion ^[b] [%]	
			THF	catalyst
1	50	21	> 99	
2	10	21	> 99	
3	5	21	> 99	
4	10	4	> 99	
5	5	4	> 99	
6	none	21	12	
7 ^[c]	10	21	0	

[a] Catalyst loading for entry 1 was simply weighed, for Entries 3–7, a stock solution in THF was used. [b] Conversions were determined from the ratio of the product and reactant signals in the ${}^1\text{H}$ NMR spectrum. [c] Control reaction performed in the dark.

reaction was completely inhibited when kept in the dark. Overall, **4b** exhibits remarkable efficiency for a non-optimized photocatalyst in this chosen [2+2] cycloaddition reaction. Further work is ongoing to test the potential of **4b** and related complexes as photocatalysts.

Conclusion

We have demonstrated for the first time that CMAs derived from copper-, silver- and gold-NHC complexes can be accessed via simple and sustainable synthetic routes. This methodology makes use of a mild base, K_2CO_3 , which proved to be superior to other mild bases both experimentally and computationally. The issue of solvent use was addressed in the deployment of green solvents (acetone and ethanol) in reactions performed in classical batch mode and under solventless conditions using a mechanochemical approach, which is also showcased for the first time for CMA synthesis. The synthesis of CMAs displays a wide scope with regard to both the NHC ligand and the amine used, while it is scalable and does not require elaborate experimental setups and/or handling. The potential of this advance is evident not only by the simplicity and mild conditions used, but also by the examples of CMA synthesis directly from imidazolium salts, metal sources and carbazole in a one-pot fashion. The combination of desirable reaction solvents, mild reagents, open-to-air conditions and wide scope are expected to significantly aid in the construction of diverse CMA libraries for photochemical and other applications. Considering the original aim of the photophysical and photocatalytic survey, two important insights are provided by this study: 1) the influence of the transition metal on the emission properties of NHC-M-Cbz is perceivable (enhanced SOC to facilitate ISC, ultimately giving pure phosphorescence for Au), but within the boundaries of this particular ligand system, highly efficient

emitters rivalling analogous CAAC or MAC complexes are not obtainable solely by changing the metal and 2) minor variations of the carbene ligand are far more consequential, as a comparison with the corresponding benzimidazole-based carbene complexes reported by Thompson and co-workers^[19b] illustrates, however, the introduction of the 4d and, particularly, 5d TM appears to be highly beneficial to fine-tune photochemical properties. This was confirmed by the impressive performance of the fairly simple gold complex [Au(SIPr)(Cbz)] (4b) in a proof-of-concept photocatalysis reaction, where complete conversion was achieved even at relatively low catalyst loadings (5 mol%) and short reaction times (4 h). This finding may provide a new perspective on the wide-ranging applicability of CMAs, especially with highly versatile carbenes such as 5-membered imidazole-based NHCs, that have attracted much less attention in studies of CMA complexes due to their lackluster performance in OLED emitter materials.

Acknowledgements

We gratefully acknowledge VLAIO (SBO project CO2PERATE), the Special Research Fund (BOF) of Ghent University is also acknowledged for Doctoral Scholarship (01D14919) to NVT, starting and project grants to SPN and CSJC, and project grant (01N03217) to KVH and MS. XM thanks the China Scholarship Council (CSC) for a PhD scholarship. The Research Foundation – Flanders (FWO) is also gratefully acknowledged for a Fundamental Research PhD fellowship to NVT (11I6921N) and project AUGE/11/029 to KVH. AS thanks the DFG (STE1834/4-2). This work was also supported by Deutsche Forschungsgemeinschaft [DFG, Priority Program SPP 2102 “Light-controlled reactivity of metal complexes” (1834/7-1)]. Umicore AG is thankfully acknowledged for generous gifts of materials. Open access funding enabled and organized by Projekt DEAL.

Conflict of Interest

The authors declare no conflict of interest.

Keywords: carbene-metal-amides • coinage metal-N-heterocyclic carbene complexes • mechanochemistry • photocatalysis • synthetic methods

- [1] a) R. Visbal, M. C. Gimeno, *Chem. Soc. Rev.* **2014**, *43*, 3551–3574; b) V. W.-W. Yam, A. K.-W. Chan, E. Y.-H. Hong, *Nat. Chem. Rev.* **2020**, *4*, 528–541; c) G. U. Mahoro, J. Fernandez-Cestau, J.-L. Renaud, P. B. Coto, R. D. Costa, S. Gaillard, *Adv. Opt. Mater.* **2020**, *8*, 2000260.
- [2] A. Steffen, B. Hupp, Reference Module in *Chemistry, Molecular Sciences and Chemical Engineering*, Elsevier, 2019.
- [3] A. S. Romanov, C. R. Becker, C. E. James, D. Di, D. Credgington, M. Linnolahti, M. Bochmann, *Chem. Eur. J.* **2017**, *23*, 4625–4637.
- [4] a) D. Di, A. S. Romanov, L. Yang, J. M. Richter, J. P. H. Rivett, S. Jones, T. H. Thomas, M. Abdi Jalebi, R. H. Friend, M. Linnolahti, M. Bochmann, D. Credgington, *Science* **2017**, *356*, 159–163; b) J. Föller, C. M. Marian, *J. Phys. Chem. Lett.* **2017**, *8*, 5643–5647.
- [5] A. S. Romanov, S. T. E. Jones, L. Yang, P. J. Conaghan, D. Di, M. Linnolahti, D. Credgington, M. Bochmann, *Adv. Opt. Mater.* **2018**, *6*, 1801347.
- [6] A. S. Romanov, L. Yang, S. T. E. Jones, D. Di, O. J. Morley, B. H. Drummond, A. P. M. Reponen, M. Linnolahti, D. Credgington, M. Bochmann, *Chem. Mater.* **2019**, *31*, 3613–3623.
- [7] a) R. Hamze, J. L. Peltier, D. Sylvinson, M. Jung, J. Cardenas, R. Haiges, M. Soleilhavoup, R. Jazzaar, P. I. Djurovich, G. Bertrand, M. E. Thomson, *Science* **2019**, *363*, 601–606; b) With regard to the discussion of the solid state aggregates of [Cu(Cbz)(CAAC)], we mainly refer to the Supporting Information (Figures S22 and S23) of this reference.
- [8] S. Shi, M.-C. Jung, C. Coburn, A. Tadle, D. Sylvinson, M. R. P. I. Djurovich, S. R. Forrest, M. E. Thomson, *J. Am. Chem. Soc.* **2019**, *141*, 3576–3588.
- [9] R. Hamze, S. Shi, S. Kapper, D. Muthiah Ravinson, L. Estergreen, M.-C. Jung, A. Tadle, R. Haiges, P. I. Djurovich, J. L. Peltier, R. Jazzaar, G. Bertrand, S. E. Bradford, M. E. Thomson, *J. Am. Chem. Soc.* **2019**, *141*, 8616–8626.
- [10] A. S. Romanov, F. Chotard, J. Rashid, M. Bochmann, *Dalton Trans.* **2019**, *48*, 15445–15454.
- [11] A. S. Romanov, S. T. E. Jones, Q. Gu, P. J. Conaghan, B. H. Drummond, J. Feng, F. Chotard, L. Buizza, M. Foley, M. Linnolahti, D. Credgington, M. Bochmann, *Chem. Sci.* **2020**, *11*, 435–446.
- [12] P. J. Conaghan, C. S. B. Matthews, F. Chotard, S. T. E. Jones, N. C. Greenham, M. Bochmann, D. Credgington, A. S. Romanov, *Nat. Commun.* **2020**, *11*, 1758.
- [13] J. Feng, E. J. Taffet, A.-P. M. Reponen, A. S. Romanov, Y. Olivier, V. Lemaur, L. Yang, M. Linnolahti, M. Bochmann, D. Beljonne, D. Credgington, *Chem. Mater.* **2020**, *32*, 4743–4753.
- [14] M. Gernert, L. Balles-Wolf, F. Kerner, U. Müller, A. Schmiedel, M. Holzapfel, C. M. Marian, J. Pflaum, C. Lambert, A. Steffen, *J. Am. Chem. Soc.* **2020**, *142*, 8897–8909.
- [15] E. J. Taffet, Y. Olivier, F. Lam, D. Beljonne, G. D. Scholes, *J. Phys. Chem. Lett.* **2018**, *9*, 1620–1626.
- [16] C. R. Hall, A. S. Romanov, M. Bochmann, S. R. Meech, *J. Phys. Chem. Lett.* **2018**, *9*, 5873–5876.
- [17] J. Feng, A.-P. M. Reponen, A. S. Romanov, M. Linnolahti, M. Bochmann, N. C. Greenham, T. Penfold, D. Credgington, *Adv. Funct. Mater.* **2021**, *31*, 2005438.
- [18] F. Chotard, V. Sivchik, M. Linnolahti, M. Bochmann, A. S. Romanov, *Chem. Mater.* **2020**, *32*, 6114–6122.
- [19] a) J. Li, L. Wang, Z. Zhao, X. Li, X. Yu, P. Huo, Q. Jin, Z. Liu, Z. Bian, C. Huang, *Angew. Chem. Int. Ed.* **2020**, *59*, 8210–8217; *Angew. Chem.* **2020**, *132*, 8287–8294; b) R. Hamze, M. Idris, D. Muthiah Ravinson, M. C. Jung, R. Haiges, P. I. Djurovich, M. E. Thomson, *Front. Chem.* **2020**, *8*, 401; c) B. M. Hockin, C. F. R. Mackenzie, D. B. Cordes, A. M. Z. Slawin, N. Robertson, E. Zysman-Colman, *J. Coord. Chem.* **2021**, *74*, 361–379.
- [20] L. Cao, S. Huang, W. Liu, H. Zhao, X.-G. Xiong, J.-P. Zhang, L.-M. Fu, X. Yan, *Chem. Eur. J.* **2020**, *26*, 17722–17729.
- [21] a) M. Bochmann, A. S. Romanov, D. Credgington, D. Di, L. Young (University of East Anglia, Cambridge Enterprise Ltd), WO 2017/046572 A1, 2017; b) M. E. Thompson, P. I. Djurovich, R. Hamze, S. Shi, J. Moon Chul (University of Southern California Los Angeles), EP 3 489 243 A1, 2019.
- [22] a) H. M. J. Wang, C. S. Vasam, T. Y. R. Tsai, S.-H. Chen, A. H. H. Chang, I. J. B. Lin, *Organometallics* **2005**, *24*, 486–493; b) V. W.-W. Yam, J. K.-W. Lee, C.-C. Ko, N. Zhu, *J. Am. Chem. Soc.* **2009**, *131*, 912–913; c) L. Jhulkil, R. Purkait, H. K. Kisan, V. Bertolasi, A. A. Isab, C. Sinha, J. Dinda, *Appl. Organomet. Chem.* **2020**, *34*, e5673.
- [23] a) M. W. Johnson, S. L. Shevick, F. D. Toste, R. G. Bergman, *Chem. Sci.* **2013**, *4*, 1023–1027; b) S. Kim, F. D. Toste, *J. Am. Chem. Soc.* **2019**, *141*, 4308–4315.
- [24] a) A. Gómez-Suárez, D. J. Nelson, D. G. Thompson, D. B. Cordes, D. Graham, A. M. Z. Slawin, S. P. Nolan, *Beilstein J. Org. Chem.* **2013**, *9*, 2216–2223; b) N. V. Tzouras, M. Saab, W. Janssens, T. Cauwenbergh, K. Van Hecke, F. Nahra, S. P. Nolan, *Chem. Eur. J.* **2020**, *26*, 5541–5551.
- [25] a) E. D. Blue, A. Davis, D. Conner, T. B. Gunnoe, P. D. Boyle, P. S. White, *J. Am. Chem. Soc.* **2003**, *125*, 9435–9441; b) S. Wiese, Y. M. Badie, R. T. Gephart, S. Mossin, M. S. Varonka, M. M. Melzer, K. Meyer, T. R. Cundari, T. H. Warren, *Angew. Chem. Int. Ed.* **2010**, *49*, 8850–8855; *Angew. Chem.* **2010**, *122*, 9034–9039; c) Y.-E. Kim, J. Kim, J. Park, K. Park, Y. Lee, *Chem. Commun.* **2017**, *53*, 2858–2861; d) A. C. Brannan, Y. Lee, *Inorg. Chem.* **2020**, *59*, 315–324.
- [26] a) L. A. Goj, E. D. Blue, C. Munro-Leighton, T. B. Gunnoe, J. L. Petersen, *Inorg. Chem.* **2005**, *44*, 8647–8649; b) M. Trose, F. Lazreg, T. Chang, F. Nahra, D. B. Cordes, A. M. Z. Slawin, C. S. J. Cazin, *ACS Catal.* **2017**, *7*,

RESEARCH ARTICLE

INORGANIC CHEMISTRY

Eliminating nonradiative decay in Cu(I) emitters: >99% quantum efficiency and microsecond lifetime

Rasha Hamze¹, Jesse L. Peltier², Daniel Sylvinson¹, Moonchul Jung¹, Jose Cardenas¹, Ralf Haiges¹, Michele Soleilhavoup², Rodolphe Jazza², Peter I. Djurovich¹, Guy Bertrand², Mark E. Thompson^{1*}

Luminescent complexes of heavy metals such as iridium, platinum, and ruthenium play an important role in photocatalysis and energy conversion applications as well as organic light-emitting diodes (OLEDs). Achieving comparable performance from more-earth-abundant copper requires overcoming the weak spin-orbit coupling of the light metal as well as limiting the high reorganization energies typical in copper(I) [Cu(I)] complexes. Here we report that two-coordinate Cu(I) complexes with redox active ligands in coplanar conformation manifest suppressed nonradiative decay, reduced structural reorganization, and sufficient orbital overlap for efficient charge transfer. We achieve photoluminescence efficiencies >99% and microsecond lifetimes, which lead to an efficient blue-emitting OLED. Photophysical analysis and simulations reveal a temperature-dependent interplay between emissive singlet and triplet charge-transfer states and amide-localized triplet states.

Organometallic complexes of heavy metals often phosphoresce from high-energy, long-lived triplet states with high luminance efficiency, enabling applications ranging from photocatalysis (*7*) and chemo- and biosensing (*2, 3*) to dye-sensitized solar cells (*4*) and organic electronics (*5, 6*). By contrast, phosphorescence of typical organocupper complexes is inefficient (*7, 8*) compared to organo-Ir and organo-Pt phosphors (*9*). This difference largely stems from the rates of two intersystem crossing (ISC) processes. The spin-orbit coupling (SOC) parameter (ξ) that facilitates ISC is smaller for the Cu nucleus ($\xi = 857 \text{ cm}^{-1}$) than for heavier metals such as Ir and Pt ($\xi = 3909$ and 4481 cm^{-1} , respectively) (*10*). Therefore, the rate of ISC from the lowest excited singlet state (S_1) to the lowest triplet excited state (T_1) typically is on the order of 10^{10} to 10^{11} s^{-1} in Cu complexes (*11, 12*) as opposed to 10^{13} to 10^{14} s^{-1} in heavy metal complexes (*13, 14*). The rate of radiative ISC from T_1 to the ground state (S_0) is markedly slower in organocupper phosphors ($k = 10^3$ to 10^4 s^{-1}) compared to Ir and Pt emitters ($k > 10^5 \text{ s}^{-1}$) (*5, 15*). Moreover, the lowest-energy optical transitions in most Cu(I) complexes are typically metal-to-ligand charge transfer (MLCT) events, which are associated with large reorganization energies. In these MLCT transitions, formal oxidation at

the d^{10} metal center induces Jahn-Teller distortion (*16*) that not only increases nonradiative decay rates but also leads to ISC rates even slower than those expected based only on SOC considerations (*17*).

In the past decade, thermally assisted delayed fluorescence (TADF) has emerged as a useful alternative for harvesting both singlet and triplet excitons generated in organic light-emitting diodes (OLEDs) (*18–21*). This process is accomplished by bringing the S_1 and T_1 manifolds close enough in energy to give high rates for exo- and endothermic ISC between them (Fig. 1A). The resulting equilibrium between S_1 and T_1 typically favors the longer-lived, weakly emissive triplet; however, a high radiative rate from S_1 can lead to a high radiative efficiency for the TADF process. A conundrum in purely organic, donor-acceptor-type TADF systems is raised by the opposing requirements for minimizing the energy gap between the two lowest excited states ($\Delta E_{S_1-T_1}$) through poor highest occupied molecular orbital (HOMO)-lowest unoccupied molecular orbital (LUMO) overlap and achieving high radiative rates for the S_1 state via large orbital overlap (*22*). TADF also occurs in Cu(I) complexes and was first observed by McMillin and co-workers (*23*). In such Cu complexes, the HOMO is typically metal-based, and the LUMO is composed of ligand π^* orbitals. However, Cu TADF systems present a major departure from their pure organic counterparts: Forward ISC in the Cu(I) compounds is fast enough to quantitatively depopulate the S_1 state, thereby completely outpacing prompt fluorescence and resulting in monoexponential

emission decay at all temperatures. To illustrate, a highly emissive Cu complex with the smallest recorded $\Delta E_{S_1-T_1} = 33 \text{ meV}$ has a radiative rate (k_r) of $2 \times 10^5 \text{ s}^{-1}$ in the solid state at room temperature (it is only weakly emissive in fluid solution) (*20*). Fitting the temperature-dependent photoluminescent decay of this complex to the modified Boltzmann Eq. 1, where k_{S_1} and k_{T_1} are the rate constants for radiative decay from the S_1 and T_1 states, respectively, k_B is Boltzmann's constant, and T is temperature, gives a derived rate of fluorescence (prompt emission from S_1) of $2 \times 10^6 \text{ s}^{-1}$ (*24*), which is a full order of magnitude faster than the recorded rate of emission (TADF) at room temperature. It is therefore reasonable to conclude that the limiting factor in determining the rate of TADF in Cu systems is the endothermic ISC from T_1 to S_1 , which is tied to SOC as shown in Eq. 2, where ρ_{FC} denotes the Frank-Condon density of states and $|<S_1|\hat{H}_{SO}|T_1>|$ denotes the SOC matrix element (*25*). Nevertheless, even the most efficient TADF-based Cu emitters have low photoluminescence (PL) quantum yields (Φ_{PL}) in fluid or polymeric matrices. High rates of nonradiative decay are observed in nonrigid environments owing to substantial distortions in the excited state of frequently studied tetrahedral motifs (*26, 27*):

$$\tau_{\text{TADF}} = \frac{3 + \exp\left(\frac{\Delta E_{S_1-T_1}}{k_B T}\right)}{3k_{T_1} + k_{S_1} \exp\left(\frac{\Delta E_{S_1-T_1}}{k_B T}\right)} \quad (1)$$

$$k_{\text{ISC}} = \frac{2\pi}{\hbar} \rho_{FC} |<S_1|\hat{H}_{SO}|T_1>|^2 \quad (2)$$

Reports of linear Cu complexes with high Φ_{PL} in nonrigid matrices highlight the appeal of low coordination in limiting excited-state reorganization (*28–30*). Unfortunately, the MLCT nature of the radiative transitions in these derivatives leads to excited-state lifetimes that are relatively long ($\tau \sim 20 \mu\text{s}$), thus limiting their luminescent efficiency. However, a recent paper by Di *et al.* has reported efficient green electroluminescence (EL) in OLEDs using two-coordinate carbene-gold and carbene-copper complexes [maximum external efficiency (EQE_{max}) = 26.3% for the former and 9.7% for the latter] (*19*). The complexes discussed by Di *et al.* consist of Au(I) or Cu(I) ions coordinated to a cyclic (alkyl)(amino)carbene (CAAC) (*31, 32*) and an N-bound amide. Here we examine a closely related family of two-coordinate, neutral CAAC-Cu(I)-amide complexes with notable photophysical properties (see Fig. 1; compound **1b** was examined by Di *et al.*) . Optimizing the steric encumbrance of substituents on the carbene, we achieve complexes with $\Phi_{PL} > 99\%$ and short emission lifetimes ($\tau = 2$ to $3 \mu\text{s}$) in fluid and polymeric media. Electrochemical, photophysical, and computational analyses reveal a picture of ligand-based frontier orbitals with minimal metal contribution. Coplanar ligand conformation in these complexes is critical to maintaining high Φ_{PL} . Finally, one of the complexes is used in blue OLEDs.

¹Department of Chemistry, University of Southern California, Los Angeles, CA, USA. ²UCSD-CNRS Joint Research Laboratory (UMI 3555), Department of Chemistry and Biochemistry, University of California, San Diego, La Jolla, CA 92093-0358, USA.

*Corresponding author. Email: met@usc.edu

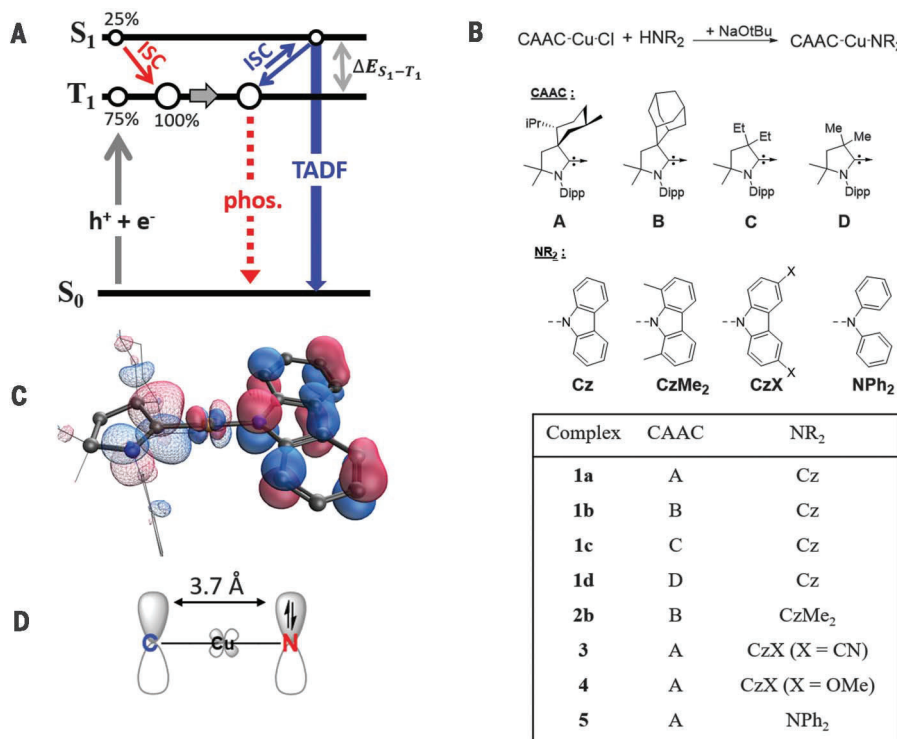


Fig. 1. Background and chemical structures of CAAC-Cu-amides. (A) Scheme depicting the radiative processes [phosphorescence (phos.) and TADF] in an OLED. (B) Complexes studied in this work. Dipp, 2,6-diisopropylphenyl; tBu, tert-butyl; iPr, isopropyl; Et, ethyl; Me, methyl. (C) HOMO (solid) and LUMO (mesh) surfaces of complex **1a**. (D) Simplified picture of the HOMO and LUMO of complex **1a**.

Structural and electronic properties of CAAC-Cu-amide complexes

The two-coordinate CAAC-Cu-amide complexes were prepared in high yields (80 to 90%) following literature procedures (Fig. 1B) (19). Complexes **1** to **5** were isolated as white to yellow powders and display varying degrees of sensitivity to O₂ and moisture depending on the steric bulk around the carbene and the nature of the amide. Complex **1b**, bearing 1,8-dimethyl carbazolidine (CzMe₂), was found to be highly sensitive to H₂O and CO₂ in ambient air as a solid and in solution (see the supplementary materials).

X-ray diffraction analysis was performed on single crystals of the complexes **1a**, **1c**, **1d**, **2b**, and **3** to **5** (see figs. S1 to S8 and tables S1 to S8). The structures all display a near-linear coordination geometry around the Cu center (174° to 179°), with a 3.73 to 3.77 Å separation between the carbene carbon and the amide nitrogen owing to similar bond lengths (C–Cu = 1.88 to 1.89 Å; Cu–N = 1.85 to 1.87 Å). Dihedral angles between the ligands are <9° in complexes **1a**, **1c**, **1d**, and **3** to **5**, whereas complex **2b** has a near orthogonal conformation (dihedral angle = 83°). Despite the asymmetry of the CAAC, only one set of ¹H NMR (nuclear magnetic resonance) spectroscopic resonances for the carbazolidine is observed in all complexes. This observation indicates rapid exchange on the NMR time scale, likely caused by rotation around the C_{carbene}–N_{amide} axis. Variable temperature NMR experiments performed on complex

1a down to -60°C show no signs of coalescence, which suggests a low energy barrier for the rotation in question. Complex **2b** also shows one set of carbazolidine resonances in its ¹H NMR spectrum, consistent with an orthogonal conformation for the ligands.

The electrochemical properties of the Cu complexes **1a** and **3** to **5**, precursors (CAAC^{Men}-CuCl, where CAAC^{Men} is ligand A in Fig. 1B, and the free amines), and potassium carbazolidine (KCz) were examined (see fig. S11 and table S11 for details). The Cu complexes undergo irreversible oxidation at potentials that vary over a 1-V range, depending on the donor strength of the amide ligand. Relative to their parent amines, the oxidation potentials of the Cu-amides decrease by 0.6 to 0.7 V. All potentials fall well below the Cu(I) oxidation potential of CAAC^{Men}-CuCl. The oxidation potential of **1a** is anodically shifted by 0.73 V compared to that of KCz, consistent with metalation. Reduction potentials are quasi-reversible, with values that are unchanged from the parent CAAC^{Men}-CuCl. The data show that the redox potentials are independently controlled by the ligands: Oxidation is primarily at the amide, and reduction at the π-accepting carbene.

The redox noninnocent nature of the ligands is also captured by density functional theory (DFT; B3LYP/LACVP**). As shown in Fig. 1C, the HOMO is principally amide-based, with substantial electron density residing in the filled p orbital of N_{amide}. The LUMO is localized largely

on the unfilled p orbital of C_{carbene}. The nature of the frontier molecular orbitals and coplanar orientation of the ligands allow for a simplified representation of the valence structure (Fig. 1D) as a donor-bridge-acceptor linear system, wherein the metal d orbitals act as a weak electronic bridge between the parallel donor (N_{amide} 2p_x) and acceptor (C_{carbene} 2p_x) orbitals, thereby illustrating the potential for long-range π interaction (33, 34). The ground state of these complexes is marked by a large permanent dipole, μ_g ~11.3 D, in close agreement with the report by Föller and Marian for an isoelectronic Au complex (35).

Absorption spectra of complexes **1a**, **1b**, **2b**, and **3** to **5** in tetrahydrofuran (THF) (Fig. 2A) show high-energy bands ($\lambda < 350$ nm) corresponding to π-π* transitions of the ligands. Broad, low-energy bands apparent in these complexes are assigned to singlet interligand charge transfer (ICT) from the electron-rich amide to the electron-accepting carbene. The onset of the ICT bands for **1a** and **3** to **5** falls in the order expected based on the oxidation potentials of their amide ligands (inset of Fig. 2A). A notable feature of the ICT transitions in these complexes is their high extinction coefficients ($\epsilon > 10^3 \text{ M}^{-1} \text{ cm}^{-1}$), which is surprising considering the ~3.7 Å separation between the HOMO and LUMO. These values are a factor of 10 greater than what is typically observed for MLCT transitions in organocupper complexes. We tentatively attribute the strongly allowed nature of the charge-transfer (CT) transitions in these complexes to the small but nonnegligible contribution of the Cu d orbitals acting as an effective electronic bridge between the donor and the acceptor components. In addition, the coplanarity of the ligands leads to a parallel orientation of the filled 2p_x orbital on the amide N and the empty 2p_x orbital on the carbene C, maximizing long-range orbital overlap.

A characteristic property of the ICT band in these complexes is the pronounced hypsochromic shift as solvent polarity increases (Fig. 2B). The absorption onset of the ICT band undergoes a blue shift of 2400 cm⁻¹ in **1a** and 2600 cm⁻¹ in **5** upon increasing solvent polarity. The magnitude of the shift reflects a strong change in the electronic dipole moment upon excitation. The direction of the shift is a consequence of the ground-state dipole being much larger in magnitude and opposite in orientation relative to its excited-state counterpart (36). Similar hypsochromic shifts of the ICT absorption band are observed upon freezing the solvent matrix and are more pronounced in methylcyclohexane (MeCy) than in 2-methyltetrahydrofuran (2-MeTHF) (Fig. 2C). The blue shift in 2-MeTHF at 77 K is likely due to the solvent dipoles being frozen around the large solute dipole, stabilizing the ground state (relaxing the potential energy surface) and destabilizing the ICT excited state. The blue shift recorded in MeCy at 77 K, where the solubility of **1a** is reduced, can be brought about by long-range dipole-dipole interactions between the solute molecules (37). In both instances, the hypsochromic shift is absent when the solvent glass is thawed.

Efficient luminescence from allowed interligand charge transfer transitions

The Cu complexes all luminesce with high efficiency in fluid solution, as well as when doped in polystyrene (PS) matrices, manifesting microsecond radiative lifetimes (Fig. 3A and Table 1). Pow-

ered samples of the carbazolide complexes **1a** to **1d** and **3** are poorly emissive, whereas **2b**, **4**, and **5** exhibit stronger luminescence in their microcrystalline forms than in solution (see figs. S22, S23, and S26 and table S15). Emission spectra of **1a** to **1d**, **4**, and **5** in 2-MeTHF solutions are

broad and featureless at room temperature, consistent with the ICT origin of these transitions. The PL efficiency improves as the steric encumbrance on the carbene increases in the series **1d** < **1c** < **1b** < **1a** ($\Phi_{PL} = 0.1$, 0.6, 0.7, and 1.0, respectively). Because **1a** to **1d** have similar

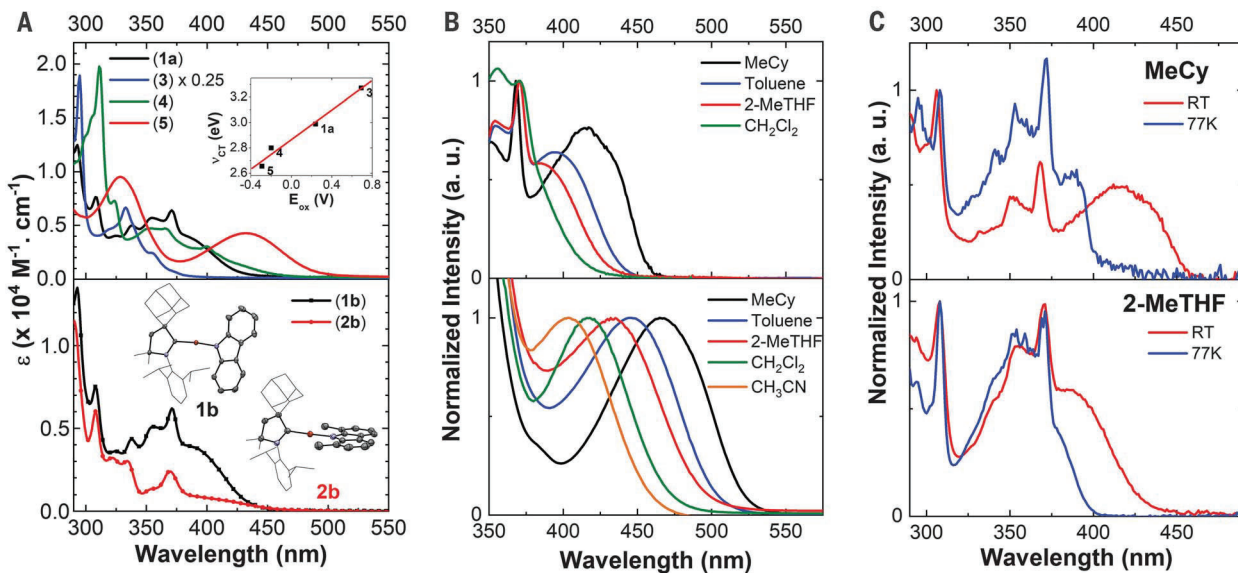


Fig. 2. Electronic spectra of CAAC-Cu-amides. (A) Absorption spectra of complexes **1a**, **1b**, **2b**, and **3** to **5** in THF. The inset in the top spectrum shows a linear relation between the energy of the CT absorption band (v_{CT}) in MeCy and the oxidation potential (E_{ox}) of the complexes. The crystal structures of complexes **1b** and **2b** are shown as insets in the bottom

spectrum. The pendant adamantyl and Dipp groups are depicted in wireframe for clarity. (B) Blue shift of the ICT absorption band with increasing solvent polarity observed in complexes **1a** and **5**. (C) Absorption spectra of complex **1a** at room temperature (RT) and 77 K, showing a blue shift at low temperature. a.u., arbitrary units.

Table 1. Photophysical data for complexes **1a, **1b**, **2b**, and **3** to **5** doped 1% by weight into PS films or dissolved at 10^{-5} M concentration in 2-MeTHF.** n.d., not determined.

Complex	Emission at room temperature				Emission at 77 K		
	λ_{max} (nm)	τ (μs)	Φ_{PL}	k_r (s ⁻¹)	k_{nr} (s ⁻¹)	λ_{max} (nm)	τ (μs)
1% weight PS films							
1a	474	2.8	1.0	3.5×10^5	3.6×10^3	480	64
3	426 1300 (30%)	240 (70%) 1300 (30%)	0.82	1.5×10^3	3.2×10^2	424	6900
4	518	2.3	1.0	4.3×10^5	$<4.4 \times 10^3$	490	550
5	532	2.6	0.78	3.0×10^5	8.5×10^4	536	264
2-MeTHF							
1a	492	2.5	1.0	3.9×10^5	$<8.0 \times 10^3$	430	7300
1b	510	2.3	0.68	3.0×10^5	1.7×10^5	430	430 nm: 3000 500 nm: 48
1c	500	1.8	0.56	3.1×10^5	2.4×10^5	430	7000
1d	510	0.54	0.11	2.0×10^5	1.6×10^6	430	5000
2b	542 2.3 (21%)	0.86 (79%) 2.3 (21%)	0.12	$1.1 \times 10^{5*}$	$8.0 \times 10^{5*}$	438	430 nm: 2400 500 nm: 37
3	428 590 [†]	450 nm: 8.3 600 nm: 8.0	0.11	n.d.	n.d.	422	12,000
4	558	0.28	0.25	8.9×10^5	2.7×10^6	470	Seconds
5	580	0.87	0.16	1.8×10^5	9.7×10^6	500	215

*Calculated from a weighted average of the two contributions to τ .

[†]Excimer peak.

radiative rate constants ($k_r = 2.0 \times 10^5$ to 4.3×10^5 s $^{-1}$), the principal effect of increasing steric bulk is to decrease the rates of nonradiative decay. Complexes **4** and **5** show red-shifted emission relative to complex **1a**, with radiative rates comparable to that of **1a** (Table 1). The sparingly soluble complex **3** shows narrow, structured emission centered at 426 nm in solution and has a radiative rate constant that is lower than the other complexes, features we attribute to emission from a state with predominant triplet-carbazole (${}^3\text{Cz}$) character, vide infra (Fig. 3D). In addition, complex **3** displays a low energy ($\lambda \sim 600$ nm) concentration-dependent emission band in solution, characterized by a rise time in its PL decay traces (see fig. S34 and table S17), which is consistent with the diffusional process required to form a luminescent excimer.

To eliminate the complications of aggregation and excimer formation in photophysical studies, we doped the complexes into thin films [1 weight

% in PS], where excimer formation is suppressed. At room temperature, samples in the rigid matrix exhibit a blue shift in their emission relative to spectra recorded in solution (i.e., rigidochromism) and suppressed rates of nonradiative decay (Fig. 3A). Complexes **1a** and **4** display broad emission with near unity quantum efficiency in PS ($\Phi_{PL} = 1.0$), whereas complex **5** is less efficient ($\Phi_{PL} = 0.78$) (Table 1). Thin films of complex **3** give narrow, structured emission at room temperature with biexponential decay lifetimes of 240 μs and 1.3 ms. The slow radiative rates in **3** ($k_r = 1.5 \times 10^3$ s $^{-1}$) are consistent with our initial ${}^3\text{Cz}$ assignment, owing to the highly destabilized ICT in this complex (Fig. 3D). Notably, the high Φ_{PL} and k_r values for complexes **1a**, **4**, and **5** in solution and thin films are comparable to phosphors containing heavy metals, such as Ir and Pt.

The photoluminescent properties are dramatically altered on cooling to 77 K. A vibronically

structured, long-lived emission (τ of ms to s, $k_r < 10^3$ s $^{-1}$) is observed for **1a** to **1d**, **3**, and **4** in frozen glasses of 2-MeTHF and MeCy (Table 1 and Fig. 3B). The emission at 77 K is assigned to a low-lying triplet state localized on the carbazole ligand (${}^3\text{Cz}$), as the phosphorescence spectrum of KCz in frozen 2-MeTHF replicates the same profile as **1a** (Fig. 3B). The blue shift in emission observed in MeCy at 77 K corresponds with the hypsochromic shift observed in ICT absorption at that temperature, as destabilizing the ICT transition leaves ${}^3\text{Cz}$ as the lowest-lying emissive state (Fig. 3E). Luminescence from **5** is broad and featureless in frozen glassy matrices, with long excited-state lifetimes ($\tau = 215$ μs in 2-MeTHF), consistent with emission from a ${}^3\text{ICT}$ state (Fig. 3D).

The luminescent properties of **1a** and **5** in thin PS films were examined as a function of temperature to probe the ICT manifold while avoiding complications from ${}^3\text{Cz}$ -dominated emission

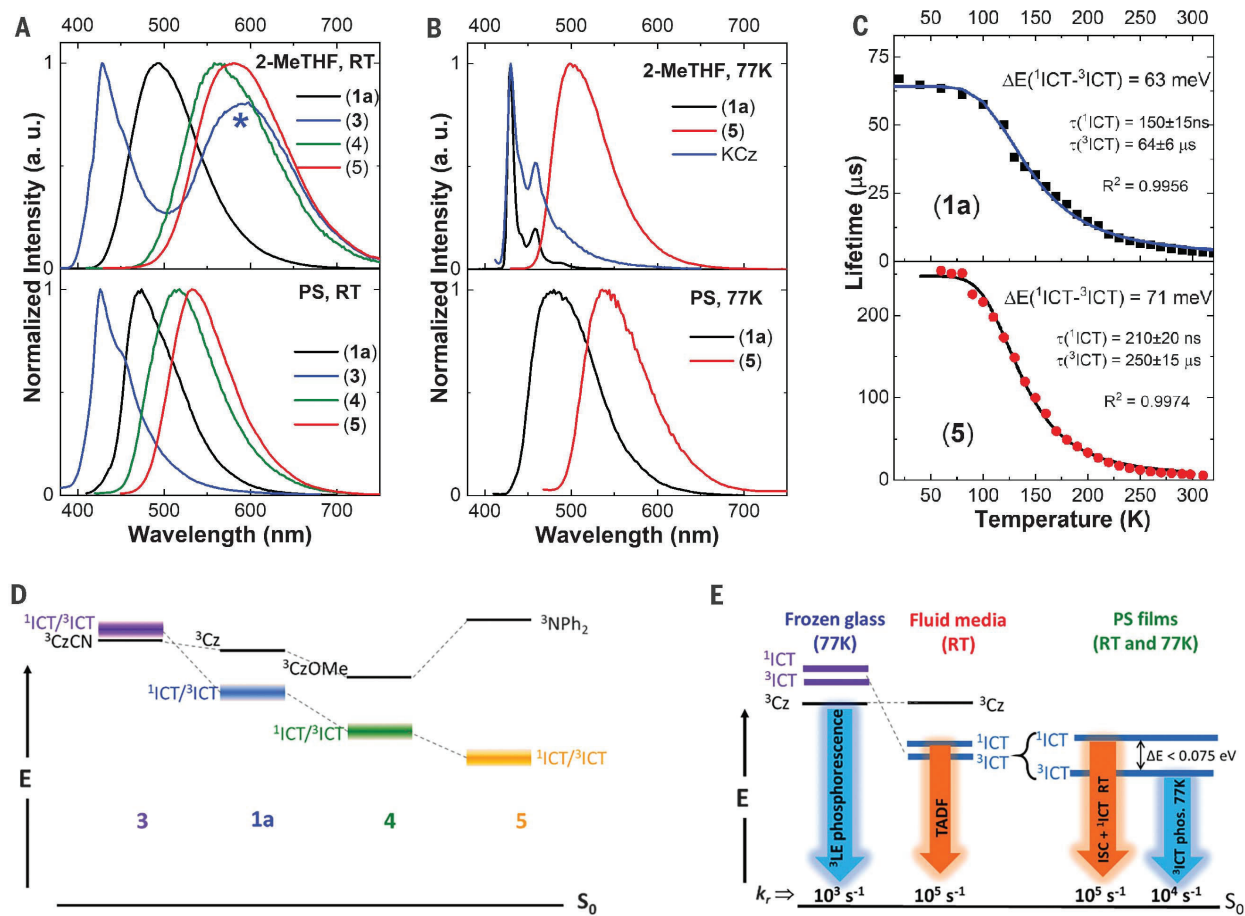


Fig. 3. Luminescence behavior of CAAC-Cu-amides. (A) Room-temperature emission spectra of complexes **1a** and **3** to **5** at 10^{-5} M in 2-MeTHF and doped 1% by weight into PS films. The asterisk indicates excimer emission. (B) 77 K emission spectra of complexes **1a** and **5** in 2-MeTHF (10^{-5} M) and 1% PS films. Also shown is the gated phosphorescence spectrum of KCz at 77 K (top). (C) Temperature-dependent PL decays of complexes **1a** (top) and **5** (bottom) as well as the data fit to Eq. 1. The parameters obtained from the fit, $\Delta E_{\text{ICT}-{}^3\text{CT}}$, τ_{ICT} , and $\tau_{{}^3\text{ICT}}$, are shown in each plot. (D) State diagram depicting ${}^1\text{ICT}$ - ${}^3\text{ICT}$ ordering in the reported complexes. The relative energies of the states are based on emission spectra. (E) Jablonski diagram depicting the different processes operating in various media at room temperature and 77 K.

and **5** (bottom) as well as the data fit to Eq. 1. The parameters obtained from the fit, $\Delta E_{\text{ICT}-{}^3\text{CT}}$, τ_{ICT} , and $\tau_{{}^3\text{ICT}}$, are shown in each plot. (D) State diagram depicting ${}^1\text{ICT}$ - ${}^3\text{ICT}$ ordering in the reported complexes. The relative energies of the states are based on emission spectra. (E) Jablonski diagram depicting the different processes operating in various media at room temperature and 77 K.

in frozen solvents. Temperature-dependent emission of thin PS films of both complexes display broad, featureless ICT spectra at all temperatures between 10 and 300 K (see figs. S30 and S31) and have excited state lifetimes that increase with decreasing temperatures (Fig. 3C). Fits of the temperature-dependent PL decay curve to a Boltzmann distribution (Eq. 1) give $\Delta E_{\text{CT}-^3\text{CT}} = 0.063 \text{ eV}$ (510 cm^{-1}) for **1a** and 0.071 eV (570 cm^{-1}) for **5** [coefficient of determination (R^2) values for the fits of **1a** and **5** in Fig. 3C are 0.996 and 0.997, respectively]. The radiative lifetimes of ^1ICT (**1a**, $\tau = 150 \pm 15 \text{ ns}$; **5**, $\tau = 210 \pm 21 \text{ ns}$) and ^3ICT (**1a**, $\tau = 64 \pm 6 \mu\text{s}$; **5**, $\tau = 250 \pm 15 \mu\text{s}$), derived from the fits to Eq. 1, are comparable to values reported by Yersin and co-workers and Bräse and co-workers in the fastest Cu(I) TADF emitters reported to date (22, 38). The rate of emission at low temperature attributed to ^3ICT -based phosphorescence is faster for **1a** than for **5**, owing to the close-lying ^3Cz in **1a**, which can enhance SOC by mixing with ^3ICT through configuration interaction (9, 12).

We also investigated the role of ligand conformation in the photophysical properties using complexes **1b** and **2b**: The former has coplanar orientation of carbene and carbazole ligands, whereas the ligands are nearly orthogonal in the latter. The ICT absorption band in **2b** has an extinction coefficient reduced threefold relative to **1b**: $\epsilon_{\text{ICT}} = 1300$ and $4000 \text{ M}^{-1} \text{ cm}^{-1}$, respec-

tively (Fig. 2A). Similarly, the efficiency and radiative rate constant for **2b** are reduced nearly fourfold relative to **1b** ($\Phi_{\text{PL}} = 0.12$ and 0.68 , and $k_r = 1.1 \times 10^5$ and $3 \times 10^5 \text{ s}^{-1}$, respectively). The marked decrease in k_r observed for **2b** is important in light of the decrease in HOMO-LUMO overlap and the expected decrease in $\Delta E_{\text{CT}-^3\text{CT}}$ (35). These observations highlight the impact of a coplanar ligand conformation on maintaining the strongly allowed nature of the ICT transitions in absorption and emission and are therefore incompatible with the rotationally accessed spin-state inversion (RASI) mechanism described by Di *et al.* (19), as previously noted by Föller and Marian and Penfold and co-workers (35, 39). Moreover, the suggestion by Di *et al.* that the S_1 state lies below the T_1 state in energy when the carbene and carbazole ligands are orthogonal is not supported by these experimental results and is counter to what is expected on the basis of fundamental quantum mechanical considerations (40).

Time-dependent DFT (TDDFT) was used to model the main electronic transitions of the excited states in these complexes (see the supplementary materials for details). The ^3ICT state shares the same orbital parentage as ^1ICT and lies within 0.25 eV of the latter (table S22), in agreement with recent reports from Föller and Marian (35) and Tafett *et al.* (41). In addition, the ^3Cz state is only 0.03 to 0.1 eV higher in en-

ergy than the ^3ICT state in all the carbazolid-based complexes except for **3**, where it is the lowest triplet state. The triplet state localized on the diphenylamide in **5**, ^3LE (i.e., $^3\text{NPh}_2$), is destabilized relative to ^3ICT by 0.5 eV.

We have further modeled the effects of solvation on the excited states of complex **1a** at 77 and 300 K using a multiscale hybrid approach that used molecular dynamics simulations in conjunction with TDDFT, as detailed in the supplementary materials. At room temperature, it was found that the ^3ICT state is the lowest triplet state in all cases owing to stabilization by the solvent dipoles (fig. S41). A similar procedure was followed to study the effect of solvation at 77 K, where single-point TDDFT calculations were performed on a frozen equilibrated cell using the hybrid scheme described in the supplementary materials. Here it was found that the ^3Cz state is the lowest-lying triplet, in accordance with the experimental observation of ^3Cz emission in 2-MeTHF at 77 K. The destabilization of the ^3ICT state can be attributed to its associated dipole (4.25 D), which is opposite in direction to the large dipole in the ground ^1ICT (11.8 D) and ^3Cz states (11.27 D). Hence, solvent molecules in a frozen matrix are expected to be ordered so as to stabilize the ground state, whereas the ^3CT state would be destabilized. Negative solvatochromic effects observed in absorption can be explained by the same rationale.

Exploration of CAAC-Cu-amides as emitters in blue OLEDs

OLEDs incorporating **1a** as an emitter were fabricated by vapor deposition (see the supplementary materials for details), following the general architecture outlined in Fig. 4A and only changing the emissive layer to screen different wide bandgap host materials. Commonly used hosts in blue OLEDs [$1,3\text{-bis}(\text{triphenylsilyl})\text{benzene}$ (UGH3); $3,3'\text{-bis}(\text{carbazol}-9\text{-yl})\text{biphenyl}$ (mCBP); and dicarbazolyl-3,5-benzene (mCP)] were examined. In addition, we also tried a Cu-based host, that is, $(\text{CAAC})\text{Cu-C}_6\text{F}_5$, with a high triplet energy; however, these devices degraded rapidly during operation (see the supplementary materials). Thin films doped into the various established hosts show similar trends with Φ_{PL} in UGH3 > mCBP > mCP (0.9, 0.6, and 0.3 respectively). OLEDs prepared with **1a** doped into UGH3 at 20 volume % give $\text{EQE}_{\text{max}} = 9.0\%$ and 16 cd/A at 2 mA/cm^2 (Fig. 4B), consistent with the high triplet energy of the UGH3 host ($T_1 = 3.5 \text{ eV}$). Although the EQE values for green- and yellow- or orange-emitting Cu-based OLEDs have been reported to be $>20\%$ (42, 43), the highest efficiencies previously reported for blue-emitting (EL $\lambda_{\text{max}} < 500 \text{ nm}$) Cu-based OLEDs are $<6\%$ (44, 45). The low EQE_{max} of the mCBP and mCP devices can be explained by a low triplet energy for the hosts (mCBP, $T_1 = 2.8 \text{ eV}$; mCP, $T_1 = 2.9 \text{ eV}$), which do not confine triplet excitons on the Cu emitter as efficiently as UGH3. The roll-off in device efficiency as the current is raised for the UGH3-based device (Fig. 4B) is

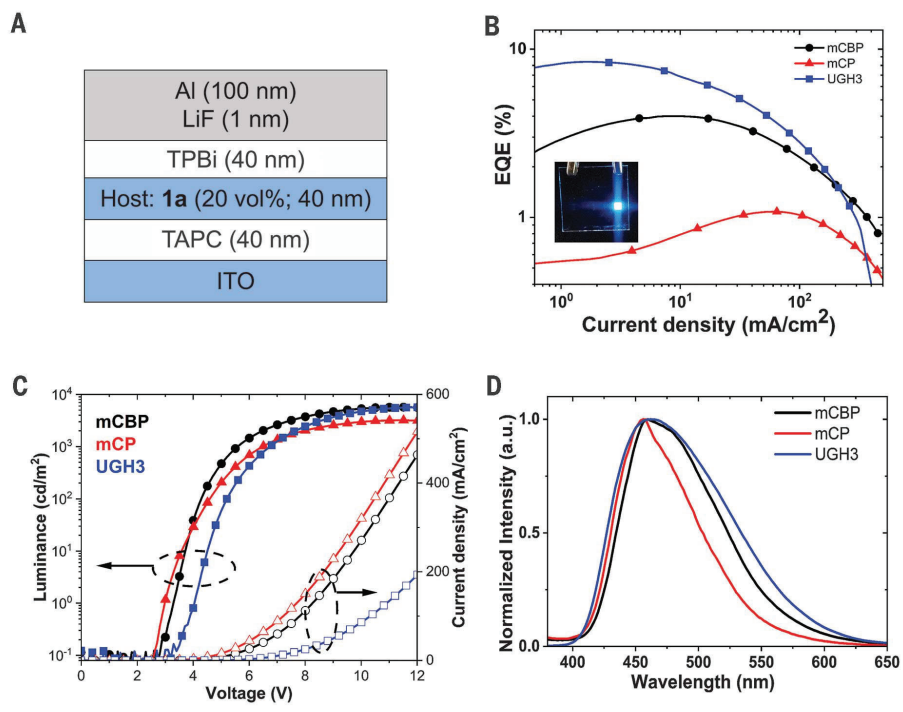


Fig. 4. OLED demonstration. (A) OLED device architecture energy scheme for **1a**-based OLEDs. TPBi, 2,2',2''-(1,3,5-benzenetriyl)-tris(1-phenyl-1-H-benzimidazole); TAPC, 4,4'-cyclohexylidenebis[N,N-bis(4-methylphenyl)benzenamine]; ITO, indium tin oxide. (B) EQE traces of devices using different hosts. The inset is a photograph of a **1a**-based device. (C and D) Current (J)-voltage (V)-luminance (L) traces (C) and EL spectra (D) of devices using different hosts.

comparable to the roll-off observed for UGH3-based OLEDs with an iridium-based emitter (46), which has been attributed to increased triplet-triplet and triplet-polaron annihilation at higher current density (47, 48). All devices exhibit blue EL, similar to the PL for **1a** in a PS film, with minor shifts due to “solvent” effects of the different host matrices. This is in contrast to the green-emissive OLEDs reported by Di *et al.* (19) for an OLED with **1b** doped into polyvinylcarbazole. We expect that stable, high-triplet energy host materials for blue OLEDs using emitter **1a** should positively affect both efficiency and device stability.

Outlook

We have prepared a series of two-coordinate CAAC-Cu-amide complexes with emission tunable across the visible spectrum, high Φ_{PL} (up to >99%) in nonrigid media, and $k_r > 10^5 \text{ s}^{-1}$. Emission stems from a strongly allowed amide-to-carbene ICT transition, with the coplanar ligand conformation and coupling through the metal d orbitals ensuring strong ϵ_{ICT} and resultant k_r . By contrast, a near-orthogonal arrangement of ligands leads to both low ϵ_{ICT} and a decrease in k_r owing to poor orbital overlap. In the Cu-carbazolide complexes, there exists a closely lying ${}^3\text{Cz}$ -centered state that dominates emission in frozen solvent glasses, owing to the destabilization of the ICT manifold in such media. Within the ICT manifold, efficient TADF is observed with $\Delta E_{ICT-{}^3CT} < 75 \text{ meV}$, among the smallest values recorded for mononuclear Cu(I)-based TADF systems (49).

The τ_{ICT} values we obtain are typical in Cu(I) TADF-based emitters; however, they are far longer than the prompt fluorescence rates recorded in pure organic TADF systems, with τ_{SI} values on the order of 10 ns (50). Another distinction from organic TADF systems is the much longer-lived (millisecond to second) phosphorescence at low temperature for organics. The discrepancy between organometallic and organic TADF suggests that a spin-pure treatment of the CT manifold is inadequate in organometallic emitters, owing to stronger SOC effects (51). The slow ${}^1\text{ICT}$ decay in Cu-based systems is likely due to considerable mixing with ${}^3\text{ICT}$ via SOC. The opposite is true for ${}^3\text{ICT}$, where considerable singlet character in the nominally triplet state leads to markedly faster decay than expected for a spin-pure triplet. The acronym TADF is an imprecise description for what is observed in Cu-based complexes of the type described here, because neither the singlet nor triplet states are spin-pure. Lifetimes as high as 0.2 μs for the ${}^1\text{ICT}$ state suggest that this state has substantial triplet contribution, thus fluorescence is not the best description for this type of emission (51, 52). The process observed here is better described as thermally enhanced luminescence, where both the lower-energy and higher-energy states are highly emissive, albeit with the lower state having a much longer radiative lifetime. Thermal enhancement here manifests in a shortening of the radiative lifetime but does not markedly increase the already high luminance efficiency.

The extent of Cu involvement in the electronic properties of these complexes appears to be the answer to the Cu-TADF conundrum we posit: The metal contribution is large enough to induce high exo- and endothermic k_{ISC} , yet low enough to ensure small reorganization energies. This work outlines the design parameters for attaining Cu(I) complexes with photophysical properties akin to their heavy metal counterparts: maintaining a two-coordinate geometry around the metal center, with redox-active ligands in a coplanar orientation. These results therefore open the door to investigation of these complexes in fields where traditional heavy metal-based phosphors have been used, for example, optical sensing, photoredox catalysis, and solar fuel generation, to name a few.

REFERENCES AND NOTES

- K. Kalyanasundaram, *Coord. Chem. Rev.* **46**, 159–244 (1982).
- M. H. Keefe, K. D. Benkstein, J. T. Hupp, *Coord. Chem. Rev.* **205**, 201–228 (2000).
- K. K.-W. Lo, M.-W. Louie, K. Y. Zhang, *Coord. Chem. Rev.* **254**, 2603–2622 (2010).
- M. Grätzel, *Inorg. Chem.* **44**, 6841–6851 (2005).
- S. Lamansky *et al.*, *J. Am. Chem. Soc.* **123**, 4304–4312 (2001).
- H. J. Bolink, E. Coronado, R. D. Costa, N. Lardiés, E. Ortí, *Inorg. Chem.* **47**, 9149–9151 (2008).
- P. C. Ford, A. Vogler, *Acc. Chem. Res.* **26**, 220–226 (1993).
- N. Armarelli, G. Accorsi, F. Cardinali, A. Listorti, in *Photochemistry and Photophysics of Coordination Compounds I*, V. Balzani, S. Campagna, Eds. (Springer, 2007), pp. 69–115.
- H. Yersin, A. F. Rausch, R. Czerwieniec, T. Hofbeck, T. Fischer, *Coord. Chem. Rev.* **255**, 2622–2652 (2011).
- S. Fraga, K. M. S. Saxena, J. Karwowski, *Handbook of Atomic Data*. Physical Science Data (Physical Science Data Series, vol. 5, Elsevier, 1976).
- L. Bergmann, G. J. Hedley, T. Baumann, S. Bräse, I. D. W. Samuel, *Sci. Adv.* **2**, e1500889 (2016).
- T. J. Penfold, E. Gindensperger, C. Daniel, C. M. Marian, *Chem. Rev.* **118**, 6975–7025 (2018).
- G. J. Hedley, A. Ruseckas, I. D. W. Samuel, *Chem. Phys. Lett.* **450**, 292–296 (2008).
- M. Kleinschmidt, C. van Wullen, C. M. Marian, *J. Chem. Phys.* **142**, 094301 (2015).
- J. Brooks *et al.*, *Inorg. Chem.* **41**, 3055–3066 (2002).
- S. Lamansky, R. C. Kwong, M. Nugent, P. I. Djurovich, M. E. Thompson, *Org. Electron.* **2**, 53–62 (2001).
- Z. A. Siddique, Y. Yamamoto, T. Ohno, K. Nozaki, *Inorg. Chem.* **42**, 6366–6378 (2003).
- H. Uoyama, K. Goushi, K. Shizu, H. Nomura, C. Adachi, *Nature* **492**, 234–238 (2012).
- D. Di *et al.*, *Science* **356**, 159–163 (2017).
- H. Yersin, R. Czerwieniec, M. Z. Shafikov, A. F. Suleymanova, *ChemPhysChem* **18**, 3508–3535 (2017).
- H. Yersin, Ed., *Highly Efficient OLEDs: Materials Based on Thermally Activated Delayed Fluorescence* (Wiley, 2019).
- R. Czerwieniec, M. J. Leitl, H. H. H. Homeier, H. Yersin, *Coord. Chem. Rev.* **325**, 2–28 (2016).
- J. R. Kirchhoff *et al.*, *Inorg. Chem.* **22**, 2380–2384 (1983).
- R. Czerwieniec, J. Yu, H. Yersin, *Inorg. Chem.* **50**, 8293–8301 (2011).
- P. K. Samanta, D. Kim, V. Coropceanu, J.-L. Brédas, *J. Am. Chem. Soc.* **139**, 4042–4051 (2017).
- M. Iwamura, H. Watanabe, K. Ishii, S. Takeuchi, T. Tahara, *J. Am. Chem. Soc.* **133**, 7728–7736 (2011).
- C. E. McCusker, F. N. Castellano, *Inorg. Chem.* **52**, 8114–8120 (2013).
- M. Gernert, U. Müller, M. Haehnel, J. Pflaum, A. Steffen, *Chemistry* **23**, 2206–2216 (2017).
- S. Shi *et al.*, *Dalton Trans.* **46**, 745–752 (2017).
- R. Hamze *et al.*, *Chem. Commun. (Camb.)* **53**, 9008–9011 (2017).
- M. Melaimi, R. Jazzaar, M. Soleilhavoup, G. Bertrand, *Angew. Chem. Int. Ed.* **56**, 10046–10068 (2017).
- O. Back, M. Henry-Ellinger, C. D. Martin, D. Martin, G. Bertrand, *Angew. Chem. Int. Ed.* **52**, 2939–2943 (2013).
- M. M. Hansmann, M. Melaimi, D. Munz, G. Bertrand, *J. Am. Chem. Soc.* **140**, 2546–2554 (2018).
- D. C. Rosenfeld, P. T. Wolczanski, K. A. Barakat, C. Buda, T. R. Cundari, *J. Am. Chem. Soc.* **127**, 8262–8263 (2005).
- J. Föller, C. M. Marian, *J. Phys. Chem. Lett.* **8**, 5643–5647 (2017).
- C. Reichardt, *Chem. Rev.* **94**, 2319–2358 (1994).
- V. Bulović, R. Deshpande, M. E. Thompson, S. R. Forrest, *Chem. Phys. Lett.* **308**, 317–322 (1999).
- D. Volz *et al.*, *Chem. Mater.* **25**, 3414–3426 (2013).
- S. Thompson, J. Eng, T. J. Penfold, *J. Chem. Phys.* **149**, 014304 (2018).
- S. P. McGlynn, T. Azumi, M. Kinoshita, *Molecular Spectroscopy of the Triplet State* (Prentice-Hall, Inc., 1969).
- E. J. Taffet, Y. Olivier, F. Lam, D. Beljonne, G. D. Scholes, *J. Phys. Chem. Lett.* **9**, 1620–1626 (2018).
- Y. Liu, S.-C. Yiu, C.-L. Ho, W.-Y. Wong, *Coord. Chem. Rev.* **375**, 514–557 (2018).
- M. Wallesch *et al.*, in *Proceedings SPIE 9183, Organic Light Emitting Materials and Devices XVIII*, F. So, C. Adachi, Eds. (SPIE, 2014), 918309.
- D. Liang *et al.*, *Inorg. Chem.* **55**, 7467–7475 (2016).
- X.-L. Chen *et al.*, *Chem. Mater.* **25**, 3910–3920 (2013).
- X. Ren *et al.*, *Chem. Mater.* **16**, 4743–4747 (2004).
- S. Reineke, K. Walzer, K. Leo, *Phys. Rev. B* **75**, 125328 (2007).
- L. Zhang, H. van Eersel, P. A. Bobbert, R. Coehoorn, *Chem. Phys. Lett.* **652**, 142–147 (2016).
- M. Osawa *et al.*, *J. Mater. Chem. C Mater. Opt. Electron. Devices* **1**, 4375–4383 (2013).
- P. L. Santos *et al.*, *J. Mater. Chem. C Mater. Opt. Electron. Devices* **4**, 3815–3824 (2016).
- R. Baková, M. Chergui, C. Daniel, A. Vlček Jr., S. Záliš, *Coord. Chem. Rev.* **255**, 975–989 (2011).
- N. J. Turro, *Modern Molecular Photochemistry* (University Science Books, 1991).

ACKNOWLEDGMENTS

Funding: This work was supported by the Universal Display Corporation for the University of Southern California authors; a National Science Foundation (NSF) Graduate Research Fellowship (grant no. DGE-1650112) supported J.L.P.; and the NSF (CHE-1661518) supported all UCSD authors. Computation for the work described in this paper was supported by the University of Southern California’s Center for High-Performance Computing (<https://hpcc.usc.edu/>). **Author contributions:** R.Ham., J.L.P., J.C., M.S., and R.J. synthesized and characterized the compounds. R.Ham. collected and analyzed the spectroscopic data. M.J. and R.Ham. fabricated and tested the OLEDs. R.Ham., J.L.P., R.J., and R.Hai. determined the x-ray structures. D.S. performed the theoretical calculations. R.Ham., P.I.D., and M.E.T. wrote the manuscript. G.B and M.E.T. directed the project.

Competing interests: R.Ham., M.J., P.I.D., and M.E.T. are inventors on a patent application submitted by the University of Southern California based partly on the intellectual property in this report. One of the authors (M.E.T.) has a financial interest in the Universal Display Corporation. **Data and materials availability:**

Structural data for all of the copper complexes reported here are freely available from the Cambridge Crystallographic Data Centre (CCDC nos. 1865272 to 1865277 for **1a**, **1c**, **1d**, and **3** to **5**; CCDC no. 1857183 for **2b**; and CCDC no. 1861278 for **Cu Host**). The supplementary materials for this paper include synthetic and characterization data (${}^1\text{H}$ and ${}^{13}\text{C}$ NMR spectra, mass spectrometry, and elemental analysis) for each copper complex; electrochemical data, ORTEP drawings, and crystallographic information on the compounds listed above; photophysical data; and details of DFT, TDDFT, and molecular dynamics calculations.

SUPPLEMENTARY MATERIALS

www.science.org/content/363/6427/601/suppl/DC1
Materials and Methods
Figs. S1 to S61
Tables S1 to S22
References (53–69)

2 September 2018; accepted 2 January 2019
10.1126/science.aav2865